UNIVERSITY OF SÃO PAULO

SÃO CARLOS SCHOOL OF ENGINEERING

DEPARTMENT OF HYDRAULICS AND SANITARY ENGINEERING

PAULO TARSO SANCHES DE OLIVEIRA

Balanço hídrico e erosão do solo no Cerrado Brasileiro

Water balance and soil erosion in the Brazilian Cerrado

São Carlos

2014

PAULO TARSO SANCHES DE OLIVEIRA

Balanço hídrico e erosão do solo no Cerrado Brasileiro

Water balance and soil erosion in the Brazilian Cerrado

Doctoral thesis submitted to the São Carlos School of Engineering, University of São Paulo, in partial fulfillment of the requirements for the Degree of Doctor in Science: Hydraulics and Sanitary Engineering.

Advisor: Prof. Dr. Edson Cezar Wendland

VERSÃO CORRIGIDA

São Carlos

2014

de Oliveira, Paulo Tarso Sanches
D48w Water balance and soil erosion in the Brazilian Cerrado / Paulo Tarso Sanches de Oliveira; orientador Edson Cezar Wendland. São Carlos, 2014.

Tese (Doutorado) - Programa de Pós-Graduação e Área de Concentração em Hidráulica e Saneamento -- Escola de Engenharia de São Carlos da Universidade de São Paulo, 2014.

1. evapotranspiration. 2. throughfall. 3. stemflow. 4. canopy interception. 5. surface runoff. 6. soil erosion. 7. rainfall erosivity. 8. deforestation. I. Título.

FOLHA DE JULGAMENTO

Candidato: Engenheiro **PAULO TARSO SANCHES DE OLIVEIRA**.

Título da tese: "Balanço hídrico e erosão do solo no cerrado brasileiro".

Data da defesa: 12/12/2014

Comissão Julgadora:	**Resultado:**
Prof. Titular **Edson Cezar Wendland (Orientador)** (Escola de Engenharia de São Carlos/EESC)	Aprovado
Profa. Titular **Luisa Fernanda Ribeiro Reis** (Escola de Engenharia de São Carlos/EESC)	Aprovado
Dr. **Silvio Crestana** (Empresa Brasileira de Pesquisa Agropecuária/EMBRAPA)	APROVADO
Prof. Titular **Humberto Ribeiro da Rocha** (Instituto de Astronomia, Geofísica e Ciências Atmosféricas/IAG-USP)	aprovado
Prof. Dr. **Sergio Koide** (Universidade de Brasília/UnB)	Aprovado

Coordenadora do Programa de Pós-Graduação em Engenharia Hidráulica e Saneamento:
Profa. Associada **Maria Bernadete A. Varesche Silva**

Presidente da Comissão de Pós-Graduação:
Prof. Associado **Paulo César Lima Segantine**

DEDICATION

To my lovely wife Dulce, the best part of me; to my parents (Walter and Damaris) and my brother (Lucas) who have always believed in me.

ACKNOWLEDGMENTS

First, I would like to acknowledge GOD to be present in my life, giving me health, wisdom, and strength to conclude one more step in my career. My wife and my entire family (despite living far away) have been very important to support my life and career. I also thank my friends in São Carlos (Brazil) and Tucson (the United States) for sharing great moments during my doctoral time.

I am grateful to my advisor, Prof. Dr. Edson Wendland, for being an example of character, a great advisor, facilitator, leader and a friend. I also thank for the opportunity to develop my doctoral study with a great group (Laboratório de Hidráulica Computacional-LHC), that made my workdays much more enjoyable.

I would like to extend my huge gratitude to my supervisor at the USDA-ARS, Southwest Watershed Research Center, Dr. Mark A. Nearing, for his sincerity, wisdom and respect, for sharing his knowledge and ideas with me, for his positive attitude about the science and the life, and for being a great mentor and friend.

I am also deeply grateful to the researchers from the USDA-ARS, Southwest Watershed Research Center and The University of Arizona for all advices, editions of the papers, and friendship. Some of these researchers are co-authors of the papers presented in this doctorate thesis, such as: Dr. Mark A. Nearing, Dr. M. Susan Moran, Dr. David C. Goodrich, Dr. Hoshin V. Gupta, Dr. Russel L. Scott, Dr. Jeffry J. Stone, Dr. Richard H. Hawkins, and Dr. Rafael Rosolem. Thank you very much to Dr. Philip Heilman (USDA-ARS, Research Leader) and Prof. Dr. David Phillip Guertin (Supervisor at the UofA) for help me in the visa process and during my time in Tucson.

This doctoral thesis could not have been done without the generous assistance of numerous individuals who shared their knowledge, expertise, and in sometimes the hard work on our experimental area, such as the graduate students at the LHC (Antonio Meira, Murilo Lucas, Davi Diniz, Cristian Youlton, Camilo Cabrera, Rafael Chaves, Ivan Marin, Frederico Martins, Thiago Matos, Marjolly Priscilla, and Jamil. The undergraduate students Ana Luisa and Petry Melo for their work in the laboratory. Many thanks to the technical staff of the USP, Roberto Bergamo and Miro that helped me to choose the experimental area, installing several equipments,

and the monitoring the experimental area. I thank to Prof. Dr. João Perea Martins for sharing his data logger design which has been used in several rain gauges in the cerrado area. I would like to thank the Arruda Botelho Institute (IAB) and São José farm that have allowed us to develop this study in the native cerrado vegetation.

My gratitude also refers to the efficient and friendly technical staff of the SHS-USP (e.g. Sá, Priscila, Flávia, Fernanda, Rose, and André). I also thank to the colleagues, professors, and technical staff of the USDA-ARS, School of Natural Resources and the Environment, and Hydrology and Water Resources department (Tucson, US), for receiving me so friendly, helping Dulce and I in every moments.

I do not have enough words to thank to my wife Dulce, which has always been on my side through the years, supporting, taking care, helping me to overcome challenges. Finally, I thank to my parents, brother, and the entire family that even living far away have supported my career.

This doctoral thesis was supported by grants from the Fundação de Amparo à Pesquisa do Estado de São Paulo - FAPESP (10/18788-5, 11/14273-3 and 12/03764-9) and the Conselho Nacional de Desenvolvimento Científico e Tecnológico - CNPq (470846/2011-9).

"All streams flow into the sea, yet the sea is never full. To the place the streams come from, there they return again."

(Ecclesiastes 1:7)

RESUMO

Oliveira, P. T. S. (2014). **Balanço hídrico e erosão do solo no Cerrado Brasileiro**. Tese de Doutorado, Escola de Engenharia de São Carlos, Departamento de Engenharia Hidráulica e Saneamento, Universidade de São Paulo, São Carlos, SP. Brasil.

O desmatamento nas regiões de Cerrado tem causado intensas mudanças nos processos hidrológicos. Essas mudanças no balanço hídrico e erosao do solo são ainda pouco entendidas, apesar de fundamentais na tomada de decisão de uso e manejo do solo nesta região. Portanto, torna-se necessário compreender a magnitude das mudanças nos processos hidrológicos e de erosão do solo, em escalas locais, regionais e continentais, e as consequências dessas mudanças. O principal objetivo do estudo apresentado nesta tese de doutorado foi de melhor entender os mecanismos dos processos hidrológicos e de erosão do solo no Cerrado Brasileiro. Para tanto, utilizou-se diferentes escalas de trabalho (vertentes, bacias hidrográficas e continental) e usando dados experimentais *in situ*, de laboratório e a partir de sensoriamento remoto. O estudo de revisão de literatura indica que a erosividade da chuva no Brasil varia de 1672 to 22,452 MJ mm ha^{-1} h^{-1} yr^{-1}. Os menores valores encontram-se na região nordeste e os maiores nas regiões norte e sudeste do Brasil. Verificou-se que os valores de interceptação da chuva variam de 4 a 20% e o escoamento pelo tronco aproximadamente 1% da precipital total no cerrado. O coeficiente de escoamento superficial foi menor que 1% nas parcelas de cerrado e o desmatamento tem o potencial de aumentar em até 20 vezes esse valor. Os resultados indicam que o método Curve Number não foi adequado para estimar o escoamento superficial nas áreas de cerrado, solo exposto (grupo hidrológico do solo A), pastagem e milheto. Portanto, nesses casos o uso do CN é inadequado e o escoamento superficial é melhor estimado a partir da equação $Q = CP$, onde C é o coeficiente de escoamento superficial. O balanço hídrico a partir de dados de sensoriamento remoto para todo o Cerrado Brasileiro indica que a principal fonte de incerteza na estimativa do escoamento superficial ocorre nos dados de precipitação do TRMM. A variação de água na superfície terrestre calculada como o resídual da equação do balanço hídrico usando dados de sensoriamento remoto (TRMM e MOD16) e valores observados de vazão mostram uma correlação significativa com os valores de variação de água na superfície terrestre provenientes dos dados do GRACE. Os dados do GRACE podem representar satisfatoriamente a variação de água na superfície terrestre para extensas regiões do Cerrado. A média anual de perda de solo nas parcelas de solo exposto e cerrado foram de 15.25 t $ha^{-1}yr^{-1}$ and 0.17 t ha^{-1} yr^{-1}, respectivamente. O fator uso e manejo do solo (fator C) da Universal Soil Loss Equation para o cerrado foi de 0.013. Os resultados mostraram que o escoamento superficial, erosão do solo e o fator C na área de cerrado variam de acordo com as estações. Os maiores valores do fator C foram encontrados no verão e outono. Os resultados encontrados nesta tese de doutorado fornecem valores de referência sobre os componentes do balanço hídrico e erosão do solo no Cerrado, que podem ser úteis para avaliar o uso e cobertura do solo atual e futuro. Além disso, conclui-se que os dados de sensoriamento remoto apresentam resultados satisfatórios para avaliar os componentes do balanço hídrico no Cerrado, identificar os períodos de seca e avaliar as alterações no balanço hídrico devido à mudanças de uso e cobertura do solo.

Palavras-chave: evapotranspiração, precipitação interna, escoamento pelo tronco, interceptação, escoamento superficial, erosão do solo, erosividade da chuva, conservação do solo e da água, savanna, desmatamento.

ABSTRACT

Oliveira, P. T. S. (2014). **Water balance and soil erosion in the Brazilian Cerrado**. Doctoral Thesis, São Carlos School of Engineering, Department of Hydraulics and Sanitary Enginiring, University of São Paulo, São Carlos, SP, Brazil.

Deforestation of the Brazilian savanna (Cerrado) region has caused major changes in hydrological processes. These changes in water balance and soil erosion are still poorly understood, but are important for making land management decisions in this region. Therefore, it is necessary to understand the magnitudes of hydrological processes and soil erosion changes on local, regional and continental scales, and the consequences that are generated. The main objective of the study presented in this doctoral thesis was to better understand the mechanism of hydrological processes and soil erosion in the Cerrado. To achieve that, I worked with different scales (hillslope, watershed and continental) and using data from experimental field, laboratory, and remote sensing. The literature review reveals that the annual rainfall erosivity in Brazil ranges from 1672 to 22,452 MJ mm ha^{-1} h^{-1} yr^{-1}. The smallest values are found in the northeastern region, and the largest in the north and the southeastern region. I found that the canopy interception may range from 4 to 20% of gross precipitation and stemflow around 1% of gross precipitation in the cerrado. The average runoff coefficient was less than 1% in the plots under cerrado and that the deforestation has the potential to increase up to 20 fold the runoff coefficient value. The results indicate that the Curve Number method was not suitable to estimate runoff under undisturbed Cerrado, bare soil (hydrologic soil group A), pasture, and millet. Therefore, in these cases the curve number is inappropriate and the runoff is more aptly modeled by the equation $Q = CP$, where C is the runoff coefficient. The water balance from the remote sensing data across the Brazilian Cerrado indicates that the main source of uncertainty in the estimated runoff arises from errors in the TRMM precipitation data. The water storage change computed as a residual of the water budget equation using remote sensing data (TRMM and MOD16) and measured discharge data shows a significant correlation with terrestrial water storage change obtained from the GRACE data. The results show that the GRACE data may provide a satisfactory representation of water storage change for large areas in the Cerrado. The average annual soil loss in the plots under bare soil and cerrado were 15.25 t $ha^{-1}yr^{-1}$ and 0.17 t ha^{-1} yr^{-1}, respectively. The Universal Soil Loss Equation cover and management factor (C-factor) for the plots under native cerrado vegetation was 0.013. The results showed that the surface runoff, soil erosion and C-factor for the undisturbed Cerrado changes between seasons. The greatest C-factor values were found in the summer and fall. The results found in this doctoral thesis provide benchmark values of the water balance components and soil erosion in the Brazilian Cerrado that will be useful to evaluate past and future land cover and land use changes for this region. In addition, I conclude that the remote sensing data are useful to evaluate the water balance components over Cerrado regions, identify dry periods, and assess changes in water balance due to land cover and land use change.

Keywords: evapotranspiration, throughfall, stemflow, canopy interception, runoff, soil erosion, rainfall erosivity, soil and water conservation, savanna, deforestation.

LIST OF FIGURES

LIST OF TABLES

TABLE OF CONTENTS

GENERAL INTRODUCTION

As global demand for agricultural products such as food and fuel grows to unprecedented levels, the supply of available land continues to decrease, which is acting as a major driver of cropland and pasture expansion across much of the developing world (Gibbs et al., 2010; Macedo et al., 2012). Vast areas of forest and savannas in Brazil have been converted into farmland, and there is little evidence that agricultural expansion will decrease, mainly because Brazil holds a great potential for further agricultural expansion in the twenty-first century (Lapola et al., 2014).

The Amazon rainforest and Brazilian savanna (Cerrado) are the most threatened biomes in Brazil (Marris, 2005). However, the high suitability of the Cerrado topography and soils for mechanized agriculture, the small number and total extent of protected areas, the lack of a deforestation monitoring program, and the pressure resulting from decreasing deforestation in Amazonia indicates that the Cerrado will continue to be the main region of farmland expansion in Brazil (Lapola et al., 2014). In fact, Soares-Filho et al. (2014) reported that the Cerrado is the most coveted biome for agribusiness expansion in Brazil, given its 40 ± 3 Mha of land that could be legally deforested.

The Brazilian Cerrado, one of the richest ecoregions in the world in terms of the biodiversity (Myers et al., 2000), covers an area of 2 million km^2 (~22% of the total area of Brazil), however, areas of remaining native vegetation represent only 51% of this total (IBAMA/MMA/UNDP, 2011). In addition to being an important ecological and agricultural region for Brazil, the Cerrado is crucial to water resource dynamics of the country, and includes portions of 10 of Brazil's 12 hydrographic regions (Oliveira et al., 2014). Furthermore, the largest hydroelectric plants (comprising 80% of the Brazilian energy) are on rivers in the Cerrado. As savannas and forests have been associated with shifts in the location, intensity and timing of rainfall events, lengthening of the dry season and changed streamflow (Davidson et al., 2012; Spracklen et al., 2012; Wohl et al., 2012), it is clear that land cover and land use change promoted by the cropland and pasture expansion in this region have the potential to affect the ecosystems services and several important economic sectors of Brazil, such as agriculture, energy production and water supply.

Therefore, it is necessary to understand the magnitudes of hydrological processes changes on local, regional and continental scales, and the consequences that are generated. The main objective of the study presented in this doctoral thesis was to better understand the

mechanism of hydrological processes and soil erosion in the Brazilian Cerrado. To achieve that, I have worked with different scales (plots, hillslope, watershed and continental) and using data from experimental field, laboratory, and remote sensing. This doctoral thesis was organized into five chapters.

In Brazil, some regression equations are used widely to obtain the local values of erosivity from pluviometric data. However, the interpretation of the input data must be realistic and must match the local climate characteristics. The **first chapter** shows a review of rainfall erosivity studies conducted in Brazil to verify the quality and representativeness of the results generated and to provide a better understanding of the rainfall erosivity in Brazil.

To understand pre-deforestation conditions, the **second chapter** determines the main components of the water balance for an undisturbed tropical woodland classified as "cerrado sensu stricto denso". An empirical model was developed to estimate actual evapotranspiration (ET) by using flux tower measurements and, vegetation conditions inferred from the enhanced vegetation index (EVI) and reference crop evapotranspiration (ETo). Canopy interception, throughfall, stemflow, and surface runoff were assessed from ground measurements. Data from two cerrado sites were used, "Pé de Gigante" - PDG and "Instituto Arruda Botelho" - IAB. Flux tower data from the PDG site collected from 2001 through 2003 was used to develop the empirical model to estimate ET. The other hydrological processes were measured at the field scale between 2011 and 2014 at the IAB site.

The curve number method is the most widely used method in Brazil for runoff estimation, despite that the tabulated Curve Numbers (CN) values have not been adapted for Brazilian conditions. In addition, there are several uncertainties in the use of CN method to estimate surface runoff from regions under undisturbed cover. Thus, the objectives of the **third chapter** are to measure natural rainfall-driven rates of runoff under undisturbed cerrado vegetation and under the main crops found in this biome, and to derive associated CN values from the five more frequently used statistical methods.

The **fourth chapter** investigates the water balance dynamics for the entire Brazilian Cerrado area, identify recent temporal trends in the major components, and assess the potential consequences of land cover and land use change for the water balance. Satellite-based TRMM, MOD16 and GRACE data were used for the period from 2003 to 2010 to quantify the primary water balance components of the region and to evaluate trends. Furthermore, the uncertainties were computed for each remotely sensed data set and the

budget closure was evaluated from measured discharge data for the three largest river basins in the Cerrado.

The magnitude of the soil erosion increases in the Cerrado region is not well understood, in part because scientific studies of surface runoff and soil erosion are scarce or nonexistent in native Cerrado vegetation. To understand the deforestation effects, the **fifth chapter** assess natural rainfall-driven rates of runoff and soil erosion under undisturbed and with bare soil, and compute the cover and management factor (C-factor) of the Universal Soil Loss Equation (USLE). Replicated data on precipitation, runoff, and soil loss on plots (5 x 20 m) under undisturbed cerrado and bare soil were collected for 55 erosive storms occurring in 2012 and 2013. C-factor was computed annually using computed values of rainfall erosivity and soil loss rate.

References

Davidson, E. A., de Araújo, A. C., Artaxo, P., Balch, J. K., Brown, I. F., C. Bustamante, M. M., … Wofsy, S. C. (2012). The Amazon basin in transition. *Nature*, *481*(7381), 321–328. doi:10.1038/nature10717

Gibbs, H. K., Ruesch, A. S., Achard, F., Clayton, M. K., Holmgren, P., Ramankutty, N., & Foley, J. A. (2010). Tropical forests were the primary sources of new agricultural land in the 1980s and 1990s. *Proceedings of the National Academy of Sciences*, *107*(38), 16732–16737. doi:10.1073/pnas.0910275107

IBAMA/MMA/UNDP. Monitoramento do desmatamento nos biomas Brasileiros por satélite. Ministério de Meio Ambiente, Brasília, Brazil. available at: http://siscom.ibama.gov.br/monitorabiomas/cerrado/index.htm.

Lapola, D. M., Martinelli, L. A., Peres, C. A., Ometto, J. P. H. B., Ferreira, M. E., Nobre, C. A., … Vieira, I. C. G. (2013). Pervasive transition of the Brazilian land-use system. *Nature Climate Change*, *4*(1), 27–35. doi:10.1038/nclimate2056

Macedo, M. N., DeFries, R. S., Morton, D. C., Stickler, C. M., Galford, G. L., & Shimabukuro, Y. E. (2012). Decoupling of deforestation and soy production in the southern Amazon during the late 2000s. *Proceedings of the National Academy of Sciences*, *109*(4), 1341–1346. doi:10.1073/pnas.1111374109

Marris, E. (2005). Conservation in Brazil: The forgotten ecosystem. *Nature*, *437*(7061), 944–945. doi:10.1038/437944a

Myers, N., Mittermeier, R. A., Mittermeier, C. G., da Fonseca, G. A. B., & Kent, J. (2000). Biodiversity hotspots for conservation priorities. *Nature*, *403*(6772), 853–858. doi:10.1038/35002501

Oliveira, P. T. S., Nearing, M. A., Moran, M. S., Goodrich, D. C., Wendland, E., & Gupta, H. V. (2014). Trends in water balance components across the Brazilian Cerrado. *Water Resources Research*, *50*, doi:10.1002/2013WR015202

Soares-Filho, B., Rajao, R., Macedo, M., Carneiro, A., Costa, W., Coe, M., … Alencar, A. (2014). Cracking Brazil's Forest Code. *Science*, *344*(6182), 363–364. doi:10.1126/science.1246663

Spracklen, D. V., Arnold, S. R., & Taylor, C. M. (2012). Observations of increased tropical rainfall preceded by air passage over forests. *Nature*, *489*(7415), 282–285. doi:10.1038/nature11390

Wohl, E., Barros, A., Brunsell, N., Chappell, N. A., Coe, M., Giambelluca, T., … Ogden, F. (2012). The hydrology of the humid tropics. *Nature Climate Change*. doi:10.1038/nclimate1556

OBJECTIVES

General Objective

The main objective of the study presented in this doctoral thesis is to better understand the mechanism of hydrological processes and soil erosion in the Brazilian Cerrado.

Specific objectives

i. To develop a review of the erosivity studies conducted in Brazil to verify the quality and representativeness of the results generated and to provide a better understanding of the rainfall erosivity (R-factor) in Brazil.
ii. To determine the main components of the water balance for an undisturbed tropical woodland classified as "cerrado sensu stricto denso".
iii. To develop an empirical model to estimate actual evapotranspiration (ET) by using flux tower measurements and, vegetation conditions inferred from the enhanced vegetation index and reference evapotranspiration.
iv. To measure natural rainfall-driven rates of runoff under undisturbed cerrado vegetation and under the main crops found in this biome, and to derive associated Curve Numbers values from the five more frequently used statistical methods.
v. To assess the water balance dynamics for the entire Brazilian Cerrado area, identify recent temporal trends in the major components, and assess the potential consequences of land cover and land use change for the water balance.
vi. To measure natural rainfall-driven rates of soil erosion under native cerrado vegetation and bare soil conditions and to derive associated USLE C-factor values.

CHAPTER 1
RAINFALL EROSIVITY IN BRAZIL: A REVIEW

Oliveira, Paulo Tarso S., Wendland, E. and Nearing, Mark A. (2013). Rainfall erosivity in Brazil: A Review. *Catena*. 100, 139-147, doi: 10.1016/j.catena.2012.08.006. (Impact factor, 2013: 2.482; Qualis CAPES: A1)

Abstract

In this paper, we review the erosivity studies conducted in Brazil to verify the quality and representativeness of the results generated and to provide a greater understanding of the rainfall erosivity (R-factor) in Brazil. We searched the ISI Web of Science, Scopus, SciELO, and Google Scholar databases and in recent theses and dissertations to obtain the following information: latitude, longitude, city, states, length of record (years), altitude, precipitation, R factor, equations calculated and respective determination coefficient (R^2). We found 35 studies in Brazil that used pluviographic rainfall data to calculate the rainfall erosivity. These studies were concentrated in the cities of the south and southeast regions (~ 60% of all the cities studied in Brazil) with a few studies in other regions, mainly in the north. The annual rainfall erosivity in Brazil ranged from 1,672 to 22,452 MJ mm ha^{-1} h^{-1} yr^{-1}. The lowest values were found in the northeast region, and the highest values were found in the north region. The rainfall erosivity tends to increase from east to west, particularly in the northern part of the country. In Brazil, there are 73 regression equations to calculate erosivity. These equations can be useful to map rainfall erosivity for the entire country. To this end, techniques already established in Brazil may be used for the interpolation of rainfall erosivity, such as geostatistics and artificial neural networks.

Keywords: erosivity; erosion; water erosion; annual precipitation; R-factor; RUSLE.

1 Introduction

Soil loss prediction is important to assess the risks of soil erosion and to determine appropriate soil use and management (Oliveira et al., 2011a). Several mathematical models (empirical, conceptual and physical-based processes) have been developed to estimate soil erosion on different spatial and temporal scales (Moehansyah et al. 2004; Ferro, 2010). The

erosion models vary from complex procedures that require a series of input parameters, such as Water Erosion Prediction Project (WEPP) (Nearing et al., 1989), Kinematic Runoff and Erosion (KINEROS) (Woolhiser et al., 1990) and European Soil Erosion Model (EUROSEM) (Morgan et al., 1998) to more simplified methods, such as the Universal Soil Loss Equation (USLE) (Wischmeier and Smith, 1978), Revised Universal Soil Loss Equation (RUSLE) (Renard et al., 1997) and Morgan-Morgan and Finney (MMF) (Morgan, 2001).

Models that require multiple input parameters may not be feasible for use in locations with no data or with difficult access, as in several regions of Brazil. Several authors consider the USLE to provide an excellent model for predicting soil loss because of its applicability (in terms of required input data) and the reliability of the obtained soil loss estimates (Risse et al., 1993; Ferro, 2010). The application of USLE on a river basin scale has been facilitated by the use of Geographic Information Systems (GIS). This combination is considered a useful tool for soil and water conservation planning (Oliveira et al., 2011a).

The USLE is the most widely used erosion model in the world, and it provides useful information for the adequate planning of soil and water conservation. This model is characterized by establishing an estimate of the average annual soil loss caused by rill and interril erosion (Kinnell, 2010; Oliveira et al., 2011a). The input data for the model are composed of natural factors (rainfall erosivity – R, erodibility – K, slope length – L, and slope – S) and anthropogenic factors (cover and management – C, and conservation practices – P). Among the factors that compose the USLE and RUSLE, the rainfall erosivity (R factor) is highly important because precipitation is the driving force of erosion and has a direct influence on aggregate breakdown and runoff. Erosivity is also an important parameter for soil erosion risk assessment under future land use and climate change (Nearing et al., 2005; Meusburger et al., 2011).

Several studies using natural and artificial rain have been conducted to understand the role of droplet size and the distribution of rainfall on the detachment of soil particles. However, the data are difficult to measure and are scarce, both spatially and temporally. Accordingly, studies related to rainfall, such as the maximum intensity over a period of time, the total energy of the rain or the rate of direct breakdown of the soil, have been conducted (Angulo-Martínez and Beguería, 2009). As an example of the erosivity index, we can cite the R factor of the USLE, which summarizes all the erosive events quantified by the EI_{30} index throughout the year (Wischmeier and Smith, 1978), the KE>25 index for southern Africa (Hudson, 1971), the AIm index for Nigeria (Lal, 1976), and the modified Fournier index for Morocco (Arnoldus, 1977).

The EI_{30} index has been the most widely used index (Hoyos et al., 2005) and provides a good correlation with soil loss in several studies in Brazil (Lombardi Neto and Moldenhauer, 1992, Bertol et al., 2007, Bertol et al., 2008, Silva et al., 2009a). However, a series of more than 20 years of rain gauge is recommended to calculate this factor, but this length of time series is not found in many parts of the world (Hoyos et al. 2005; Capolongo et al. 2008; Lee and Heo, 2011). Simplified methods for predicting rainfall erosivity using readily available data have been presented and are used in many countries because the high-resolution rainfall data needed to directly compute the rainfall erosivity are not available for many locations; moreover, calculations of such data (when available) are intricate and time consuming (Lee and Heo, 2011). Models that relate the erosivity index with pluviometric data (e.g., monthly precipitation, annual total precipitation and modified Fournier index) were proposed to obtain the R factor. These daily pluviometric records are generally available for most locations with good spatial and temporal coverage, allowing the calculation of the erosivity index in regions that have no pluviographic rainfall data (Renard and Freimund, 1994; Silva, 2004; Angulo-Martínez and Beguería, 2009).

In Brazil, some regression equations are used widely to obtain the local values of erosivity from pluviometric data. However, the interpretation of the input data must be realistic and must match the local climate characteristics. In this paper, we review the erosivity studies conducted in Brazil to verify the quality and representativeness of the results generated and to provide a better understanding of the rainfall erosivity in Brazil. The R factor was used as the index to show the rainfall erosivity.

2 Materials and Methods

Rainfall erosivity has been calculated for Brazilian regions using recording rain gauge data as the source of input. We review the ISI Web of Science, Scopus, SciELO, and Google Scholar databases and recent theses and dissertations that have not been published in journals. The following information was obtained from the published works: latitude, longitude, city, states, length of record (years), altitude, precipitation, R factor, equations calculated and respective determination coefficient (R^2).

We analyze the spatial distribution of the erosivity studies for the regions of Brazil to determine which areas have an abundance or lack of information. In addition, the erosivity information was compared with the calculated values of erosivity derived from regression equations.

3 Results and Discussion

3.1 Calculation of the erosivity index (EI_{30}) in Brazil

The erosivity index (EI_{30}) is determined for isolated rainfalls and classified as either erosive or nonerosive. In Brazil, periods of rainfall are considered to be isolated and non-erosive when they are separated by periods of precipitation between 0 (no rain) and 1.0 mm for at least 6 h and are considered to be erosive when 6.0 mm of rain falls in 15 min or 10.0 mm of rain falls over a longer time period (Wischmeier, 1959, Oliveira et al., 2011a).

Erosive rain is analyzed by identifying the segments with the same inclination that represent periods of rain with the same intensity. For each segment with uniform rainfall, the unitary kinetic energy is determined by Eq. 1 (Wischmeier and Smith, 1978).

$$e = 0.119 + 0.0873 \log_{10} i \quad (1)$$

where *e* is the unitary kinetic energy (MJ ha^{-1} mm^{-1}) and *i* represents the segments of rainfall intensity (mm h^{-1}).

The rainfall kinetic energy can be directly calculated from drop size distribution and terminal velocity of the drops. This way, is important to study better these relationship at different regions (Cerdà, 1997). In Brazil, Wagner and Massambani (1988) developed the relationship between kinetic energy and rainfall intensity from 533 samples of the drop size distribution. The authors concluded that the equation generated (from observed data) to calculate kinetic energy do not have any significant difference of the equation from Wischmeier and Smith (1978). Thus, the Eq. 1 still widely used in Brazil.

The value obtained in Eq. 1 is multiplied by the amount of rain in the respective uniform segment to express the kinetic energy of the segment in MJ ha^{-1}. The total kinetic energy of rain (Ect) is obtained by adding the kinetic energy of all the uniform segments of rain. The EI_{30} is defined as the product of the maximum rain intensity during a 30-minute period (I_{30}) and the Ect.

$$EI_{30} = Ect\ I_{30} \quad (2)$$

where EI_{30} is the rainfall erosivity index (MJ mm ha^{-1} h^{-1}), *Ect* is the total kinetic energy of the rain (MJ ha^{-1}), and I_{30} is the maximum rain intensity during a 30-minute period (mm h^{-1}).

The RUSLE R-factor is obtained from the average annual values of the EI_{30} erosion index:

$$R = \frac{1}{n}\sum_{j=1}^{n}\sum_{k=1}^{m_j}(EI_{30})_k \quad (3)$$

where *R* is the average of the annual rainfall erosivity (MJ mm ha^{-1} h^{-1} yr^{-1}), *n* is the number of years of records, m_j is the number of erosive events in a given year *j*, and EI_{30} is the rainfall erosivity index of a single event *k*.

After calculating the values of $EI_{30,}$ a regression analysis is performed, usually using the Fournier index modified by Lombardi Neto (1977) or mean annual precipitation (P) (Eq. 4) as independent variables. In Brazil, several researchers showed that the modified Fournier index (MFI) have achieved best results in the calculating of the R Factor (Lombardi Neto and Moldenhauer, 1992; Carvalho et al., 2005; Cassol et al., 2008, Oliveira et al., 2011b). These resulting regression equations generally are used to calculate the erosivity from pluviometric data in regions that have no pluviographic rainfall data.

$$MFI = p_i^2\ P^{-1} \quad (4)$$

where *MFI* is the modified Fournier index, *p* is the mean monthly precipitation at month *i* (mm), and *P* is the mean annual precipitation (mm).

3.2 Mapping rainfall erosivity

The erosivity map can be obtained by interpolation methods using sampled values to estimate the erosivity values in places where no rainfall data are available (Montebeller et al., 2007). Until the late 1980s, interpolation techniques such as inverse distance, Thiessen polygons, or isohyetal method were the most popular techniques for the interpolation of rainfall data (Goovaerts, 1999). Silva (2004) used point erosivity values (calculated from regression equations) and the inverse distance method to obtain an erosivity map of Brazil. This study provided a good overall understanding of the occurrence of larger and smaller values of erosivity throughout the country.

Since the 1990s, a geostatistical interpolation method based on the regionalized variables theory has been widely used (Goovaerts, 1999) because it allows estimation at nonsampled points without bias and with minimum variance (Montebeller et al., 2007). Several studies were performed using the Kriging interpolation method to obtain erosivity maps. We can cite the works of Shamshad et al. (2008) in Peninsular Malaysia, Angulo-Martínez et al. (2009) in northeastern Spain, Zhang et al. (2010) in northeastern China, Meusburger et al. (2011) in Switzerland, and Bonilla and Vidal (2011) in central Chile. In Brazil, erosivity maps were created by Vieira and Lombardi Neto (1995) in São Paulo State, Mello et al. (2007) in Minas Gerais State, Montebeller et al. (2007) in Rio de Janeiro State, and Oliveira et al. (2011b) in Mato Grosso do Sul State.

In addition to the use of the geostatistical method for erosivity mapping, the application of machine learning techniques (ML) also is successfully used as a tool to obtain values of erosivity in places where no rainfall data are available. One of the main techniques of ML is Artificial Neural Networks (ANN), which have been used satisfactorily for this purpose (Licznar, 2005). In Brazil, ANN was used to estimate the rainfall erosivity in the States of São Paulo (Moreira et al., 2006), Minas Gerais (Moreira et al., 2008), and Mato Grosso do Sul (Alves Sobrinho et al., 2011), and Silva et al. (2010a) worked in the Vale do Ribeira, in southern São Paulo State. Like the rainfall erosivity mapping by geostatistical techniques, studies using ANN are concentrated in the southeastern region of Brazil. Thus, we find it necessary to perform further studies in other regions of Brazil because this kind of regional approach helps in effective land-use planning.

3.3 Spatial distribution of erosivity studies in Brazil

We found 35 studies that used pluviographic rainfall data to calculate the rainfall erosivity. These studies focused on 80 cities in 14 of the 26 Brazilian states, i.e. with no studies on erosivity in the other half of the states. Most studies concentrated on the cities of the south and southeast regions (~ 60% of all the cities studied in Brazil), with only a few studies in other regions, mainly in the north and central-west (Figure 1 and Table 1). This concentration occurs because the south and southeast regions are the most economically prosperous and have a higher population density.

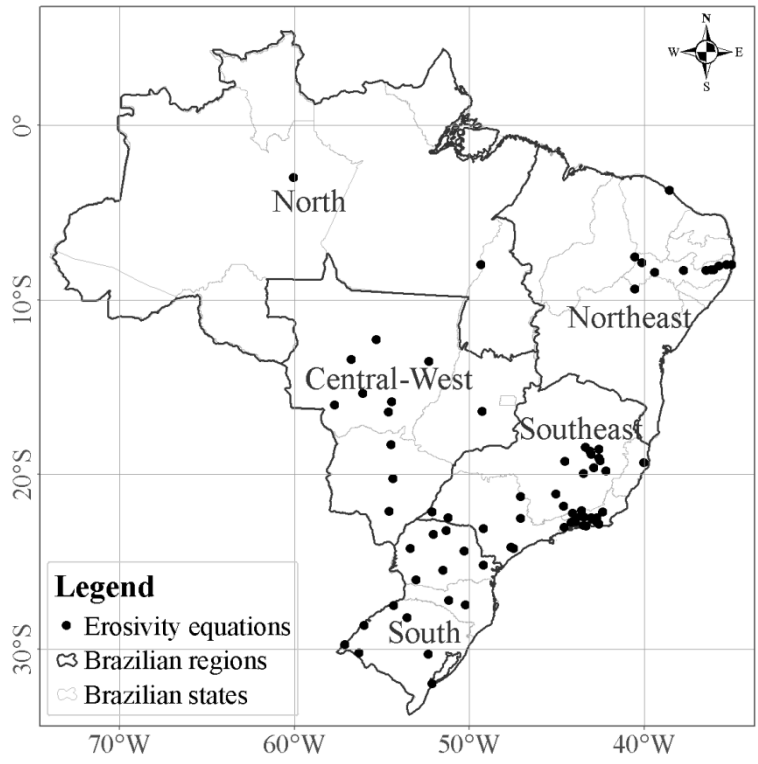

Figure 1. Spatial distribution of studies on erosivity in Brazil.

The rainfall erosivity values observed in Brazil ranges from 1,672 to 22,452 MJ mm ha^{-1} h^{-1} yr^{-1}. The average erosivity (± sd) observed is 8,403 ± 4,090 MJ mm ha^{-1} h^{-1} yr^{-1}. Lower values are found in the northeastern region, in the state of Pernambuco (PE), and the highest values are found in the north region (States of Para - PA and Amazonas - AM) and southeast

region (States of Minas Gerais - MG, Rio de Janeiro - RJ, and Sao Paulo - SP) (Table 1 and Figure 2a). Figure 2a was derived using the data presented in Table 1 and kriging interpolation method. However, this map is illustrative only because it is based on a sparse data set. To obtain a more accurate erosivity map, we recommend applying the equations presented in Table 1 in pluviometric data of other Brazilian places and after with several data points elaborating the map.

Table 1. Studies on erosivity in Brazil

Latitude	Longitude	City	States	Years	Altitude	Precipitation	R-factor	Equations	R^2	Authors
3° 0' 0"S	60° 0' 0"W	Manaus	AM	-	-	2,219	14,129	$EI_{30} = 42.77 + 3.76$ (MFI)	-	Oliveira Jr. and Medina, 1990
3° 44' 0"S	38° 33' 0"W	Fortaleza	CE	20	20	1,677	6,774	-	-	Dias and Silva, 2003
19° 35' 0"S	40° 0' 0"W	Aracruz	ES	7	40	1,400	8,536	$EI_{30} = 40.578 + 7.9075$ (P)	0.61	Martins et al., 2010
16° 41' 0"S	49° 23' 0"W	Goiânia	GO	5	750	1,280	8,353	$EI_{30} = 215.33 + 30.23$ (MFI)	0.77	Silva et al., 1997
21° 8' 24"S	45° 0' 0"W	Lavras	MG	15	919	1,530	5,403	-	-	Evangelista et al., 2006
19° 25' 0"S	44° 15' 0"W	Sete Lagoas	MG	3	732	1,340	5,835	$EI_{30} = 25.3 + 43.35$ (MFI) - 0.232 $(MFI)^2$	-	Marques et al., 1997
19° 04' 11"S	42° 32' 56"W	Açucena	MG	3	493	1,481	18,646	$EI_{30} = 158.35\ (MFI)^{0.85}$	0.88	Silva et al., 2010b
19° 38' 23"S	42° 51' 13"W	Antônio Dias	MG	3	420	1,198	12,919	$EI_{30} = -119.27 + 7.84$ (P)	0.9	Silva et al., 2010b
19° 13' 20"S	42° 29' 41"W	Belo Oriente	MG	3	280	1,223	8,670	$EI_{30} = 215.4\ (MFI)^{0.65}$	0.89	Silva et al., 2010b
19° 47' 55"S	42° 08' 51"W	Caratinga	MG	3	660	1,037	10,115	$EI_{30} = 321.63\ (MFI)^{0.48}$	0.86	Silva et al., 2010b
18° 33' 25"S	42° 32' 35"W	Peçanha	MG	3	890	1,100	9,013	$EI_{30} = -141.07 + 9.63$ (P)	0.9	Silva et al., 2010b
18° 40' 23"S	43° 04' 52"W	Sabinópolis	MG	3	760	1,078	8,670	$EI_{30} = 123.33\ (MFI)^{0.74}$	0.95	Silva et al., 2010b
19° 57' 26"S	43° 24' 60"W	Santa Bárbara	MG	3	810	1,272	9,145	$EI_{30} = 170.59\ (MFI)^{0.64}$	0.93	Silva et al., 2010b
18° 27' 19"S	43° 18' 16"W	Sto. Ant. Itambé	MG	3	720	1,411	15,280	$EI_{30} = 179.33\ (MFI)^{0.77}$	0.9	Silva et al., 2010b
18° 51' 87"S	42° 58' 29"W	Sto D. do Prata	MG	3	621	1,102	13,145	$EI_{30} = 114.42\ (MFI)^{0.81}$	0.86	Silva et al., 2010b
22° 6' 54"S	54° 33' 39"W	Dourados	MS	8	458	1,378	9,256	$EI_{30} = 73.464 + 56.562$ (MFI) $EI_{30} = 80.305\ (MFI)^{0.8966}$	0.80 0.88	Oliveira et al., 2011b
18° 18' 10"S	54° 26' 43"W	Coxim	MS	4	238	1,371	10,439	$EI_{30} = 247.35 + 41.036$ (MFI) $EI_{30} = 138.33\ (MFI)^{0.7431}$	0.90 0.91	Oliveira et al., 2011b
20° 15' 57"S	54° 18' 54"W	Campo Grande	MS	3	592	1,419	9,872	$EI_{30} = 171.40 + 42.173$ (MFI) $EI_{30} = 139.44\ (MFI)^{0.6784}$	0.78 0.91	Oliveira et al, 2011b
15° 37' 18"S	56° 06' 30"W	Cuiabá	MT	18	151	1,387	8,810	$EI_{30} = 109.412\ (MFI)^{0.744}$	0.91	Almeida et al., 2011a
16° 27' 0"S	54° 34' 12"W	Rondonopolis	MT	6	284	1,274	6,641	$EI_{30} = 133.2004291\ (MFI)^{0.5372499}$	0.90	Almeida et al., 2011b
16° 03' 0"S	57° 40' 48"W	Caceres	MT	7	118	1,191	5,056	$EI_{30} = 172.6326451\ (MFI)^{0.5245258}$	0.94	Almeida et al., 2011b
15° 39' 0"S	57° 29' 00"W	Caceres	MT	9	135	1,369	8,493	$EI_{30} = 56.115\ (MFI)^{0.9504}$	0.87	Morais et al., 1991
16° 02' 0"S	57° 16' 00"W	Caceres	MT	7	155	1,316	7,830	$EI_{30} = 36.849\ (MFI)^{1.0852}$	0.84	Morais et al., 1991
13° 33' 0"S	52° 15' 36"W	Canarana	MT	-	406	1,796	12,516	$EI_{30} = 317.397829\ (MFI)^{0.484654}$	0.86	Almeida et al., 2011c

Table 1. Continued.

Latitude	Longitude	City	States	Years	Altitude	Precipitation	R Factor	Equations	R^2	Authors
12° 17' 24"S	55° 17' 24"W	Vera	MT	-	379	2,259	15,965	$EI_{30} = 399.538719\ (MFI)^{0.458718}$	0.84	Almeida et al., 2011c
15° 50' 24"S	54° 23' 24"W	Poxoréo	MT	-	370	1,688	8,652	$EI_{30} = 272.865645\ (MFI)^{0.419164}$	0.66	Almeida et al., 2011c
13° 26' 24"S	56° 42' 36"W	São J. Rio Claro	MT	-	360	1,881	7,107	$EI_{30} = 147.262400\ (MFI)^{0.533025}$	0.83	Almeida et al., 2011c
8° 13' 42"S	49° 21' 58"W	Conc. Araguaia	PA	8	203	1,729	11,487	$EI_{30} = 321.5 + 36.2\ (MFI)$	0.89	Oliveira Jr, 1996
5° 24' 35"S	49° 06' 48"W	Marabá	PA	-	98	1,969	13,915	-	-	Oliveira Jr. et al., 1992
1° 04' 48"S	46° 47' 21"W	Bragança	PA	-	21	2,318	12,351	-	-	Oliveira Jr. et al., 1992
2° 15' 30"S	49° 31' 06"W	Cametá	PA	-	11	2,255	14,756	-	-	Oliveira Jr. et al., 1989
3° 47' 04"S	49° 42' 18"W	Tucuruí	PA	-	203	2,207	14,487	-	-	Oliveira Jr. et al., 1989
3° 01' 41"S	47° 21' 10"W	Paragominas	PA	-	140	1,954	13,251	-	-	Oliveira Jr. et al., 1989
1° 26' 37"S	48° 28' 30"W	Belem	PA	-	15	3,144	22,452	- $EI_{30} = 57.25 + 30.8\ (MFI)$	- 0.88	Oliveira Jr. et al., 1995
7° 58' 48"S	35° 8' 60"W	Olinda	PE	10	61	1,852	6,325	$EI_{30} = 69.24(MFI)^{0.75}$	0.87	Cantalice et al., 2009
8° 24' 4"S	35° 25' 54"W	Catende	PE	5	160	699	3,601	$EI_{30} = 57.32\ (MFI)^{0.618}$ $EI_{30} = 97.79 + 15\ (MFI)$	0.75 0.72	Cantalice et al., 2009
8° 0' 1"S	35° 10' 42"W	Gloria do Goitá	PE	10	153	956	3,212	$EI_{30} = 50.75\ (MFI)^{0.724}$	0.78	Cantalice et al., 2009
8° 17' 17"S	35° 58' 56"W	Caruaru	PE	9	540	501	1,909	$EI_{30} = 61.81\ (MFI)^{0.58}$	0.67	Cantalice et al., 2009
8° 11' 33"S	36° 4' 53"W	São Caetano	PE	11	650	500	1,672	$EI_{30} = 61.81\ (MFI)^{0.58}$	0.67	Cantalice et al., 2009
8° 20' 38"S	36° 25' 26"W	Belo Jardim	PE	7	610	628	2,862	$EI_{30} = 61.81(MFI)^{0.58}$ $EI_{30} = 73.34 + 23.18\ (MFI)$	0.67 0.94	Cantalice et al., 2009
7° 34' 12"S	40° 30' 02"W	Araripina	PE	9	630	719	2,860	$EI_{30} = 95.48\ (MFI)^{0.56}$ $EI_{30} = 73.34 + 23.18\ (MFI)$	0.82 0.94	Cantalice et al., 2009
8° 17' 1"S	39° 14' 7"W	Cabrobó	PE	9	336	446	2,518	$EI_{30} = 95.48\ (MFI)^{0.56}$ $EI_{30} = 73.34 + 23.18\ (MFI)$	0.82 0.94	Cantalice et al., 2009
7° 52' 57"S	40° 04' 49"W	Ouricuri	PE	11	450	580	2,538	$EI_{30} = 95.48(MFI)0.56$ $EI_{30} = 73.34 + 23.18\ (MFI)$	0.82 0.94	Cantalice et al., 2009
9° 23' 33"S	40° 30' 16"W	Petrolina	PE	8	370	438	3,480	$EI_{30} = 95.48\ (MFI)^{0.56}$ $EI_{30} = 73.34 + 23.18\ (MFI)$	0.82 0.94	Cantalice et al., 2009
8° 19' 16"S	37° 43' 26"W	Poço da Cruz	PE	8	470	498	3,159	$EI_{30} = 95.48\ (MFI)^{0.56}$	0.82	Cantalice et al., 2009
24° 15' 18"S	53° 20' 35"W	Oeste Paraná	PR	-	-	-	-	$EI_{30} = 182.86 + 56.21\ (MFI)$	-	Rufino et al., 1993

Table 1. Continued.

Latitude	Longitude	City	States	Years	Altitude	Precipitation	R Factor	Equations	R^2	Authors
26° 4' 21"S	53° 1' 31"W	Sudoeste Paraná	PR	-	-	-	-	EI_{30} = 144.86 + 55.20 (MFI)	-	Rufino et al., 1993
22° 28' 57"S	51° 11' 29"W	Norte Paraná	PR	-	-	-	-	EI_{30} = 216.31 + 41.30 (MFI)	-	Rufino et al., 1993
23° 13' 25"S	51° 16' 13"W	Noroeste Paraná	PR	-	-	-	-	EI_{30} = 164.12 + 39.44 (MFI)	-	Rufino et al., 1993
23° 26' 43"S	52° 1' 54"W	Centro Paraná	PR	-	-	-	-	EI_{30} = 191.79 + 48.40 (MFI)	-	Rufino et al., 1993
25° 30' 55"S	51° 27' 51"W	Centro S. Paraná	PR	-	-	-	-	EI_{30} = 107.52 + 46.89 (MFI)	-	Rufino et al., 1993
24° 24' 19"S	50° 15' 45"W	Centro L. Paraná	PR	-	-	-	-	EI_{30} = 93.29 + 41.20 (MFI)	-	Rufino et al., 1993
25° 13' 30"S	49° 8' 32"W	Leste Paraná	PR	-	-	-	-	EI_{30} = 33.26 + 40.71 (MFI)	-	Rufino et al., 1993
22° 10' 12"S	42° 19' 17"W	Nova Friburgo	RJ	5	857	1,063	5,431	EI_{30} = -67.99 + 33.86 (MFI)	0.85	Carvalho et al., 2005
22° 27' 30"S	43° 24' 39"W	Seropédica	RJ	7	33	1,118	5,472	EI_{30} = 64.87 + 38.14 (MFI)	0.82	Carvalho et al., 2005
22° 04' 04"S	43° 33' 30"W	Rio das Flores	RJ	5	400	1,028	4,118	EI_{30} = 112.54 + 20.70 (MFI)	0.82	Gonçalves et al., 2006
22° 13' 39"S	44° 03' 41"W	Valença	RJ	7	567	1,550	6,971	EI_{30} = 194.08 + 27.74 (MFI)	0.82	Gonçalves et al., 2006
23° 1' 48"S	44° 31' 12"W	Angra dos Reis	RJ	6	6	2,034	10,140	EI_{30} = 73.21+ 44.61 (MFI)	0.84	Gonçalves et al., 2006
21° 50' 24"S	44° 34' 48"W	Carmo	RJ	15	146	1,013	5,653	EI_{30} = 223.87 + 21.00 (MFI)	0.72	Gonçalves et al., 2006
22° 28' 48"S	43° 50' 24"W	Barra do Piraí	RJ	14	371	1,486	4,985	EI_{30} = 50.36 + 24.53 (MFI)	0.96	Gonçalves et al., 2006
22° 41' 60"S	43° 52' 48"W	Pirai	RJ	15	462	1,451	6,696	EI_{30} = 112.54 + 20.70 (MFI)	0.82	Gonçalves et al., 2006
22° 45' 0"S	44° 7' 12"W	Rio Claro	RJ	15	479	1,466	9,031	EI_{30} = 118.71 + 38.48 (MFI)	0.98	Gonçalves et al., 2006
22° 42' 36"S	42° 42' 0"W	Rio Bonito	RJ	16	40	1,387	5,289	EI_{30} = 38.48 + 35.13 (MFI)	0.81	Gonçalves et al., 2006
22° 34' 48"S	42° 56' 24"W	Magé	RJ	19	10	1,859	10,235	EI_{30} = 64.59 + 47.68 (MFI)	0.89	Gonçalves et al., 2006
22° 28' 48"S	42° 39' 36"W	Conc. Macabu	RJ	15	40	1,915	7,961	EI_{30} = 39.86 + 37.90 (MFI)	0.91	Gonçalves et al., 2006
22° 28' 48"S	43° 0' 0"W	Magé	RJ	16	640	3,006	15,806	EI_{30} = 146.28 + 46.37 (MFI)	0.70	Gonçalves et al., 2006
22° 51' 0"S	42° 32' 60"W	Saquarema	RJ	15	10	1,252	5,448	EI_{30} = -13.36 + 50.02 (MFI)	0.65	Gonçalves et al., 2006
22° 55' 12"S	43° 25' 12"W	Rio de Janeiro	RJ	17	40	1,280	4,439	EI_{30} = 3.89 + 37.76 (MFI)	0.79	Gonçalves et al., 2006
22° 57' 36"S	43° 16' 48"W	Rio de Janeiro	RJ	16	460	2,170	9,331	EI_{30} = -76.27 + 53.31 (MFI)	0.40	Gonçalves et al., 2006
22° 42' 38"S	43° 52' 41"W	Piraí	RJ	18	462	-	6,772	-	-	Machado et al., 2008

Table 1. Continued.

Latitude	Longitude	City	States	Years	Altitude	Precipitation	R Factor	Equations	R^2	Authors
30° 23' 0"S	56° 26' 0"W	Quaraí	RS	38	100	1,513	9,292	EI_{30} = -47.35 + 82.72 (MFI)	0.84	Bazzano et al., 2007
32° 01' 0"S	52° 09' 0"W	Rio Grande	RS	23	15	1,162	5,135	non-significant correlation	-	Bazzano et al., 2010
								EI_{30} = 99.646 + 63.874 (MFI)	0.77	
28° 39' 0"S	56° 0' 0"W	São Borja	RS	48	99	1,540	9,751	$EI_{30} = 55.564\ (MFI)^{1.1054}$	0.84	Cassol et al., 2008
30° 32' 0"S	52° 31' 0"W	Enc. do Sul	RS	31	420	1,279	5,534	non-significant correlation	-	Eltz et al., 2011
29° 45' 0"S	57° 05' 0"W	Uruguaiana	RS	29	74	1,171	8,875	EI_{30} = -96735 + 81.967 (MFI)	0.94	Hickmann et al., 2008
								EI_{30} = 330.86 + 34.54 (MFI)	0.40	
28° 33' 0"S	53° 54' 0"W	Ijuí	RS	31	448	1,667	8,825	$EI_{30} = 109.65\ (MFI)^{0.76}$	0.53	Cassol et al., 2007
								EI_{30} = 354.71 + 44.927 (MFI)	0.41	
27° 51' 0"S	54° 29' 0"W	Santa Rosa	RS	29	273	1,832	11,217	$EI_{30} = 118.52\ (MFI)^{0.8034}$	0.50	Mazurana et al., 2009
								EI_{30} = 238.585 + 22.626 (MFI)	0.50	
27° 24' 0"S	51° 12' 0"W	Campos Novos	SC	10	947	1,754	6,329	$EI_{30} = 59.265\ (MFI)^{1.087}$	0.86	Bertol, 1994
27° 49' 0"S	50° 20' 0"W	Lages	SC	10	953	1,549	5,790	-	-	Bertol et al.. 2002
22° 37' 0"S	52° 10' 0"W	Teod. Sampaio	SP	19	255	1,282	7,172	EI_{30} = 106.8183 + 46.9562 (MFI)	0.93	Colodro et al., 2002
22° 31' 12"S	47° 2' 40"W	Campinas	SP	22	670	1,280	6,738	$EI_{30} = 68.730\ (MFI)^{0.841}$	0.98	Lombardi Neto and Moldenhauer, 1992
23° 13' 0"S	49° 14' 0"W	Piraju	SP	23	571	1,482	7,074	$EI_{30} = 72.5488\ (MFI)^{0.8488}$	0.93	Roque et al., 2001
24° 17' 0"S	47° 57' 0"W	Sete Barras	SP	9	30	1,434	12,664	EI_{30} = 316.20 + 55.40 (MFI)	0.98	Silva et al., 2009b
24° 24' 0"S	47° 45' 0"W	Juquiá	SP	7	60	824	6,145	EI_{30} = 207.21 +40.65 (MFI)	0.90	Silva et al., 2009b
21° 16' 58"S	47° 0' 36"W	Mococa	SP	-	-	-	-	$EI_{30} = 111.173\ (MFI)^{0.691}$	0.98	Carvalho et al., 1991

Years = length of record, Altitude (m), P = average annual precipitation (mm), R = R factor (MJ mm ha^{-1} h^{-1} yr^{-1}), and (-) No available

States by region: North (Amazonas, AM and Pará, PA); Northeast (Ceará, CE and Pernambuco, PE); Central-weast (Mato Grosso do Sul, MS; Mato Grosso, MT and Goiás, GO); Southeast (Espírito Santo,ES; Minas Gerais, MG; Rio de Janeiro, RJ and São Paulo, SP) and South (Paraná, PR; Rio Grande do Sul, RS and Santa Catarina, SC).

The influence of the climate in the annual rainfall erosivity can be observed in Figure 2. The lower values are found in the northeast, in regions with climates hot arid steppe (BSh), and hot arid desert (BWh). In these regions, the average annual precipitation is below 800 mm. We found the highest annual erosivity values, such as those in the cities of Belem, PA and Tucurui, PA, with erosivity values of the 22,452 and 14,756 MJ mm ha^{-1} h^{-1} yr^{-1}, respectively. This region has an equatorial, humid (Af) and equatorial monsoonal (Am) climates, with average annual precipitation of the 2,300 mm and high intensity rainfall , thus resulting in high erosivity values.

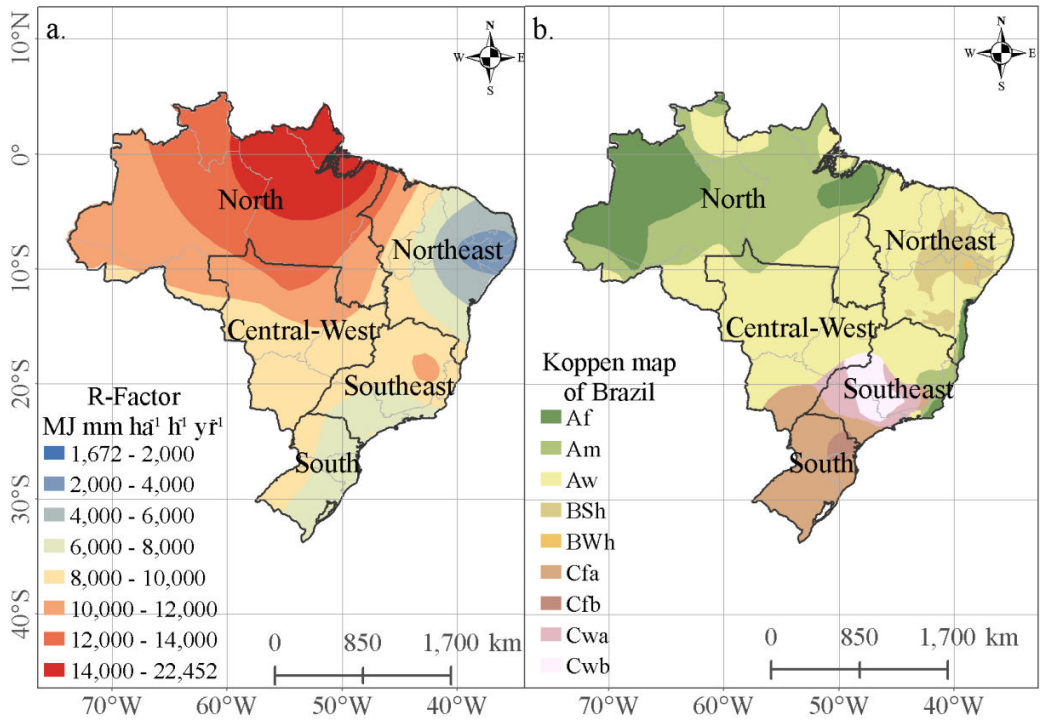

Figure 2. a. R-factor map of Brazil (an approximation). b. Koppen climate classification of Brazil. Where Af, equatorial, fully humid; Am, equatorial, monsoonal; Aw, equatorial, winter dry; BSh, hot arid steppe; BWh, hot arid desert; Cfa, humid, warm temperate, hot summer; Cfb, humid, warm temperate, warm summer; Cwa, winter dry, warm temperate, hot summer; Cwb, winter dry, warm temperate, warm summer.

The range of rainfall erosivity values of Brazil is similar the range observed in other tropical regions, and they are higher than the observed in temperate climate regions (Table 2). These higher erosivity values observed in the tropics are caused by the high amount of precipitation, intensity and kinetic energy of rain. The main rainfall generating mechanism in

most tropical regions is convection. As a result, the tropics receive more rain at higher intensities than the temperate regions, dominated by midlatitude cyclones (Hoyos et al., 2005).

Table 2. Range of rainfall erosivity values for several locations of the world.

Locate	Erosivity (MJ mm ha^{-1} $h^{-1}yr^{-1}$)	Source
Tropical sites		
Honduras	2,980 - 7,297	Mikhailova et al. (1997)
Peninsular Malaysia	9,000 - 14,000	Shamshad et al. (2008)
Colombian Andes	10,409 - 15,975	Hoyos et al. (2005)
El Salvador Republic	7,196 - 17,856	Silva et al. (2011)
Southeastern Nigeria	12,814 - 18,611	Obi and Salako (1995)
Brazil	1,672 - 22,452	Present paper
Australia's tropics	1,080 - 33,500	Yu (1998)
Temperate sites		
Slovenia	1,318 - 2,995	Mikos et al. (2006)
Mediterranean region	100 - 3,203	Diodato and Bellocchi (2010)
Northeastern Spain	40 - 4,500	Angulo-Martínez et al. (2009)
Switzerland	124- 5,611	Meusburger et al. (2011)
Korea	2,109 - 6,876	Lee and Heo (2011)
Central Chile	50 - 7,400	Bonilla and Vidal (2011)
United States	85 - 11,900	Renard and Freimund (1994)

The correlation between annual precipitation and erosivity ($r = 0.77$) was significant at the 0.05 level (Figure 3). However, the pattern of rainfall erosivity in Brazil cannot be explained only by annual precipitation. Several researchers found that high values of annual precipitation does not necessarily produce higher values of erosivity (Mello et al., 2007; Bazzano et al., 2010; Silva et al., 2010b; Oliveira et al., 2011b). In Brazil, the greatest erosivity values are caused by intense rainfall occurring in certain times of the year.

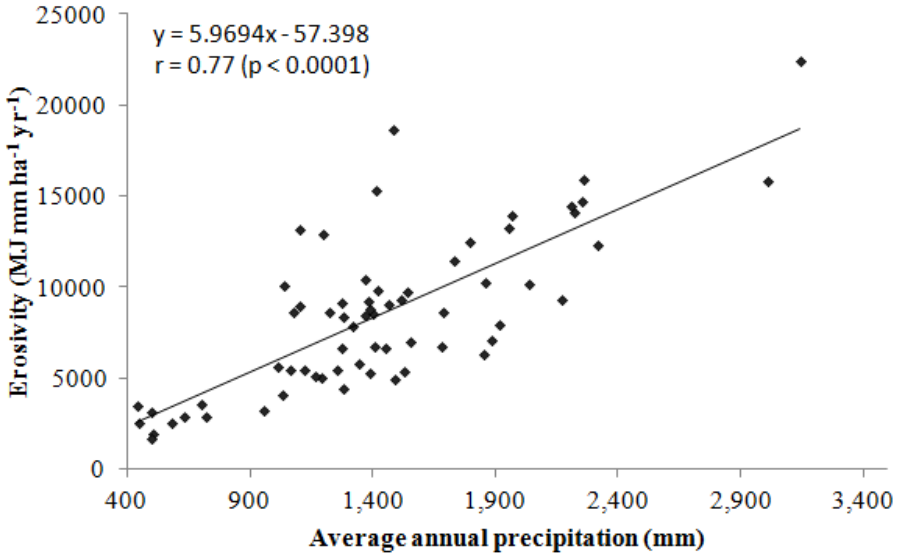

Figure 3. Correlation between annual erosivity and annual precipitation.

We found that there was a significant correlation between longitude (r = 0.36) and annual erosivity at the 0.05 level (Figure 4). Despite of the low value of the correlation coefficient, it is possible to verify the erosivity increase from east to west. It occurs mainly due to the low erosivity in the northeastern region and high in northwest region. We did not find significant correlation between latitude (r = 0.13) and annual erosivity at the 0.05 level.

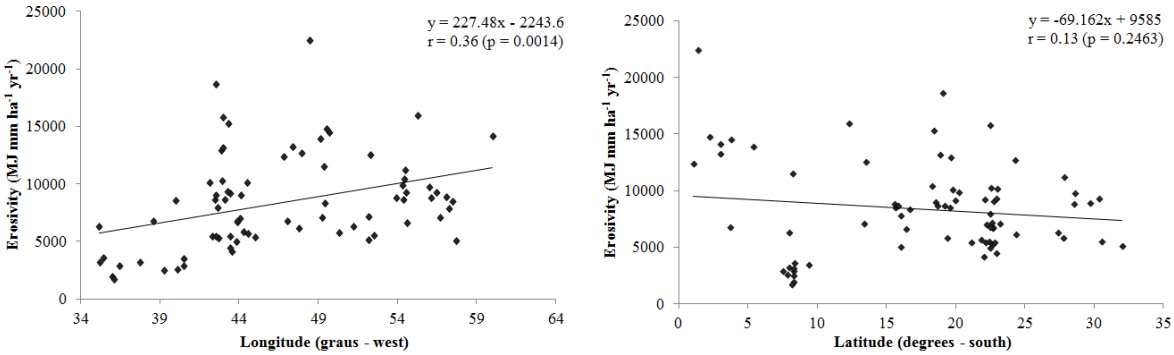

Figure 4. Correlation of the longitude and latitude with the annual erosivity.

According to classifications for the interpretation of the annual erosivity index of Brazil, we found that the erosivity rainfall values exceed 7,357 MJ mm ha^{-1} h^{-1} yr^{-1} (strong erosivity) in 52.6% of the data (Table 3). From this results we found that in Brazil there are several areas of water erosion risk, mainly southeastern and central-west regions. In these regions is occurring the

rapid expansion of sugar cane cultivation for production sugar and biofuel (Loarie et al., 2011). Thus, the knowledge of these areas with higher erosivity rainfall values is essential to assess the soil erosion risk and to support to soil and water conservation planning (Oliveira et al., 2011a).

Table 3. Classifications for the interpretation of the annual erosivity index of Brazil.

*Erosivity (MJ mm ha^{-1} h^{-1})	Erosivity class	Observed data (%)
$R \leq 2,452$	Low erosivity	2.6
$2,452 < R \leq 4,905$	Medium erosivity	13.2
$4,905 < R \leq 7,357$	Medium-strong erosivity	31.6
$7,357 < R \leq 9,810$	Strong erosivity	23.7
$R > 9,810$	Very strong erosivity	28.9

Source: *Carvalho (2008), modified to S.I. metric units according to Foster et al. (1981).

In Brazil, 73 equations correlate the rainfall erosivity index (EI_{30}) with the mean annual precipitation (P) or the modified Fournier index (MFI) (Table 1 and Figure 1). The equations presented in Table 1 can be used in areas that have no pluviographic rainfall data but that have similar climatic conditions. However, the equations cannot be extrapolated to a generalized form without underestimating or overestimating the erosivity values. Studies must be conducted on the local climate to determine which equation is best suited to the desired region.

Silva (2004) proposed the division of Brazil into eight homogeneous regions according to rainfall. A single equation was designated for each region to allow the rainfall erosivity for each month to be estimated from the rainfall coefficient. In this proposal, the same equation was applied to several states. We compare the R factor values presented in Table 1 with the results calculated by Silva (2004). We conclude that despite providing a significant contribution to the understanding of rainfall erosivity in Brazil, the generalization of these equations produces many errors (Figure 5). Therefore, the choice of equation to be used in different locations should be performed with caution and should be based on local climate studies.

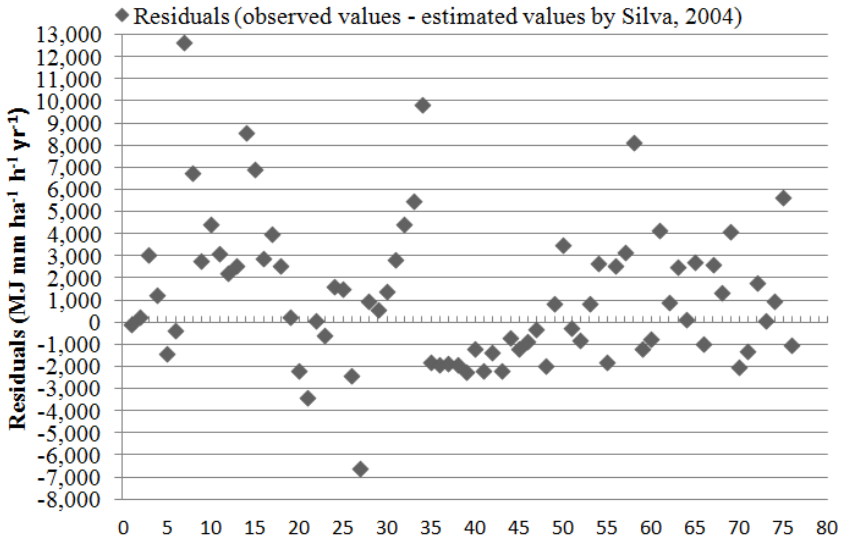

Figure 5. Residual values of erosivity (observed values – estimated values by Silva, 2004).

Before Silva (2004), there were few studies on rainfall erosivity and few equations adjusted for the regions of Brazil. Since 2005, the number of publications on rainfall erosivity has increased significantly (Figure 6). From the information presented in this present paper, new studies can be developed to map rainfall erosivity for the entire country. The equations that we found (Table 1) can be used with pluviometric data available for all Brazil by Agência Nacional de Águas (ANA) on website (http://hidroweb.ana.gov.br/). Furthermore, we recommend the inclusion of the rainfall return periods and the climate change in future studies.

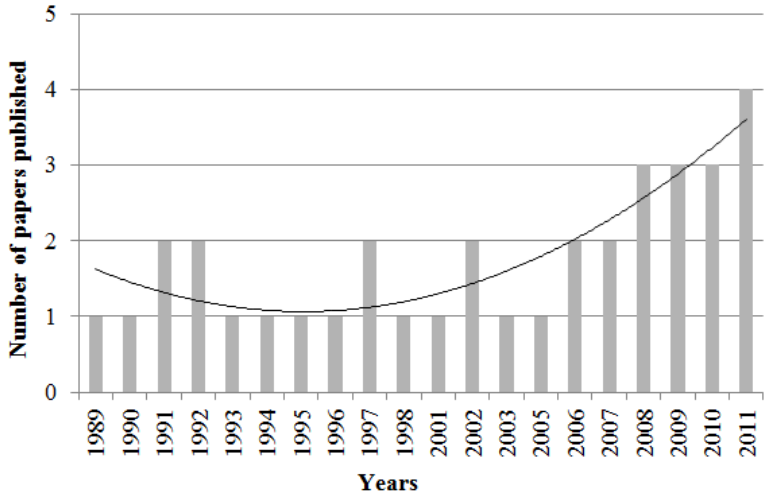

Figure 6. Number of papers published per year.

In addition, the computational advances and the consolidation of the use of methodologies such as artificial neural networks and geostatistics techniques to obtain the rainfall erosivity can help to develop a more precise study for Brazil. These studies are fundamental for achieving effective environmental planning and may assist in analyzing vulnerability, risk forecasting and allocating financial resources for farmers in risk areas (Oliveira et al., 2011a; Rodrigues et al., 2011).

We found that 85% of the analyzed studies were developed using a historical series of less than 20 years, so only 15% of these studies used the minimum series required for RUSLE calculation (Renard et al., 1997) (Figure 7).

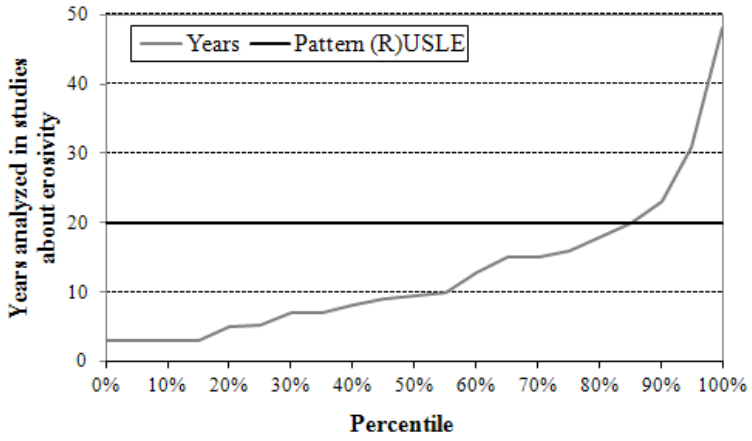

Figure 7. Years of data analyzed in studies on erosivity.

In Brazil, in general, hydrological and meteorological information is scarce or difficult to access (Montebeller et al., 2007; Oliveira et al., 2011b). This is a constant problem in the development of research models in this country. We recommend maintaining the existing stations and establishing new stations because this is the only way to obtain more realistic results. In addition, the development of new regional and global models and new scientific discoveries are needed to obtain basic data for the calibration and validation of the results.

4 Conclusions

The annual rainfall erosivity in Brazil, based on our review, ranges from 1672 to 22,452 MJ mm ha^{-1} h^{-1} yr^{-1}. The lowest values are found in the northeastern region, and the highest values are found in the north region and the southeastern region. The rainfall erosivity tends to increase from east to west, particularly in the northern part of the country.

We conclude that there are few studies on erosivity in Brazil and that these studies are concentrated in the south and southeast regions. In addition, the number of years of data used in most of those studies was less than the recommended standard for the application of RUSLE (20 years of data).

The regression equations of rainfall erosivity cannot be extrapolated to a generalized form without underestimating or overestimating the erosivity values. Studies must be conducted on the local climate to determine which equation is best suited to the desired region.

In Brazil, there are 73 regression equations to calculate erosivity. These equations can be useful to map rainfall erosivity for the entire country. To this end, techniques already established in Brazil may be used for the interpolation of rainfall erosivity, such as geostatistics and artificial neural networks.

5 Acknowledgments

The authors thank the Fundação de Amparo à Pesquisa do Estado de São Paulo - FAPESP (Processes 2010/18788-5 and 2011/14273-3) and the Conselho Nacional de Desenvolvimento Científico e Tecnológico - CNPq (Process 470846/2011-9) whose financial support made the development of the present study feasible.

6 References

Almeida C.O.S., Amorin R.S.S., Eltz F.L.F., Couto E.G., & Jordani S.A. (2011c). Erosividade em quatro municípios do estado de Mato Grosso e suas correlações com dados pluviométricos. *Proc. XXXIII Congresso Brasileiro de Ciência do Solo*, Uberlândia, 1-4.

Almeida C.O.S., Amorin R.S.S., Eltz F.L.F., Couto E.G., & Pelissari, A.L. (2011b). Correlação do índice de erosividade (EI 30) com o coeficiente de chuvas em Cáceres (MT) e Rondonópolis (MT). Proc. *XXXIII Congresso Brasileiro de Ciência do Solo*, Uberlândia, 1-4.

Almeida, C. O. S., Amorim, R. S. S., Couto, E. G., Eltz, F. L. F., & Borges, L. E. C. (2011a). Erosive potential of rainfall in Cuiabá, MT: distribution and correlation with rainfall. *Revista Brasileira de Engenharia Agrícola E Ambiental*, *15*(2), 178–184. doi:10.1590/S1415-43662011000200011

Alves Sobrinho, T., Pertussatti, C. A., Rebucci, L. C. S., & Oliveira, P. T. S. (2011). Estimativa da erosividade em local das chuvas, utilizando redes neurais artificiais. *Ambiente E Agua - An Interdisciplinary Journal of Applied Science*, *6*(2), 246–254. doi:10.4136/ambi-agua.197

Angulo-Martínez, M., & Beguería, S. (2009). Estimating rainfall erosivity from daily precipitation records: A comparison among methods using data from the Ebro Basin (NE Spain). *Journal of Hydrology*, *379*(1-2), 111–121. doi:10.1016/j.jhydrol.2009.09.051

Angulo-Martínez, M., López-Vicente, M., Vicente-Serrano, S. M., & Beguería, S. (2009). Mapping rainfall erosivity at a regional scale: a comparison of interpolation methods in the Ebro Basin (NE Spain). *Hydrology and Earth System Sciences*, *13*(10), 1907–1920. doi:10.5194/hess-13-1907-2009

Arnoldus, H.M.J. (1977). *Methodology used to determine the maximum potential average annual soil loss due to sheet and rill erosion in Morocco*. FAO Soils Bulletin 34, 39-51.

Bazzano, M. G. P., Eltz, F. L. F., & Cassol, E. A. (2007). Erosividade, coeficiente de chuva, padrões e período de retorno das chuvas de Quaraí, RS. *Revista Brasileira de Ciência Do Solo*, *31*(5), 1205–1217. doi:10.1590/S0100-06832007000500036

Bazzano, M. G. P., Eltz, F. L. F., & Cassol, E. A. (2010). Erosividade e características hidrológicas das chuvas de Rio Grande (RS). *Revista Brasileira de Ciência Do Solo*, *34*(1), 235–244. doi:10.1590/S0100-06832010000100024

Bertol I. (1994). Evaluation for rain erosivity for Campos Novos (SC) during the 1981-1990 period. *Pesquisa Agropecuária Brasileira*, 29, 1453-1458.

Bertol, I., Leite, D., Engel, F. L., Cogo, N. P., & González, A. P. (2007). Erodibilidade de um nitossolo háplico alumínico determinada em condições de campo. *Revista Brasileira de Ciência Do Solo*, *31*(3), 541–549. doi:10.1590/S0100-06832007000300014

Bertol, I., Schick, J., Batistela, O., Leite, D., Visentin, D., & Cogo, N. P. (2002). Erosividade das chuvas e sua distribuição entre 1989 e 1998 no município de Lages (SC). *Revista Brasileira de Ciência Do Solo*, *26*(2), 455–464. doi:10.1590/S0100-06832002000200019

Bertol, I., Zoldan Junior, W. A., Fabian, E. L., Zavaschi, E., Pegoraro, R., & González, A. P. (2008). Efeito de escarificação e da erosividade de chuvas sobre algumas variáveis de valores de erosão hídrica em sistemas de manejo de um nitossolo háplico. *Revista Brasileira de Ciência Do Solo*, *32*(2), 747–757. doi:10.1590/S0100-06832008000200029

Bonilla, C. A., & Vidal, K. L. (2011). Rainfall erosivity in Central Chile. *Journal of Hydrology*, *410*(1-2), 126–133. doi:10.1016/j.jhydrol.2011.09.022

Cantalice, J. R., Bezerra, S. A., Figueira, S. B., Inácio, E. S., & Silva, M. D. (2009). LINHAS ISOEROSIVAS DO ESTADO DE PERNAMBUCO - 1ª APROXIMAÇÃO. *Revista Caatinga*, *22*(2). Retrieved from http://periodicos.ufersa.edu.br/revistas/index.php/sistema/article/view/205

Carvalho M.P.E., Lombardi Neto F., Vasques Filho J., & Catâneo A. (1991). Correlação entre o índice de erosividade EI_{30} médio mensal e o coeficiente de chuva do município de Mococa, SP. *Científica - Revista de Agronomia*, 19, 1-7.

Carvalho, D. F. de, Montebeller, C. A., Franco, E. M., Valcarcel, R., & Bertol, I. (2005). Padrões de precipitação e índices de erosividade para as chuvas de Seropédica e Nova Friburgo, RJ. *Revista Brasileira de Engenharia Agrícola E Ambiental*, *9*(1), 7–14. doi:10.1590/S1415-43662005000100002

Carvalho, N.O. (2008). *Hidrossedimentologia Prática*. 2ª Ed., Interciência, Rio da Janeiro, Brazil. 599p.

Cassol, E. A., Eltz, F. L. F., Martins, D., Lemos, A. M. de, Lima, V. S. de, & Bueno, A. C. (2008). Erosividade, padrões hidrológicos, período de retorno e probabilidade de ocorrência das chuvas em São Borja, RS. *Revista Brasileira de Ciência Do Solo*, *32*(3), 1239–1251. doi:10.1590/S0100-06832008000300032

Cassol, E. A., Martins, D., Foletto Eltz, F. L., de Lima, V. S., & Camara Bueno, A. (2007). Erosividade e padrões hidrológicos das chuvas de Ijuí (RS) no período de 1963 a 1993. *Revista Brasileira de Agrometeorologia*, *15*(3), p. 220–231.

Cerdá, A. (1997). Rainfall drop size distribution in the Western Mediterranean basin, València, Spain. *CATENA*, *30*(2-3), 169–182. doi:10.1016/S0341-8162(97)00019-2

Colodro, G., Carvalho, M. P., Roque, C. G., & Prado, R. M. (2002). Erosividade da chuva: distribuição e correlação com a precipitação pluviométrica de Teodoro Sampaio (SP).

Revista Brasileira de Ciência Do Solo, *26*(3), 809–818. doi:10.1590/S0100-06832002000300027

Dias, A. S., & Silva, J. R. C. (2003). A erosividade das chuvas em Fortaleza (CE): I - distribuição, probabilidade de ocorrência e período de retorno - 1ª aproximação. *Revista Brasileira de Ciência Do Solo*, *27*(2), 335–345. doi:10.1590/S0100-06832003000200013

Diodato, N., & Bellocchi, G. (2010). MedREM, a rainfall erosivity model for the Mediterranean region. *Journal of Hydrology*, *387*(1-2), 119–127. doi:10.1016/j.jhydrol.2010.04.003

Eltz, F. L. F., Cassol, E. A., & Pascotini, P. B. (2011). Potencial erosivo e características das chuvas de Encruzilhada do Sul, RS. *Revista Brasileira de Engenharia Agrícola E Ambiental*, *15*(4), 331–337. doi:10.1590/S1415-43662011000400001

Evangelista A.W.P., Carvalho L.G., Dantas A.A.A., & Bernadino D.T. (2006). Rainfall erosive potential in Lavras, Minas Gerais state, Brazil: distribution, occurrence probability and return period. *Irriga*, 11, 1-11.

Ferro, V. (2010). Deducing the USLE mathematical structure by dimensional analysis and self-similarity theory. *Biosystems Engineering*, *106*(2), 216–220. doi:10.1016/j.biosystemseng.2010.03.006

Foster, G.R., McCool, D.K., Renard, K.G., Moldenhauer, W. C. (1981). Conversion of the universal soil loss equation to SI metric units. *Journal of Soil & Water Conservation*, *36*(6), 355–359.

Gonçalves, F. A., Silva, D. D. da, Pruski, F. F., Carvalho, D. F. de, & Cruz, E. S. da. (2006). Índices e espacialização da erosividade das chuvas para o Estado do Rio de Janeiro. *Revista Brasileira de Engenharia Agrícola E Ambiental*, *10*(2), 269–276. doi:10.1590/S1415-43662006000200004

Goovaerts, P. (1999). Using elevation to aid the geostatistical mapping of rainfall erosivity. *CATENA*, *34*(3-4), 227–242. doi:10.1016/S0341-8162(98)00116-7

Hickmann, C., Eltz, F. L. F., Cassol, E. A., & Cogo, C. M. (2008). Erosividade das chuvas em Uruguaiana, RS, determinada pelo índice EI30, com base no período de 1963 a 1991. *Revista Brasileira de Ciência Do Solo*, *32*(2), 825–831. doi:10.1590/S0100-06832008000200036

Hoyos, N., Waylen, P. R., & Jaramillo, Á. (2005). Seasonal and spatial patterns of erosivity in a tropical watershed of the Colombian Andes. *Journal of Hydrology*, *314*(1-4), 177–191. doi:10.1016/j.jhydrol.2005.03.014

Hudson N. (1971). *Soil Conservation*. Cornell University Press, Ithaca.

Kinnell, P. I. A. (2010). Event soil loss, runoff and the Universal Soil Loss Equation family of models: A review. *Journal of Hydrology*, *385*(1-4), 384–397. doi:10.1016/j.jhydrol.2010.01.024

Lal, R. (1976). Soil erosion on Alfisols in Western Nigeria. *Geoderma*, *16*(5), 389–401. doi:10.1016/0016-7061(76)90003-3

Lee, J.-H., & Heo, J.-H. (2011). Evaluation of estimation methods for rainfall erosivity based on annual precipitation in Korea. *Journal of Hydrology*, *409*(1-2), 30–48. doi:10.1016/j.jhydrol.2011.07.031

Licznar P. (2005). Artificial neural networks use for rainfall-runoff erosivity factor estimation. *EJPAU*. 8, #4.

Loarie, S. R., Lobell, D. B., Asner, G. P., Mu, Q., & Field, C. B. (2011). Direct impacts on local climate of sugar-cane expansion in Brazil. *Nature Climate Change*, *1*(2), 105–109. doi:10.1038/nclimate1067

Lombardi Neto, F. (1977). *Rainfall erosivity - its distribution and relationship with soil loss at Campinas, Brazil*. West Lafayette: Purdue Univ., 53p. M.Sc. Thesis.

Lombardi Neto, F., & Moldenhauer, W. C. (1992). Erosividade da chuva: sua distribuição e relação com as perdas de solo em Campinas (SP). *Bragantia*, *51*(2). doi:10.1590/S0006-87051992000200009

Machado, R. L., Carvalho, D. F. de, Costa, J. R., Oliveira Neto, D. H. de, & Pinto, M. F. (2008). Análise da erosividade das chuvas associada aos padrões de precipitação pluvial na região de Ribeirão das Lajes (RJ). *Revista Brasileira de Ciência Do Solo*, *32*(5), 2113–2123. doi:10.1590/S0100-06832008000500032

Marques, J. J. G. S. M., Alvarenga, R. C., Curi, N., Santana, D. P., & Silva, M. L. N. (1997). Rainfall erosivity indices, soil losses and erodibility factor for two soils from the cerrado region - first approximation. *Revista Brasileira de Ciencia do Solo (Brazil)*. Retrieved from http://agris.fao.org/agris-search/search.do?recordID=BR1998001270

Martins, S. G., Avanzi, J. C., Silva, M. L. N., Curi, N., Norton, L. D., & Fonseca, S. (2010). Rainfall erosivity and rainfall return period in the experimental watershed of Aracruz, in the coastal plain of Espirito Santo, Brazil. *Revista Brasileira de Ciência Do Solo*, *34*(3), 999–1004. doi:10.1590/S0100-06832010000300042

Mazurana, J., Cassol, E. A., Santos, L. C. dos, Eltz, F. L. F., & Bueno, A. C. (2009). Erosividade, padrões hidrológicos e período de retorno das chuvas erosivas de Santa Rosa (RS). *Revista Brasileira de Engenharia Agrícola E Ambiental*, *13*, 975–983. doi:10.1590/S1415-43662009000700021

Mello, C. R. de, Sá, M. A. C. de, Curi, N., Mello, J. M. de, Viola, M. R., & Silva, A. M. da. (2007). Erosividade mensal e anual da chuva no Estado de Minas Gerais. *Pesquisa Agropecuária Brasileira*, *42*(4), 537–545. doi:10.1590/S0100-204X2007000400012

Meusburger, K., Steel, A., Panagos, P., Montanarella, L., & Alewell, C. (2011). Spatial and temporal variability of rainfall erosivity factor for Switzerland. *Hydrology and Earth System Sciences Discussions*, *8*(5), 8291–8314. doi:10.5194/hessd-8-8291-2011

Mikhailova, E. A., Bryant, R. B., Schwager, S. J., & Smith, S. D. (1997). Predicting Rainfall Erosivity in Honduras. *Soil Science Society of America Journal*, *61*(1), 273. doi:10.2136/sssaj1997.03615995006100010039x

Mikoš, M., JošT, D., & PetkovšEk, G. (2006). Rainfall and runoff erosivity in the alpine climate of north Slovenia: a comparison of different estimation methods. *Hydrological Sciences Journal*, *51*(1), 115–126. doi:10.1623/hysj.51.1.115

Moehansyah, H., Maheshwari, B. L., & Armstrong, J. (2004). Field Evaluation of Selected Soil Erosion Models for Catchment Management in Indonesia. *Biosystems Engineering*, *88*(4), 491–506. doi:10.1016/j.biosystemseng.2004.04.013

Montebeller, C. A., Ceddia, M. B., Carvalho, D. F. de, Vieira, S. R., & Franco, E. M. (2007). Variabilidade espacial do potencial erosivo das chuvas no Estado do Rio de Janeiro. *Engenharia Agrícola*, *27*(2), 426–435. doi:10.1590/S0100-69162007000300011

Morais L.F.B., Silva V., Naschenveng C., Hardoin P.C., Almeida J.E.L., Weber O.L.S., Boel E., & Durigon V. (1991). Índice EI_{30} e sua relação com o coeficiente de chuva do sudoeste do Mato Grosso. *Revista Brasileira de Ciência Do Solo*, 15, 339-344.

Moreira, M. C., Cecílio, R. A., Pinto, F. de A. de C., & Pruski, F. F. (2006). Desenvolvimento e análise de uma rede neural artificial para estimativa da erosividade da chuva para o Estado de São Paulo. *Revista Brasileira de Ciência Do Solo*, *30*(6). doi:10.1590/S0100-06832006000600016

Moreira, M. C., Pruski, F. F., Oliveira, T. E. C. de, Pinto, F. de A. de C., & Silva, D. D. da. (2008). NetErosividade MG: erosividade da chuva em Minas Gerais. *Revista Brasileira de Ciência Do Solo*, *32*(3), 1349–1353. doi:10.1590/S0100-06832008000300042

Morgan, R. P. . (2001). A simple approach to soil loss prediction: a revised Morgan–Morgan–Finney model. *CATENA*, *44*(4), 305–322. doi:10.1016/S0341-8162(00)00171-5

Morgan, R. P. C., Quinton, J. N., Smith, R. E., Govers, G., Poesen, J. W. A., Auerswald, K., … Styczen, M. E. (1998). The European Soil Erosion Model (EUROSEM): a dynamic approach for predicting sediment transport from fields and small catchments. *Earth Surface Processes and Landforms*, *23*(6), 527–544. doi:10.1002/(SICI)1096-9837(199806)23:6<527::AID-ESP868>3.0.CO;2-5

Nearing, M. A., Foster, G. R., Lane, L. J., & Finkner, S. C. (1989). A process-based soil erosion model for USDA-Water Erosion Prediction Project technology. *Trans. ASAE*, *32*(5), 1587–1593.

Nearing, M. A., Jetten, V., Baffaut, C., Cerdan, O., Couturier, A., Hernandez, M., … van Oost, K. (2005). Modeling response of soil erosion and runoff to changes in precipitation and cover. *CATENA*, *61*(2-3), 131–154. doi:10.1016/j.catena.2005.03.007

Obi, M. E., & Salako, F. K. (1995). Rainfall parameters influencing erosivity in southeastern Nigeria. *CATENA*, *24*(4), 275–287. doi:10.1016/0341-8162(95)00024-5

Oliveira Jr R.C. (1996). *Índice de Erosividade das Chuvas na Região de Conceicão do Araguaia, Pará*. Belém: EMBRAPA-CPATU, 20p.

Oliveira Jr R.C., & Medina B.F. (1990). A erosividade das chuvas em Manaus (AM). *Revista Brasileira de Ciência Do Solo*, 14, 235-239.

Oliveira Jr R.C., Chaves R.S., & Melo A.S. (1995). A erosividade das chuvas em Belém. Boletim da FCAP, Belém, 22, 35-52.

Oliveira Jr R.C., Lopes O.M.N., & Melo A.S. (1989). A erosividade das chuvas em Cametá, Tucuruí e Paragominas, no Estado do Pará. Boletim da FCAP, Belém, 18, 2-26.

Oliveira Jr RC., Rodrigues T.E., & Melo, A.S. (1992). A erosividade das chuvas nos municípios de Bragança e Marabá no Estado do Pará. Boletim do Museu Paraense Emílio Goeldi Série Ciências da Terra, Belém, 4, 45-57.

Oliveira, P. T. S., Rodrigues, D. B. B., Sobrinho, T. A., Carvalho, D. F. de, & Panachuki, E. (2012). Spatial variability of the rainfall erosive potential in the State of Mato Grosso do Sul, Brazil. *Engenharia Agrícola*, *32*(1), 69–79. doi:10.1590/S0100-69162012000100008

Oliveira, P. T. S., Sobrinho, T. A., Rodrigues, D. B. B., & Panachuki, E. (2011). Erosion Risk Mapping Applied to Environmental Zoning. *Water Resources Management*, *25*(3), 1021–1036. doi:10.1007/s11269-010-9739-0

Renard K.G., Foster G.R., Weesies G.A., Mccool D.K., & Yoder D.C. (1997). *Predicting soil erosion by water: A guide to conservation planning with the Revised Universal Soil Loss Equation (RUSLE)*. Washington: USDA Agriculture Handbook, n.703.

Renard, K. G., & Freimund, J. R. (1994). Using monthly precipitation data to estimate the R-factor in the revised USLE. *Journal of Hydrology*, *157*(1-4), 287–306. doi:10.1016/0022-1694(94)90110-4

Risse, L. M., Nearing, M. A., Laflen, J. M., & Nicks, A. D. (1993). Error assessment in the universal soil loss equation. *Soil Science Society of America Journal*, *57*(3), 825–833.

Rodrigues, D. B. B., Sobrinho, T. A., Oliveira, P. T. S. de, & Panachuki, E. (2011). Nova abordagem sobre o modelo Brasileiro de serviços ambientais. *Revista Brasileira de Ciência Do Solo*, *35*(3), 1037–1045. doi:10.1590/S0100-06832011000300037

Roque C.G., Carvalho M.P., & Prado R.M. (2001). Rainfall erosivity factor at Piraju (SP), Brazil: distribution, probability of occurrence, return period and correlation with rainfall coefficient. *Revista Brasileira de Ciência Do Solo*, 25, 147-156.

Rufino R.L., Biscaia R.C.M., & Merten G.H. (1993). Determinação do potencial erosivo da chuva do estado do Paraná através da pluviometria: terceira aproximação. *Revista Brasileira de Ciência Do Solo*, 17, 439-444.

Shamshad, A., Azhari, M. N., Isa, M. H., Hussin, W. M. A. W., & Parida, B. P. (2008). Development of an appropriate procedure for estimation of RUSLE EI30 index and preparation of erosivity maps for Pulau Penang in Peninsular Malaysia. *CATENA*, *72*(3), 423–432. doi:10.1016/j.catena.2007.08.002

Silva M.L.N., Freitas P.L., Blancaneaux P., & Curi N. (1997). Rainfall erosivity indices in the Goiânia region, Goiás state, Brazil. *Pesquisa Agropecuária Brasileira*, 32, 977-985.

Silva R.B., Iori P., & Silva F.A.M. (2009b). Proposition and compare of equations to estimate the rainfall erosivity in two cities of São Paulo state. *Irriga*, 14, 533-547.

Silva, A. M. (2004). Rainfall erosivity map for Brazil. *CATENA*, *57*(3), 251–259. doi:10.1016/j.catena.2003.11.006

Silva, A. M. da, Silva, M. L. N., Curi, N., Avanzi, J. C., & Ferreira, M. M. (2009a). Erosividade da chuva e erodibilidade de Cambissolo e Latossolo na região de Lavras, sul de Minas Gerais. *Revista Brasileira de Ciência Do Solo*, *33*(6), 1811–1820. doi:10.1590/S0100-06832009000600029

Silva, A. M., Wiecheteck, M., & Zuercher, B. W. (2011). Spatial Assessment of Indices for Characterizing the Erosive Force of Rainfall in El Salvador Republic. *Environmental Engineering Science*, *28*(4), 309–316. doi:10.1089/ees.2010.0296

Silva, M. A. da, Silva, M. L. N., Curi, N., Santos, G. R. dos, Marques, J. J. G. de S. e M., Menezes, M. D. de, & Leite, F. P. (2010b). Avaliação e espacialização da erosividade da chuva no Vale do Rio Doce, região centro-leste do Estado de Minas Gerais. *Revista Brasileira de Ciência Do Solo*, *34*(4), 1029–1039. doi:10.1590/S0100-06832010000400003

Silva, R. B., Iori, P., Armesto, C., & Bendini, H. N. (2010a). Assessing Rainfall Erosivity with Artificial Neural Networks for the Ribeira Valley, Brazil. *International Journal of Agronomy*, *2010*, 1–7. doi:10.1155/2010/365249

Vieira, S. R., & Lombardi Neto, F. (1995). Variabilidade espacial do potencial de erosão das chuvas do Estado de São Paulo. *Bragantia*, *54*(2), 405–412. doi:10.1590/S0006-87051995000200019

Wagner C.S., & Massambini O. (1988). Análise da relação intensidade de chuva: energia de Wischmeier & Smith e sua aplicabilidade à região de São Paulo. *Revista Brasileira de Ciência Do Solo*, 12, 197-203.

Wischmeier W.H., & Smith D.D. (1978). *Predicting rainfall erosion losses*. A guide to conservation planning. Washington: USDA Agriculture Handbook, n. 537, 58p.

Wischmeier, W. H. (1959). A rainfall erosion index for a universal soil-loss equation. *Soil Science Society of America Journal*, *23*(3), 246–249.

Woolhiser D.A., Smith R.E., & Goodrich D.C. (1990). *KINEROS: A Kinematic Runoff and Erosion Model: Documentation and User Manual*. U.S. Department of Agriculture, Agricultural Research Service, ARS-77, 130p.

Yu, B. (1998). Rainfall erosivity and its estimation for Australia's tropics. *Australian Journal of Soil Research*, *36*(1), 143. doi:10.1071/S97025

Zhang, Y.-G., Nearing, M. A., Zhang, X.-C., Xie, Y., & Wei, H. (2010). Projected rainfall erosivity changes under climate change from multimodel and multiscenario projections in Northeast China. *Journal of Hydrology*, *384*(1-2), 97–106. doi:10.1016/j.jhydrol.2010.01.013

CHAPTER 2

THE WATER BALANCE COMPONENTS OF UNDISTURBED TROPICAL WOODLANDS IN THE BRAZILIAN CERRADO

Oliveira, Paulo Tarso S., Wendland, E., Nearing, Mark A., Scott, Russel L., Rosolem, R., and da Rocha, Humberto R. (2014). The water balance components of undisturbed tropical woodlands in the Brazilian Cerrado. *Hydrology and Earth System Sciences Discussions,* 11, 12987-13018, doi:10.5194/hessd-11-12987-2014. (Impact factor, 2013: 3.642; Qualis CAPES: A1)

Abstract

Deforestation of the Brazilian Cerrado region has caused major changes in hydrological processes. These changes in water balance components are still poorly understood, but are important for making land management decisions in this region. To understand pre-deforestation conditions, we determined the main components of the water balance for an undisturbed tropical woodland classified as "cerrado sensu stricto denso". We developed an empirical model to estimate actual evapotranspiration (ET) by using flux tower measurements and, vegetation conditions inferred from the enhanced vegetation index and reference evapotranspiration. Canopy interception, throughfall, stemflow, surface runoff, and water table level were assessed from ground measurements. We used data from two Cerrado sites, "Pé de Gigante" - PDG and "Instituto Arruda Botelho" - IAB. Flux tower data from the PDG site collected from 2001 to 2003 was used to develop the empirical model to estimate ET. The other hydrological processes were measured at the field scale between 2011 and 2014 in the IAB site. The empirical model showed significant agreement (R^2=0.73) with observed ET at the daily scale. The average values of estimated ET at the IAB site ranged from 1.91 to 2.60 mm d^{-1} for the dry and wet season, respectively. Canopy interception ranged from 4 to 20% and stemflow values were approximately 1% of gross precipitation. The average runoff coefficient was less than 1%, while Cerrado deforestation has the potential to increase that amount up to 20 fold. As relatively little excess water runs off (either by surface water or groundwater) the water storage may be estimated by the difference between precipitation and evapotranspiration. Our results provide benchmark values of water balance dynamics in the undisturbed Cerrado that will be useful to evaluate past and future land cover and land use changes for this region.

Keywords: evapotranspiration, throughfall, stemflow, runoff, savanna, deforestation, water balance, canopy interception.

1 Introduction

As global demand for agricultural products such as food and fuel grows to unprecedented levels, the supply of available land continues to decrease, which is acting as a major driver of cropland and pasture expansion across much of the developing world (Gibbs et al., 2010; Macedo et al., 2012). Vast areas of forest and savannas in Brazil have been converted into farmland, and there is little evidence that agricultural expansion will decrease, mainly because Brazil holds a great potential for further agricultural expansion in the twenty-first century (Lapola et al., 2014).

The Amazon rainforest and Brazilian savanna (Cerrado) are the most threatened biomes in Brazil (Marris, 2005). However, the high suitability of the Cerrado topography and soils for mechanized agriculture, the small number and total extent of protected areas, the lack of a deforestation monitoring program, and the pressure resulting from decreasing deforestation in Amazonia indicates that the Cerrado will continue to be the main region of farmland expansion in Brazil (Lapola et al., 2014). In fact, Soares-Filho et al. (2014) reported that the Cerrado is the most coveted biome for agribusiness expansion in Brazil, given its 40 ± 3 Mha of land that could be legally deforested.

The Brazilian Cerrado, one of the richest ecoregions in the world in terms of the biodiversity (Myers et al., 2000), covers an area of 2 million km^2 (~22% of the total area of Brazil), however, areas of remaining native vegetation represent only 51% of this total (IBAMA/MMA/UNDP, 2011). In addition to being an important ecological and agricultural region for Brazil, the Cerrado is crucial to water resource dynamics of the country, and includes portions of 10 of Brazil's 12 hydrographic regions (Oliveira et al., 2014). Further, the largest hydroelectric plants (comprising 80% of the Brazilian energy) are on rivers in the Cerrado. As savannas and forests have been associated with shifts in the location, intensity and timing of rainfall events, lengthening of the dry season and changed streamflow (Davidson et al., 2012; Spracklen et al., 2012; Wohl et al., 2012), it is clear that land cover and land use change promoted by the cropland and pasture expansion in this region have the potential to affect the ecosystems services and several important economic sectors of Brazil, such as agriculture, energy production and water supply.

Although all indications are that farmland expansion will continue in the Cerrado and that the land cover and land use will promote changes in water balance dynamics, few studies have been developed to investigate the hydrological processes at the field scale (plots or hillslope). In general, the studies on the Cerrado hydroclimatic variability have been done on large areas (Loraie et al., 2011; Davidson et al., 2012; Oliveira et al., 2014). Evapotranspiration (ET) has been the most intensively studied component of the water balance at the field scale, and is based on eddy covariance methods (Vourlitis et al., 2002; Santos et al., 2003; da Rocha et al., 2009; Giambelluca et al., 2009) or by the water balance in the soil (Oliveira et al., 2005; Garcia-Montiel et al., 2008). However, other water balance components such as rainfall interception, canopy throughfall, stemflow, surface runoff, infiltration, percolation, subsurface flow and groundwater recharge are poorly understood in the Cerrado.

To understand pre-deforestation conditions, we determined the main components of the water balance for an undisturbed tropical woodland classified as "cerrado sensu stricto denso". We developed an empirical model to estimate actual evapotranspiration (ET) by using flux tower measurements and, vegetation conditions inferred from the enhanced vegetation index (EVI) and reference crop evapotranspiration (ETo). Canopy interception, throughfall, stemflow, and surface runoff were assessed from ground measurements. We used data from two cerrado sites, "Pé de Gigante" - PDG and "Instituto Arruda Botelho" - IAB. Flux tower data from the PDG site collected from 2001 to 2003 was used to develop the empirical model to estimate ET. The other hydrological processes were measured at the field scale between 2011 and 2014 in the IAB site.

2 Materials and Methods

2.1 Cerrado area

We developed this study using data from two cerrado sites, "Pé de Gigante" - PDG and "Instituto Arruda Botelho" - IAB, referenced throughout the text as PDG and IAB, respectively. Both sites are located in the State of São Paulo and have a distance of approximately 60 km

between them (Fig. 1). The physiognomy of PDG and IAB sites was classified as "cerrado sensu stricto denso", which is also known as cerrado woodland, and has a characteristic arborous cover of 50% to 70% and trees with heights of 5 to 8 m (Furley 1999). Similar soil characteristics, hydroclimatology and phenology were found between these sites (details given below).

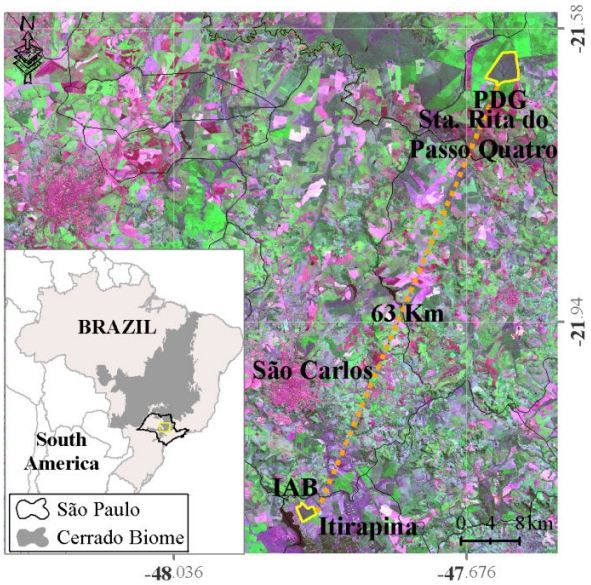

Figure 1. Location of study areas.

'Pé de Gigante - PDG' site

We used field measurements collected at the PDG flux tower located on a contiguous 1060 ha undisturbed woodland in the municipality of Santa Rita do Passo Quatro, São Paulo State (latitude 21°37' S, longitude 47°39' W, elevation:~ 700 m). According to the Köppen climate classification system, the climate in this area is Cwa humid subtropical, with a dry winter (April to September) and hot and rainy summer (October to March). The average annual precipitation and temperature are 1478 mm and 21.1 ºC, respectively. The soil is classified in the Brazilian Soil Classification System (SiBCS) as Ortic Quartzarenic Neosol (RQo) with less than 15% clay. Net radiation (Rn), latent heat (LE), sensible heat (H) fluxes and ancillary meteorological data were measured at a height of 21 m and recorded every half-hour from January 2001 to December 2003. Details about the equipment and measurement procedures used are provided by da Rocha et al. (2002, 2009).

'Instituto Arruda Botelho - IAB' site

The IAB site is a 300 ha, undisturbed woodland located in the municipality of Itirapina, São Paulo State (latitude 22°10' S, longitude 47°52' W, elevation: 780 m). The absolute density of trees was of 15,278 individuals per hectare, with a Shannon diversity index of 4.03 (Reys 2008), which are similar to characteristics reported at the PDG site (Fidelis and Godoy, 2003). The climate in the IAB site is similar to that for the PDG (Cwa subtropical), with an average annual precipitation of 1506 mm and temperature of 20.8 ºC. The soil is also classified as Ortic Quartzarenic Neosol with sandy texture in the entire profile (85.7% sand, 1.7% silt, and 12.6% clay), and soil bulk density of 1.7 g cm^{-3}. We installed a 11 m instrumental platform to measure basic above-canopy meteorological and soil variables (Table 1). A datalogger (Campbell CR1000, Logan UT, USA) sampled the weather station and soil data every 15 s and recorded averages on a 10 min basis.

Table 1. Data collected at the IAB site.

Variable description	**Sensor**	**Height or depth (m)**
Temperature and relative humidity	Psychrometer HC2S3	9
Wind speed and direction anemometer	Anemometer RM Young 05103-5	10
Net radiation	NR-LITE2	10
Global solar radiation	LiCor 200X	10
Precipitation	Texas TB4	10
Atmospheric pressure	Barometer Vaisala CS106	2
Soil moisture	EnviroScan SENTEK	0.10, 0.50, 0.70, 1.00, 1.50

2.2 Modeling ET

In Brazil, there are a few flux tower sites in native cerrado vegetation. These sites were located in the States of São Paulo ("Pé de Gigante - PDG", da Rocha et al., 2002 and 2009), Brasilia ("Instituto Brasileiro de Geografia e Estatistica - IBGE" ecological reserve, Giambelluca et al., 2009; and "Reserva Ecologica de Aguas Emendadas", Miranda et al., 1997), and Mato Grosso (municipality of Sinop, a transitional Amazonia–Cerrado fores, Vourlitis et al., 2002).

There is a lack of information about ET in other Cerrado regions. To fill this gap, some authors have combined vegetation indices (VI) from the remote sensing data with ground measures of ET (usually flux tower) to spatially extrapolate ET measurements over nearby regions with few or no ground data. This process consists in the use of ground measurements of ET from flux towers set in natural ecosystems to develop a best-fit equation between ET, satellite-derived VIs, ancillary remote sensing data, and ground meteorological data (Glenn et al., 2010, 2011). Such an approach has been successfully applied to determine ET in natural ecosystems such as: riparian zones (Scott et al., 2008), shrublands (Nagler et al., 2007), rangeland and native prairie (Wang et al., 2007) temperate grassland, boreal forest, tundra (Mu et al., 2009) and Amazon rainforest (Joarez et al., 2008).

VIs are a ratio derived from the red and near-infrared spectral reflectance, and are strongly correlated with physiological processes that depend on photosynthetically active radiation absorbed by a canopy, such as transpiration and photosynthesis (Glenn et al., 2010). Normalized Difference Vegetation Index (NDVI) and the Enhanced Vegetation Index (EVI) from the Moderate Resolution Imaging Spectrometer (MODIS) on the NASA Terra satellite are VIs widely used in environmental studies. However, previous studies have shown that EVI can better capture canopy structural variation, seasonal vegetation variation, land cover variation, and biophysical variation for high biomass vegetation (Huete et al. 2002; Joarez et al., 2008). In addition, EVI has been a better predictor of ET than NDVI (Nagler et al., 2005a, b; Glenn et al., 2007; Wang et al., 2007).

We developed an empirical relationship between ET from the PDG flux tower, MODIS Enhanced Vegetation Index (EVI) and reference crop evapotranspiration (ETo) following the approach used by Nagler et al. (2013):

$$ET = ETo\ [\ a\ (1 - e^{(-bEVI)}) - c] \qquad (1)$$

where *a, b* and *c* are fitting coefficients and $(1 - e^{(-bEVI)})$ is derived from the Beer-Lambert Law modified to predict absorption of light by a canopy. The coefficient *c* accounts for the fact that EVI is not zero at zero ET since bare soil has a low but positive EVI (Nagler et al., 2004, 2013).

Daily average ET values from the PDG flux tower were computed by first filling the gaps in the 1-hour data that were due to sensor malfunctions or bad measurements. Gaps were filled using 1-hour averages of photosynthetically active radiation (PAR) and a 14-day look-up tables of ET values averaged over 100 micromoles m^{-2} s^{-1} intervals (Falge et al., 2001). Then we computed daily ET averages over every 16 days to be in sync with the 16-day EVI data. We used EVI data provided by the MODIS product MOD13Q1 (http://daac.ornl.gov/MODIS/). These data are provided by National Aeronautics and Space Administration (NASA) as atmospherically and radiometrically corrected 16-day composite images with a 250 m spatial resolution. We obtained the MODIS EVI pixel centered on the flux tower. ETo was computed daily according to the FAO-56 method (Allen et al., 1998) and then averaged over 16 days.

We used the parameter optimization tool Genetic Algorithm from the Matlab (Mathworks, Natick, MA, USA) Global Optimization Toolbox global to fit the Eq. 1 incorporating the time series of measured ET, EVI and ETo for 2001 to 2003. This process consisted in minimizing the sum of squared differences between the ET observed from eddy covariance and estimated by Eq. 1:

$$function = \sum_{i=1}^{n} [ET(i)obs - ET(i)sim]^2 \quad (2)$$

where *ET(i)obs* is the observed ET and *ET(i)sim* is modeled ET at time (i).

For model validation, we calibrated the model using 2001 and 2002 data and then predicted ET for 2003. After this validation process we fitted the Eq. 1 again, but now considering the full time series available. The coefficient of determination (R^2), standard deviation of differences between observed and estimated ET (*SD*), root mean square (*RMSE*) and the Student's t-test with a 95% confidence level were used to evaluate the significance of the linear relationship between the observed and estimated ET.

2.3 Hydrological processes measured in the IAB site

2.3.1 Canopy interception

Canopy interception (CI) was computed as the difference between the gross precipitation (P_g) and the net precipitation (P_n), where P_g is the total precipitation that fell at the top of the canopy and P_n is computed as the sum of two components: throughfall (TF) and stemflow (SF):

$$CI = P_g - P_n = P_g - (TF + SF) \quad (3)$$

We measured the P_g from an automated tipping bucket rain gauge (model TB4) located above the canopy at 10 m height (Table 1). TF was obtained from 15 automated tipping bucket rain gauges (Davis Instruments, Hayward, CA) distributed below the cerrado canopy and randomly relocated every month during the wet season (Fig. 2a). Each rain gauge was installed considering an influence area of 10 x 10 m. SF was measured on 12 trees using a plastic hose wrapped around the trees trunks, sealed with neutral silicone sealant, and a covered bucket to store the water (Fig. 2b). Selected trees to be monitored were divided into two groups considering the diameter at breast height (DBH). Therefore, we monitored 7 trees with 5 cm < DBH < 20 cm and 5 trees with DBH > 20 cm. The volume of water in each SF collector was measured after each rainfall event that generated stemflow, totaling 42 SF measurements during the study period. The volume of water measured from each sample tree was expressed as an equivalent volume per m^2 of basal area, and then this value was multiplied by the site basal area (27.75 m^2 ha^{-1}) to compute stemflow in mm (Dezzeo and Chacón, 2006 and MacJannet et al., 2007). We measured P_g, TF and SF from September 2012 to July 2014.

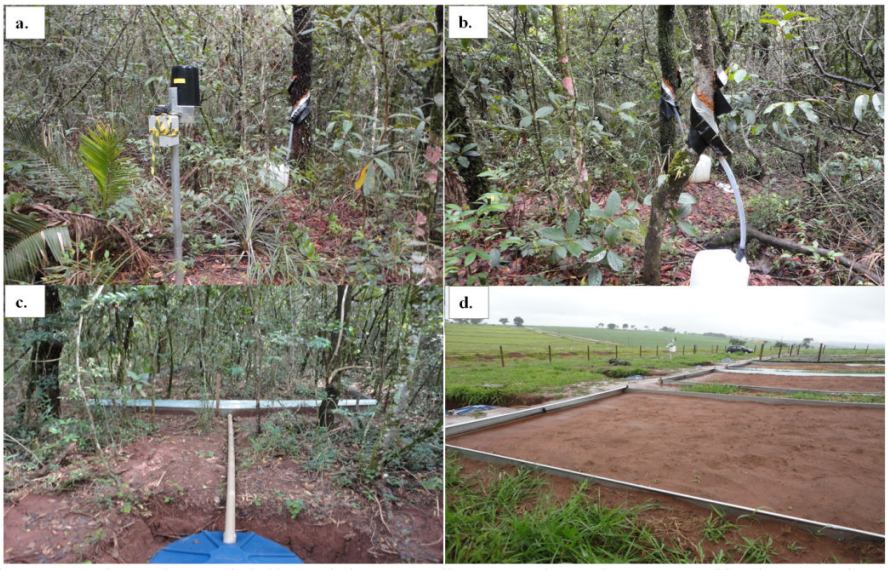

Figure 2. Collectors of a. throughfall and b. stemflow, and surface runoff plots under undisturbed c. cerrado and d. bare soil.

2.3.2 Surface runoff

Surface runoff was measured from 100 m^2 experimental plots of 5 m width and 20 m length from January 2012 to July 2014. To evaluate the cover influence on the surface runoff, experimental plots were installed under native vegetation and bare soil with steepness of approximately 0.09 m m^{-1}. Each treatment had three replications and plots on bare soil were located about 1 km from the plots under undisturbed cerrado (Fig. 2c, d). The boundaries of the plots were made using galvanized sheet placed 30 cm above the soil and into the soil to a depth of 30 cm. Surface runoff was collected in storage tanks at the end of each plot. Plots under bare soil were built with three storage tanks with 310 liters capacity each and two splitters of one seventh, i.e. one seventh were collected in the second tank and one forty ninth in the third tank. In the plots under cerrado vegetation only one storage tank with a capacity of 310 liters for each plot was used to collect runoff and soil loss because of the expected lower runoff amounts from those plots.

Surface runoff was measured for each erosive rain event under the undisturbed cerrado and bare soil. Periods of rainfall were considered to be isolated events when they were separated by

periods of precipitation between 0 (no rain) and 1.0 mm for at least 6 h, and were classified as erosive events when 6.0 mm of rain fell within 15 min or 10.0 mm of rain fell over a longer time period (Oliveira et al., 2013). We used this approach because in general only erosive rainfall has promoted surface runoff in the study area. A total of 65 erosive rainfall events were evaluated during the study period.

2.3.3 Groundwater recharge

The water table level was monitored from December 2011 to July 2014 from a well with 42 m in depth installed in the undisturbed cerrado. Water-table fluctuation data were measured daily from a pressure sensor (Mini-Diver model DI501, Schlumberger Limited, Houston, USA).

2.3.4 Water balance at the IAB site

We evaluated the water balance components in the IAB site at the daily, monthly and annual scale from January 2012 to March 2014 (Eq. 4). We used measured data of precipitation, surface runoff, and direct recharge. Evapotranspiration was estimated using the fitted equation from the EVI and reference evapotranspiration data.

$$\frac{dS}{dt} = P - ET - Q - R \quad (4)$$

where S is the water storage change with time, P is precipitation, ET is evapotranspiration, Q is runoff, and R groundwater recharge.

3 Results and Discussion

3.1 Modeling ET

The daily average (± standard deviation) reference evapotranspiration (ETo), measured evapotranspiration (ET), and EVI in the PDG site were 4.56 ± 0.73 mm d^{-1}, 2.31 ± 0.87 mm d^{-1}, and 0.41 ± 0.09, respectively. We found a significant correlation between observed ET and EVI with a correlation coefficient of 0.75 ($p < 0.0001$). EVI showed similar seasonality that was observed for the ET and ETo during wet and dry seasons (Fig. 3). The average ET and EVI values for the wet season were 2.81 ± 0.57 mm d^{-1} and 0.48 ± 0.05, and for the dry season 1.70 ± 0.70 mm d^{-1} and 0.33 ± 0.05, respectively.

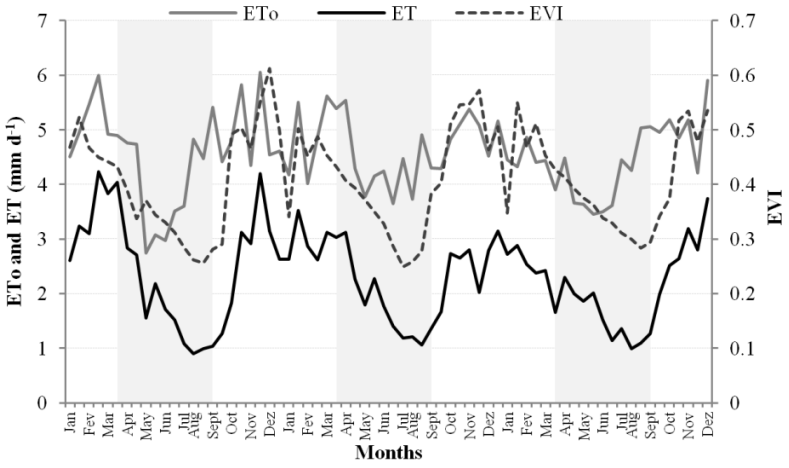

Figure 3. Seasonality of enhanced vegetation index (EVI), reference evapotranspiration (ETo) and observed actual evapotranspiration (ET) data from 2001 through 2003 at the PDG site. The grey shaded bar shows the dry season.

The fitted equation considering the periods of calibration, validation and full time series at 16-day averages showed good results in the ET estimates, with a coefficient of determination (R^2) greater than 0.70 and standard deviation of differences between observed and estimated ET (SD) and root mean square (RMSE) less than 0.50 mm d^{-1} and 21%, respectively (Table 2). The final form of the fitted equation was:

$$ET = ETo\ [\ 10.36\ (1 - e^{(-12.31EVI)}) - 9.74] \quad (5)$$

Table 2. Model calibration and validation results reported as the coefficient of determination (R^2), standard deviation of differences (SD), and root mean square errors (RMSE) for 16-day averages.

Time series	R^2	SD (mm day^{-1})	RMSE (%)
Calibration, 2001-2002	0.71	0.50	20.92
Validation, 2003	0.83	0.33	15.69
Full time series, 2001-2003	0.73	0.45	19.53

The modeled values of ET estimated for the full period, wet and dry seasons (2.30 ± 0.76 mm d^{-1}, 2.81 ± 0.31 mm d^{-1}, and 1.69 ± 0.60 mm d^{-1}, respectively) were not significantly different (p = 0.05) from the observed values of ET during the same period. Furthermore, we found better values of R^2, SD, and RMSE of 0.78, 0.16 mm month^{-1}, and 17.07% at the monthly scale. The annual average ET observed and estimated for the three years studied (2001-2003) were 822mm yr^{-1} and 820 mm yr^{-1}, respectively, with an RMSE of 6.12%. Juarez et al. (2008) used EVI and net radiation to estimate ET for four flux towers in Amazon rain forest and found values of R^2 ranging from 0.31 to 0.80 at a monthly scale. Observed ET between 2000 and 2002 from the PDG site was compared previously by Ruhoff et al. (2013) with the ET estimated from the product MOD16 (Mu et al., 2011). The authors found values of R^2 = 0.61 and RMSE = 0.46 mm d^{-1}, which were not as good as for the present study results. In a review paper about ET estimation in natural ecosystems using vegetation index methods, Glenn et al. (2010) reported values for different temporal scales ranging from 0.45 to 0.95 for the R^2 and of 10 to 30% for the RMSE. They concluded that the uncertainty associated with remote sensing estimates of ET is constrained by the accuracy of the ground measurements, which for the flux tower data are on the order of 10 to 30%. Hence, the values of SD and RMSE reported in the present study are within the error bounds of the likely ground measurement errors. Our findings indicate that the fitted equation may be used to compute ET at daily, monthly and annual scales.

3.2 Canopy interception, throughfall, and stemflow

The gross precipitation (P_g) in the IAB site during the 23 month study period was 1929 mm, where 78% of this total occurred from October through March (wet season). We found similar values of 766 mm and 734 mm for the two wet seasons studied, 2012-2013 and 2013-2014. There were also a significant number of rainfall events in the "dry" season of May, June and September with a total of 429 mm (Fig. 4a). The sum of throughfall (TF) was 1566 mm, which corresponded to 81.2% of P_g. Individual wet season TF values were 81.9 and 82.3% of P_g while total dry season P_g was 74.8%. The coefficient of determination between P_g and TF was 0.99 ($p < 0.0001$) over the 253 rainfall days (Fig. 4b). Stemflow values (by 42 events) ranged from 0.3 to 2.7% with an average of 1.1% of P_g. The greatest values of SF were found in the beginning of the wet season (October and November) and the smallest values occurred in the middle of the wet season (January and February). This suggests that there is an influence of condition of trees trunks (dry and wet) and canopy dynamic in the stemflow. Furthermore, we found greater values of SF in the trees with 5 cm < DBH < 20 cm (1.6% of P_g) than the trees with DBH > 20 cm (0.4% of P_g), which is consistent with results reported by Bäse et al. (2012) for the transitional Amazonia–Cerrado forest.

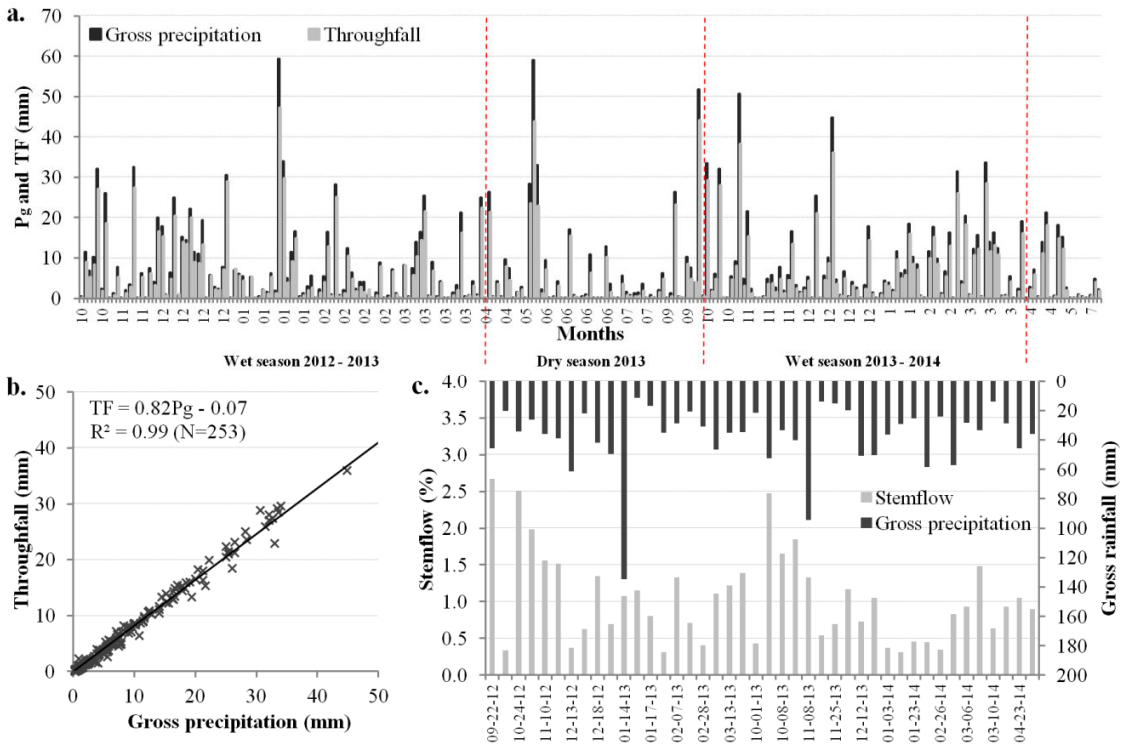

Figure 4. a. Gross precipitation and throughfall for each rain event measured from October, 2012 through July, 2014. Dotted lines in red show the beginning and the end of dry seasons (April through September). b. Scatter plot of throughfall against gross precipitation. c. Gross precipitation and stemflow measured from September 2012 through May 2014.

We found only three previous studies about interception process in the Brazilian Cerrado. The values reported in the literature for TF and SF, ranged from 80 to 95% of P_g. and <1 to 2.4% of P_g, respectively (Table 3). In the present study the canopy interception (CI) was 17.7% of P_g. Therefore, considering our findings and previous studies presented in Table 3 we can suggest that CI in the undisturbed cerrado ranges from 4 to 20% of P_g. However, future studies are necessary to understand the influence of physiognomies of the Cerrado in the CI processes. This region is large and complex and varies from grassland to savanna to forest (Furley, 1999; Ferreira and Huete, 2004). In addition, other characteristics such as conditions trees trunks (crooked and twisted), stand structure, canopy cover, rainfall features, and the litter interception should be better studied in specific studies of rainfall interception processes.

Table 3. Previous studies of throughfall (TF) and stemflow (SF) in the Brazilian Cerrado. Percentages denote percent of total rainfall.

Location	Land cover	TF (%)	SF (%)	Source
Agudos, São Paulo Satate	"cerradão"	72.7	-	Lima and Nicolielo, 1983
Uberlândia, São Paulo Satate	"cerrado sensu stricto"	89.0	< 1	Lilienfein and Wilcke, 2004
Assis, São Paulo Satate	"cerrado sensu stricto"	95.0	0.7	Honda, 2013
Assis, São Paulo Satate	"cerrado sensu stricto denso"	89.0	1.5	Honda, 2013
Assis, São Paulo Satate	"cerradão"	80.0	2.4	Honda, 2013
Itirapina, São Paulo Satate	"cerrado sensu stricto denso"	81.2	1.1	Present study

3.3 Cerrado water balance

The measured annual precipitation at the IAB site was 1248 mm, 1195 mm, 421 mm for 2012, 2013 and January through July of 2014, respectively. We measured 65 rainfall events that generated surface runoff during the study. The runoff coefficient for individual rainfall events (total runoff divided by total rainfall) ranged from 0.003 to 0.860 with an average value and standard deviation of 0.197 ± 0.179 in the bare soil plots. The highest values were found for larger, more intense rainfall events, or in periods with several consecutive rainfall events, which induced high soil moisture contents and consequently greater runoff generation. Moreover, the runoff coefficient found for the bare soil plots (~20%) indicates that the soil in the study area (sandy soil) has a high infiltration capacity. Runoff coefficients ranged from 0.001 to 0.030 with an average of less than 1% (0.005 ± 0.005) in the plots under undisturbed cerrado. Youlton (2013) studied in two hydrological years (2011-12 and 2012-13) the surface runoff using plots installed in the same experimental area as the present study and found values of 3.6 to 5.1% and 2.0 to 5.0% for the runoff coefficient under pasture and sugarcane, respectively. Cogo et al. (2003) reported values of runoff coefficient for soybeans and oat ranging from 2.0 to 4.0% depending to the soil tillage and management. Pasture, sugarcane and soybeans are the main cover types that have been used to replace the undisturbed cerrado lands (Loarie et al., 2011; Lapola et al., 2014). Therefore our results indicate that the cerrado deforestation has the potential to increase surface runoff around 5 fold when the cerrado is replaced for pasture and croplands and up to 20 fold for bare soil conditions.

Infiltration was calculated after subtracting interception (without accounting for the litter interception) and surface runoff from the gross precipitation. Thereby we found that 79% of gross rainfall infiltrated into the soil. Fig. 5 shows the amount of infiltration and the volumetric water content (VWC) up to 1.5 m in depth. We found a rapid increase in the VWC as a function of infiltration, indicating that the sandy soil found in the IAB site promoted fast infiltration, mainly in the first meter depth of the soil profile. The VWC ranged from 0.08 to 0.23 m^3 m^{-3} and 0.08 to 0.17 m^3 m^{-3} for 0.1 and 1.5 m soil depths, respectively. However, it is important to note that the root zone for trees in the cerrado is usually deep (more than 10 m in depth) and limited by the water table level (Oliveira et al, 2005; Garcia-Montiel et al., 2008; Villalobos-Vega et al., 2014). Therefore, the 1.5 m soil profile is not representative for evaluating the water use by vegetation, but is useful to evaluate the response for rainfall events and evaporative processes. Oliveira et al. (2005) concluded that the water stored in deep soil layers (1 to 4 m) provides approximately 75% of the total water used for an undisturbed cerrado classified as "cerrado sensu stricto denso", the class that includes the IAB and PDG sites.

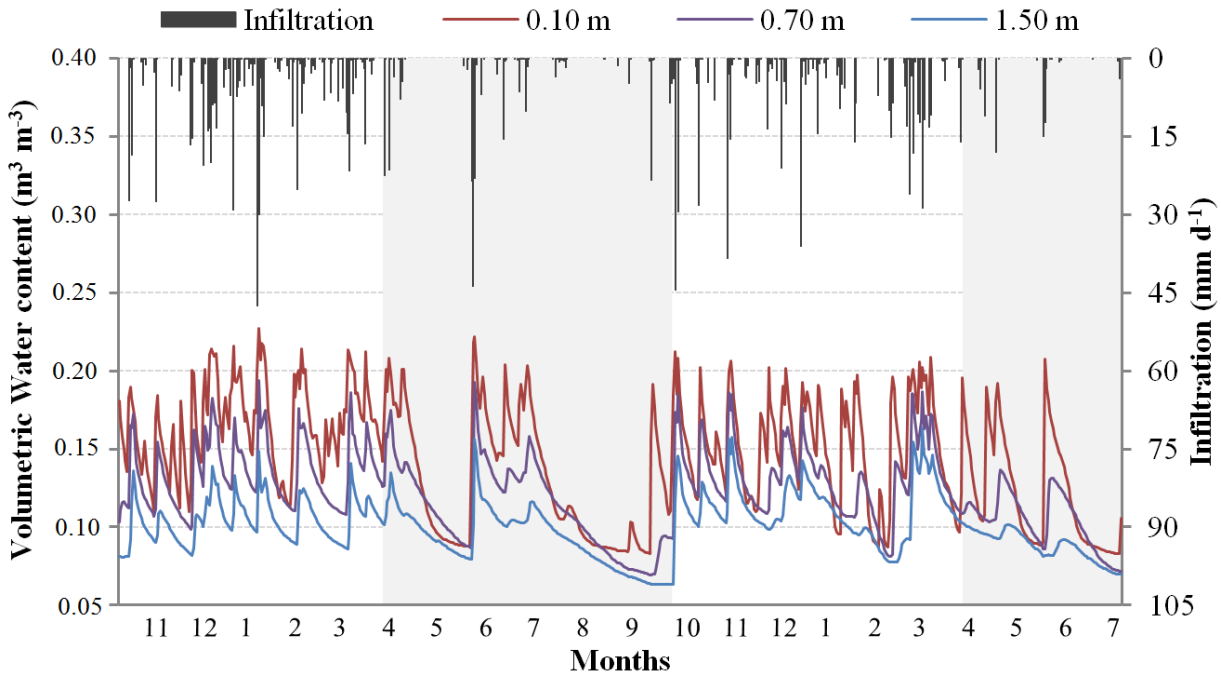

Figure 5. Estimated infiltration and volumetric water content measured at the depth of 0.10 m, 0.70 m, and 1.50 m. Data were collected from October 2012 through July 2014. The grey shaded bar shows the dry season.

The amount of water infiltrated into the soil was not enough to elevate the water table level in the well during the study period, from December 2011 to July 2014. This happened because the water table in the monitored well was approximately 35 m deep. In other words, there is a large distance from the soil surface to the water table, and the amount of water that eventually reached the saturated zone was not enough to cause a change in the water table level. The first study about the influence of groundwater dynamics in the undisturbed cerrado was conducted by Villalobos-Vega et al., (2014) from 11 monitored wells with water tables ranging from 0.18 to 15.56 m. The authors found little water table change in regions with deep water table (up to 15.56 m), and in some wells the recharge water took up to 5 months to reach the groundwater table. They also concluded that water table depth has a strong influence on variations in tree density and diversity, i.e. regions with deep water tables such as the IAB site (35 m) tend to exhibit greater tree abundance and diversity than sites with shallow water table. Therefore, the infiltrated water in the present study was likely either extracted and transpired by the vegetation, drained by lateral subsurface flow (not measured in this studied, but probably small due to the flat topography of the site) or stored in the vadose zone.

Groundwater recharge is also affected by land use and land cover change (Scanlon et al., 2005; Dawes et al., 2012). We found that the undisturbed cerrado tends to provide more infiltration than areas covered with pasture and cropland. On the other hand, the cerrado vegetation has signficant canopy interception and evapotrasnpiration that result in little groundwater recharge as compared to pasture and cropland. Using 23 monitoring wells distributed in a watershed located 5 km away from the IAB site, Wendland et al. (2007) showed that the groundwater recharge varies with the land cover. The authors reported values of annual recharge and water table depth, respectively, ranging from 145 to 703 mm yr^{-1} (5 to16 m) in pasture, 324–694 mm yr^{-1} (9 to 22 m) in orange citrus, and 37–48 mm yr^{-1} (21 m) in eucalyptus forests. Therefore, cerrado deforestation has the potential to change groundwater recharge dynamics.

The average values of actual evapotranspiration (ET) estimated by Eq. 5 for the IAB cerrado site for the full period, wet and dry seasons (2.30 ± 0.67 mm d^{-1}, 2.60 ± 0.38 mm d^{-1}, and 1.91 ± 0.60 mm d^{-1}, respectively) were similar to that observed in the PDG site. The annual average ET estimated for the two years studied (2012-2013) was 823 mm yr^{-1}, which also is consistent with that found by Giambelluca et al. (2009) of 823 mm yr^{-1} and the PDG site of 822

mm yr^{-1}. Given that surface runoff was less than 1% of precipitation and groundwater recharge and subsurface lateral flow was likely small, vadose zone water storage is basically the difference between precipitation and evapotranspiration (Fig. 6).

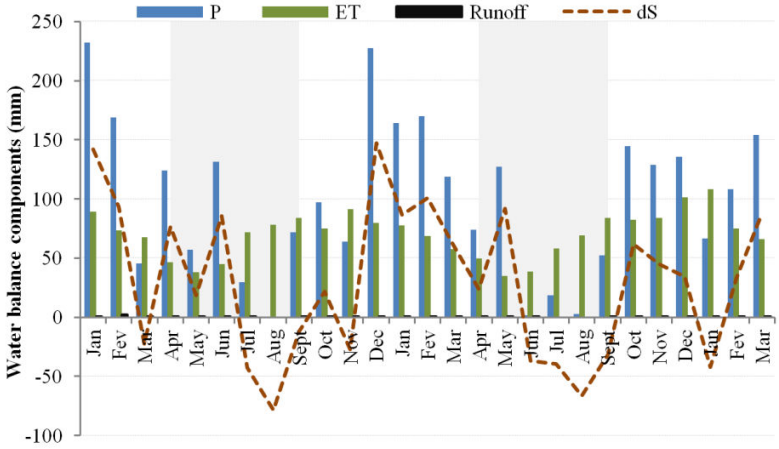

Figure 6. Water balance components at monthly scale from January 2012 through March 2014. The grey shaded bar shows the dry season.

The water deficits in the Cerrado region usually happen from April through September (dry season), however we found an atypical water decrease in the wet season (months of March and November 2012, and January 2014). Indeed, the rainfall amounts in these months were 71%, 56% and 39% less than the historical mean of 1973 to 2013 (156 mm, 147 mm and 270 mm) observed at the climatological station from the Centro de Recursos Hídricos e Ecologia Aplicada at the University of São Paulo, located approximately 3 km from the study area. In addition, we note that the annual rainfall during the period of study (1248 mm and 1195 mm for 2012 and 2013, respectively) were approximately 20% less than the historical mean of the 1500 mm. The decreased rainfall in São Paulo State in recent years has caused problems of water scarcity (Rodrigues et al., 2014).

4 Conclusions

Deforestation of the Brazilian Cerrado has caused major changes in hydrological processes; however these changes are still poorly understood at the field scale. Thus, to understand pre-deforestation conditions, we determined the main components of the water balance for an undisturbed dense cerrado. We developed an empirical model to estimate actual evapotranspiration by using flux tower measurements and, vegetation conditions inferred from the enhanced vegetation index and reference evapotranspiration. Canopy interception, throughfall, stemflow, surface runoff, and water table level were assessed from ground-measurements. We used flux tower data from the PDG site collected during 2001 to 2003 to develop the empirical model to estimate ET. The other hydrological processes were measured at the field scale between 2011 and 2014 in the IAB site.

The empirical model developed in the present study showed a satisfactory agreement with observed ET and better results than from the product MOD16 ET. From this empirical model it is possible to compute ET at daily, monthly and annual scales for undisturbed cerrado areas with similar characteristics of hydroclimatology and phenology that observed in the PDG site. Furthermore, from this approach is possible to assess the ET for large areas of the Cerrado with a good spatial and temporal resolution (250 m and 16 days), therefore, it may be useful for monitoring evapotranspiration dynamics in this region.

We conclude that the canopy interception may range from 4 to 20% of gross precipitation in the cerrado and that stemflow values are around 1% of gross precipitation. Our results also indicate that the average runoff coefficient was less than 1% in the plots under undisturbed cerrado and that the deforestation has the potential to increase up to 20 fold the runoff coefficient value. In addition, we did not find evidence of net groundwater table changes, possibly because the water table is at significant depth at the IAB site, the deep rooting depth of the trees, and the study period with rainfall smaller than the historical mean. As only little excess water runs off (either by surface water or groundwater) the water storage may be estimated by the difference between precipitation and evapotranspiration. Our results provide benchmark values of water balance dynamics in the undisturbed Cerrado that will be useful to evaluate past and future land use in different sceneries of water scarcity and climate change for this region.

5 Acknowledgments

This study was supported by grants from the Fundação de Amparo à Pesquisa do Estado de São Paulo - FAPESP (10/18788-5, 11/14273-3 and 12/03764-9) and the Conselho Nacional de Desenvolvimento Científico e Tecnológico - CNPq (470846/2011-9). USDA is an equal opportunity provider and employer. We would like to thank the Arruda Botelho Institute (IAB) and São José farm that have allowed us to develop this study in the native Cerrado vegetation.

6 References

Allen, R., Pereira, L., Rais, D., Smith, M., Solomon, K., & O'Halloran, T. (1998). Crop Evapotranspiration-Guidelines for Computing Crop Water Requirements; FAO Irrigation and Drainage Paper 56; Food and Agriculture Organization of the United Nations: Rome, Italy.

Bäse, F., Elsenbeer, H., Neill, C., & Krusche, A. V. (2012). Differences in throughfall and net precipitation between soybean and transitional tropical forest in the southern Amazon, Brazil. *Agriculture, Ecosystems & Environment*, *159*, 19–28. doi:10.1016/j.agee.2012.06.013

Cogo, N. P., Levien, R., & Schwarz, R. A. (2003). Perdas de solo e água por erosão hídrica influenciadas por métodos de preparo, classes de declive e níveis de fertilidade do solo. *Revista Brasileira de Ciência Do Solo*, *27*(4), 743–753. doi:10.1590/S0100-06832003000400019

da Rocha, H. R., Manzi, A. O., Cabral, O. M., Miller, S. D., Goulden, M. L., Saleska, S. R., … Maia, J. F. (2009). Patterns of water and heat flux across a biome gradient from tropical forest to savanna in Brazil. *Journal of Geophysical Research*, *114, 1-8*. doi:10.1029/2007JG000640

da Rocha, H. R. da, Freitas, H. C., Rosolem, R., Juárez, R. I. N., Tannus, R. N., Ligo, M. A., … Dias, M. A. F. S. (2002). Measurements of CO2 exchange over a woodland savanna (Cerrado Sensu stricto) in southeast Brasil. *Biota Neotropica*, *2*(1), 1–11. doi:10.1590/S1676-06032002000100009

Davidson, E. A., de Araújo, A. C., Artaxo, P., Balch, J. K., Brown, I. F., C. Bustamante, M. M., … Wofsy, S. C. (2012). The Amazon basin in transition. *Nature*, *481*(7381), 321–328. doi:10.1038/nature10717

Dawes, W., Ali, R., Varma, S., Emelyanova, I., Hodgson, G., & McFarlane, D. (2012). Modelling the effects of climate and land cover change on groundwater recharge in south-west Western Australia. *Hydrol. Earth Syst. Sci.*, *16*(8), 2709–2722. doi:10.5194/hess-16-2709-2012

Dezzeo, N., & Chacón, N. (2006). Nutrient fluxes in incident rainfall, throughfall, and stemflow in adjacent primary and secondary forests of the Gran Sabana, southern Venezuela. *Forest Ecology and Management*, *234*(1-3), 218–226. doi:10.1016/j.foreco.2006.07.003

Falge, E., Baldocchi, D., Olson, R., Anthoni, P., Aubinet, M., Bernhofer, C., … Wofsy, S. (2001). Gap filling strategies for long term energy flux data sets. *Agricultural and Forest Meteorology*, *107*(1), 71–77. doi:10.1016/S0168-1923(00)00235-5

Ferreira, L. G., & Huete, A. R. (2004). Assessing the seasonal dynamics of the Brazilian Cerrado vegetation through the use of spectral vegetation indices. *International Journal of Remote Sensing*, *25*(10), 1837–1860. doi:10.1080/0143116031000101530

Fidelis, A. T., & Godoy, S. A. P. de. (2003). Estrutura de um cerrado strico sensu na Gleba Cerrado Pé-de-Gigante, Santa Rita do Passa Quatro, SP. *Acta Botanica Brasilica*, *17*(4), 531–539. doi:10.1590/S0102-33062003000400006

Furley, P. A. (1999). The nature and diversity of neotropical savanna vegetation with particular reference to the Brazilian cerrados. *Global Ecology and Biogeography*, *8*(3-4), 223–241. doi:10.1046/j.1466-822X.1999.00142.x

Garcia-Montiel, D. C., Coe, M. T., Cruz, M. P., Ferreira, J. N., da Silva, E. M., & Davidson, E. A. (2008). Estimating Seasonal Changes in Volumetric Soil Water Content at Landscape Scales in a Savanna Ecosystem Using Two-Dimensional Resistivity Profiling. *Earth Interactions*, *12*(2), 1–25. doi:10.1175/2007EI238.1

Giambelluca, T. W., Scholz, F. G., Bucci, S. J., Meinzer, F. C., Goldstein, G., Hoffmann, W. A., … Buchert, M. P. (2009). Evapotranspiration and energy balance of Brazilian savannas with contrasting tree density. *Agricultural and Forest Meteorology*, *149*(8), 1365–1376. doi:10.1016/j.agrformet.2009.03.006

Gibbs, H. K., Ruesch, A. S., Achard, F., Clayton, M. K., Holmgren, P., Ramankutty, N., & Foley, J. A. (2010). Tropical forests were the primary sources of new agricultural land in the 1980s and 1990s. *Proceedings of the National Academy of Sciences*, *107*(38), 16732–16737. doi:10.1073/pnas.0910275107

Glenn, E. P., Huete, A. R., Nagler, P. L., Hirschboeck, K. K., & Brown, P. (2007). Integrating Remote Sensing and Ground Methods to Estimate Evapotranspiration. *Critical Reviews in Plant Sciences*, *26*(3), 139–168. doi:10.1080/07352680701402503

Glenn, E. P., Nagler, P. L., & Huete, A. R. (2010). Vegetation Index Methods for Estimating Evapotranspiration by Remote Sensing. *Surveys in Geophysics*, *31*(6), 531–555. doi:10.1007/s10712-010-9102-2

Glenn, E. P., Neale, C. M. U., Hunsaker, D. J., & Nagler, P. L. (2011). Vegetation index-based crop coefficients to estimate evapotranspiration by remote sensing in agricultural and natural ecosystems. *Hydrological Processes*, *25*(26), 4050–4062. doi:10.1002/hyp.8392

Honda, E. A. (2013). *Repartição da água da chuva sob o dossel e umidade do solo no gradiente fisionômico da vegetação do Cerrado*, Ph.D. Dissertation , Universidade de São Paulo, São Carlos, SP, Brazil.

Huete, A., Didan, K., Miura, T., Rodriguez, E. P., Gao, X., & Ferreira, L. G. (2002). Overview of the radiometric and biophysical performance of the MODIS vegetation indices. *Remote Sensing of Environment*, *83*(1–2), 195–213. doi:10.1016/S0034-4257(02)00096-2

IBAMA/MMA/UNDP. Monitoramento do desmatamento nos biomas Brasileiros por satélite. Ministério de Meio Ambiente, Brasília, Brazil. available at: http://siscom.ibama.gov.br/monitorabiomas/cerrado/index.htm., 2011.

Juárez, N. R. I., Goulden, M. L., Myneni, R. B., Fu, R., Bernardes, S., & Gao, H. (2008). An empirical approach to retrieving monthly evapotranspiration over Amazonia. *International Journal of Remote Sensing*, *29*(24), 7045–7063. doi:10.1080/01431160802226026

Lapola, D. M., Martinelli, L. A., Peres, C. A., Ometto, J. P. H. B., Ferreira, M. E., Nobre, C. A., … Vieira, I. C. G. (2013). Pervasive transition of the Brazilian land-use system. *Nature Climate Change*, *4*(1), 27–35. doi:10.1038/nclimate2056

Lilienfein, J., & Wilcke, W. (2004). Water and element input into native, agri- and silvicultural ecosystems of the Brazilian savanna. *Biogeochemistry*, *67*(2), 183–212. doi:10.1023/B:BIOG.0000015279.48813.9d

Lima, W. P. & Nicolielo N. (1983). Precipitação efetiva e interceptação em florestas de pinheiros tropicais e em reserva de cerradão. *IPEF*, 24, 43-46.

Loarie, S. R., Lobell, D. B., Asner, G. P., Mu, Q., & Field, C. B. (2011). Direct impacts on local climate of sugar-cane expansion in Brazil. *Nature Climate Change*, *1*(2), 105–109. doi:10.1038/nclimate1067

Macedo, M. N., DeFries, R. S., Morton, D. C., Stickler, C. M., Galford, G. L., & Shimabukuro, Y. E. (2012). Decoupling of deforestation and soy production in the southern Amazon during the late 2000s. *Proceedings of the National Academy of Sciences*, *109*(4), 1341–1346. doi:10.1073/pnas.1111374109

Marris, E. (2005). Conservation in Brazil: The forgotten ecosystem. *Nature*, *437*(7061), 944–945. doi:10.1038/437944a

McJannet, D., Wallace, J., & Reddell, P. (2007). Precipitation interception in Australian tropical rainforests: I. Measurement of stemflow, throughfall and cloud interception. *Hydrological Processes*, *21*(13), 1692–1702. doi:10.1002/hyp.6347

Miranda, A. C., Miranda, H. S., Lloyd, J., Grace, J., Francey, R. J., Mcintyre, J. A., … Brass, J. (n.d.). Fluxes of carbon, water and energy over Brazilian cerrado: an analysis using eddy covariance and stable isotopes. *Plant, Cell and Environment*, *20*(3), 315–328.

Mu, Q., Jones, L. A., Kimball, J. S., McDonald, K. C., & Running, S. W. (2009). Satellite assessment of land surface evapotranspiration for the pan-Arctic domain. *Water Resources Research*, *45*(9), 1-20. doi:10.1029/2008WR007189

Mu, Q., Zhao, M., & Running, S. W. (2011). Improvements to a MODIS global terrestrial evapotranspiration algorithm. *Remote Sensing of Environment*, *115*(8), 1781–1800. doi:10.1016/j.rse.2011.02.019

Myers, N., Mittermeier, R. A., Mittermeier, C. G., da Fonseca, G. A. B., & Kent, J. (2000). Biodiversity hotspots for conservation priorities. *Nature*, *403*(6772), 853–858. doi:10.1038/35002501

Nagler, P. (2004). Leaf area index and normalized difference vegetation index as predictors of canopy characteristics and light interception by riparian species on the Lower Colorado River. *Agricultural and Forest Meteorology*, *125*(1-2), 1–17. doi:10.1016/j.agrformet.2004.03.008

Nagler, P., Glenn, E., Nguyen, U., Scott, R., & Doody, T. (2013). Estimating Riparian and Agricultural Actual Evapotranspiration by Reference Evapotranspiration and MODIS Enhanced Vegetation Index. *Remote Sensing*, *5*(8), 3849–3871. doi:10.3390/rs5083849

Nagler, P. L., Cleverly, J., Glenn, E., Lampkin, D., Huete, A., & Wan, Z. (2005b). Predicting riparian evapotranspiration from MODIS vegetation indices and meteorological data. *Remote Sensing of Environment*, *94*(1), 17–30. doi:10.1016/j.rse.2004.08.009

Nagler, P. L., Glenn, E. P., Kim, H., Emmerich, W., Scott, R. L., Huxman, T. E., & Huete, A. R. (2007). Relationship between evapotranspiration and precipitation pulses in a semiarid rangeland estimated by moisture flux towers and MODIS vegetation indices. *Journal of Arid Environments*, *70*(3), 443–462. doi:10.1016/j.jaridenv.2006.12.026

Nagler, P. L., Scott, R. L., Westenburg, C., Cleverly, J. R., Glenn, E. P., & Huete, A. R. (2005a). Evapotranspiration on western U.S. rivers estimated using the Enhanced Vegetation Index from MODIS and data from eddy covariance and Bowen ratio flux towers. *Remote Sensing of Environment*, *97*(3), 337–351. doi:10.1016/j.rse.2005.05.011

Oliveira, P. T. S., Nearing, M. A., Moran, M. S., Goodrich, D. C., Wendland, E., & Gupta, H. V. (2014). Trends in water balance components across the Brazilian Cerrado. *Water Resources Research*, *50*, 7100-7114, doi:10.1002/2013WR015202

Oliveira, P. T. S., Wendland, E., & Nearing, M. A. (2013). Rainfall erosivity in Brazil: A review. *Catena*, *100*, 139–147. doi:10.1016/j.catena.2012.08.006

Oliveira, R. S., Bezerra, L., Davidson, E. A., Pinto, F., Klink, C. A., Nepstad, D. C., & Moreira, A. (2005). Deep root function in soil water dynamics in cerrado savannas of central Brazil. *Functional Ecology*, *19*(4), 574–581. doi:10.1111/j.1365-2435.2005.01003.x

Reys, P.A.N. (2008). Estrutura e fenologia da vegetação de borda e interior em um fragmento de cerrado sensu stricto no sudeste do Brasil (Itirapina, São Paulo). PhD dissertation, Universidade Estadual Paulista, Rio Claro, Brazil. (124pp).

Rodrigues, D., Gupta, H., Serrat-Capdevila, A., Oliveira, P., Mario Mendiondo, E., Maddock, T., & Mahmoud, M. (2014). Contrasting American and Brazilian Systems for Water Allocation and Transfers. *Journal of Water Resources Planning and Management*, 04014087. doi:10.1061/(ASCE)WR.1943-5452.0000483

Ruhoff, A. L., Paz, A. R., Aragao, L. E. O. C., Mu, Q., Malhi, Y., Collischonn, W., … Running, S. W. (2013). Assessment of the MODIS global evapotranspiration algorithm using eddy covariance measurements and hydrological modelling in the Rio Grande basin. *Hydrological Sciences Journal*, *58*(8), 1658–1676. doi:10.1080/02626667.2013.837578

Santos, A. J. B., Silva, G. T. D. A., Miranda, H. S., Miranda, A. C., & Lloyd, J. (2003). Effects of fire on surface carbon, energy and water vapour fluxes over campo sujo savanna in central Brazil. *Functional Ecology*, *17*(6), 711–719. doi:10.1111/j.1365-2435.2003.00790.x

Scanlon, B. R., Reedy, R. C., Stonestrom, D. A., Prudic, D. E., & Dennehy, K. F. (2005). Impact of land use and land cover change on groundwater recharge and quality in the southwestern US. *Global Change Biology*, *11*(10), 1577–1593. doi:10.1111/j.1365-2486.2005.01026.x

Scott, R. L., Cable, W. L., Huxman, T. E., Nagler, P. L., Hernandez, M., & Goodrich, D. C. (2008). Multiyear riparian evapotranspiration and groundwater use for a semiarid watershed. *Journal of Arid Environments*, *72*(7), 1232–1246. doi:10.1016/j.jaridenv.2008.01.001

Soares-Filho, B., Rajao, R., Macedo, M., Carneiro, A., Costa, W., Coe, M., … Alencar, A. (2014). Cracking Brazil's Forest Code. *Science*, *344*(6182), 363–364. doi:10.1126/science.1246663

Spracklen, D. V., Arnold, S. R., & Taylor, C. M. (2012). Observations of increased tropical rainfall preceded by air passage over forests. *Nature*, *489*(7415), 282–285. doi:10.1038/nature11390

Villalobos-Vega, R., Salazar, A., Miralles-Wilhelm, F., Haridasan, M., Franco, A. C., & Goldstein, G. (2014). Do groundwater dynamics drive spatial patterns of tree density and diversity in Neotropical savannas? *Journal of Vegetation Science*, n/a–n/a. doi:10.1111/jvs.12194

Vourlitis, G. L., Filho, N. P., Hayashi, M. M. S., de S. Nogueira, J., Caseiro, F. T., & Campelo, J. H. (2002). Seasonal variations in the evapotranspiration of a transitional tropical forest of Mato Grosso, Brazil. *Water Resources Research*, *38*(6), 30–1–30–11. doi:10.1029/2000WR000122

Wang, K., Wang, P., Li, Z., Cribb, M., & Sparrow, M. (2007). A simple method to estimate actual evapotranspiration from a combination of net radiation, vegetation index, and temperature. *Journal of Geophysical Research*, *112*(D15), 1-14. doi:10.1029/2006JD008351

Wendland, E., Barreto, C., & Gomes, L. H. (2007). Water balance in the Guarani Aquifer outcrop zone based on hydrogeologic monitoring. *Journal of Hydrology*, *342*(3–4), 261–269. doi:10.1016/j.jhydrol.2007.05.033

Wohl, E., Barros, A., Brunsell, N., Chappell, N. A., Coe, M., Giambelluca, T., … Ogden, F. (2012). The hydrology of the humid tropics. *Nature Climate Change*. doi:10.1038/nclimate1556

Youlton, C. (2013) Quantificação experimental da alteração no balanço hidríco e erosão em um neossolo quartzarênico devido à substituição de pastagem por cana-de-açúcar, Ph.D. Dissertation, Universidade de São Paulo, São Carlos, SP, Brazil.

CHAPTER 3
CURVE NUMBER ESTIMATION FROM BRAZILIAN CERRADO RAINFALL AND RUNOFF DATA

Oliveira, Paulo Tarso S., Nearing, Mark . A., Stone, Jeffry J., Hawkins, Richard H., Rodrigues, Dulce B.B., Panachuki, E., Wendland, E. Curve number estimation from Brazilian Cerrado rainfall and runoff data. *Journal of Hydrologic Engineering*. Under Review. (Impact factor, 2013: 1.624; Qualis CAPES: A2)

Abstract

The Curve Number (CN) method has been widely used to estimate runoff from rainfall events in Brazil, however, CN values for use in the Brazilian savanna (Cerrado) are poorly documented. In this study we used experimental plots to measure natural rainfall-driven rates of runoff under undisturbed cerrado and under the main crops found in this biome, and derive associated CN values from the measured data using five different statistical methods. Curve numbers obtained from the standard table was suitable to estimate runoff for bare soil, soybeans, and sugarcane. However, CN values obtained from measured rainfall-runoff data (CN calibrated) provide better runoff estimates than the CN values from the standard table. The best CN values for the bare soil (hydrologic soil group B), soybeans, and sugarcane were 81.2 (78.5-83.9), 78.7 (75.9-81.5), and 70.2 (67.8-72.6). We concluded that the Curve Number method was not suitable to estimate runoff under undisturbed cerrado, bare soil (hydrologic soil group A), pasture, and millet.

Keywords: runoff; rainfall; savanna; deforestation hydrology; hydrologic models.

1 Introduction

The Brazilian savanna (Cerrado) is the second largest biome in South America, covering an area of 2 million km^2 (equivalent to 22% of Brazil). This biome provides an important role in water resources dynamics because it distributes fresh water to the largest river basins in Brazil

and South America. In addition, approximately one half of the outcrop area of the Guarani aquifer system, one of the largest aquifers worldwide, is located in this biome. Thus, the Cerrado has been considered one of the most important biomes for Brazilian water resources. However, vast areas of this biome have been converted into farmland, and there is little evidence that agricultural expansion will decrease, mainly because Brazil holds the great potential for further agricultural expansion in the twenty-first century (Lapola et al., 2014). Some authors have reported variations in hydrological processes promoted by the land cover and land use changes in the Cerrado (Costa et al., 2003; Coe et al., 2011; Loarie et al., 2011; Oliveira et al., 2014).

Several models have been developed to evaluate changes in hydrological processes. The Curve Number (CN) method developed in 1954 by the United States Department of Agriculture, Soil Conservation Service (USDA-SCS), currently the Natural Resources Conservation Service (USDA-NRCS), has been one of the methods most often used to estimate direct surface runoff from a given rainfall event (Hawkins et al., 2009). Because of the simplicity, versatility, and availability of necessary data, this method has been quite popular within the United States and other countries (Ponce and Hawkins, 1996; Sartori et al., 2011; Hawkins et al., 2009). Several hydrologic, soil erosion and water quality models have used the curve number method, such as: CREAMS (Knisel, 1980), SWRRB (Wiliams et al., 1985), AGNPS (Young et al., 1989), EPIC (Sharpley & Williams, 1990), SWAT (Arnold et al., 1998), Curve Number-based modeling of sediment yield (Mishra et al., 2006; Tyagi et al., 2008) and the curve number method coupled with the RUSLE model (Gao et al., 2012).

In the curve number method several different factors that affect surface runoff generation, such as soil type, land cover and land use, surface condition, and antecedent soil moisture are incorporated into a single CN parameter (Hawkins et al., 2009). Using data from 24 watersheds in the United States the SCS developed a standard table of curve numbers. The CN values can be obtained by the standard table, however, the CN estimated by *in situ* data from plots or watersheds are preferable. The tabulated curve numbers can result in large errors in surface runoff estimation (Hawkins et al., 2009; Soulis et al., 2009). Shi et al. (2009) shown that the tabulated CN underestimate the runoff for large rainfall events and overestimate small rainfall events. Several authors have reported better runoff estimates from the *in situ* data than from using tabulated CN (King & Balogh, 2008; Elhakeem and Papanicolaou, 2009; Shi et al., 2009; Tedela et al., 2012; Hoomehr et al., 2012; D'Asaro et al., 2014; Ajmal and Kim, 2014).

Tabulated curve numbers derived for rainfall-runoff data were originally computed from a graphical method, where surface runoff and rainfall volumes were plotted to obtain the curve that divides the plotted points into two equal groups, thus corresponding the median curve number (NRCS, 2004). Other methods for calculating the curve number from rainfall-runoff data include the geometric mean (NRCS, 2004), arithmetic mean (Bonta, 1997; Tedela et al., 2012), nonlinear, least squares fit (Hawkins, 1993), standard asymptotic fit (Hawkins, 1993) and lognormal frequency (Schneider and McCuen, 2005). However, a consensus is lacking for which method is best or should be used as a standard for curve number estimation. Most investigations use several methods to estimate the curve number, and then choose the best method for each condition (Tedela et al., 2012).

The curve number method is the most widely used method in Brazil for runoff estimation, despite that the tabulated CN values have not been adapted for Brazilian conditions (Sartori et al., 2011). In addition, there are several uncertainties in the use of CN method to estimate surface runoff from regions under undisturbed cover (Tedela et al., 2012). Thus, the objectives of this study were to measure natural rainfall-driven rates of runoff under undisturbed Cerrado vegetation and under the main crops found in this biome, and to derive associated CN values from the five more frequently used statistical methods.

2 Materials and Methods

2.1 Study area

This study was developed in two Brazilian States locates in the Cerrado biome. In area 1 (Fig. 1a), we measured runoff from six plots of 5 x 20 m (100 m^2) with slope steepness of approximately 0.09 m m^{-1}. We used three replications of under undisturbed Cerrado and three with bare soil (Ortic Quartzarenic Neosol, hydrologic soil group A). The plots under cerrado were installed in an area with approximately 300 ha of undisturbed cerrado located in the municipality of Itirapina, São Paulo State (latitude 22°10' S, longitude 47°52' W and average

elevation of the 780 m). The area 2 (Fig. 1b) is located in the municipality of Aquidauna, Mato Grosso Sul State (latitude 20°27' S, longitude 55°40' W and average elevation of the 170 m). In this area we used 10 plots of 3.5 x 22.15 m (77.5 m^2) with slope steepness of approximately 0.05 m m^{-1}. We used two replications for pasture, soybeans, millet, sugarcane and bare soil (Dystrophic Red Argisol, hydrologic soil group B).

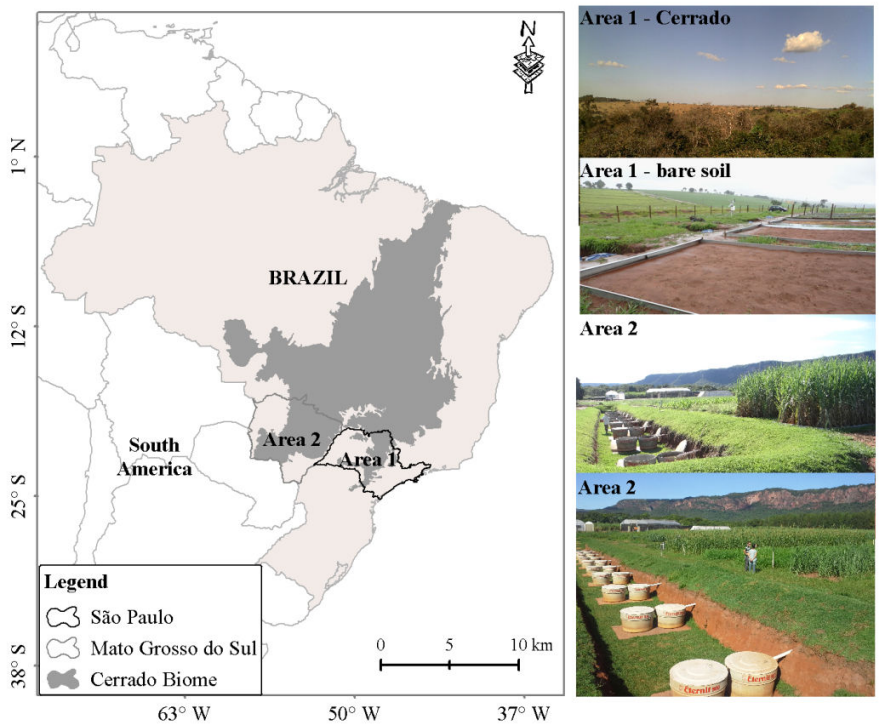

Figure 1. Location of study areas: area 1. cerrado, and bare soil (hydrologic soil group A); and area 2. crops, pasture and bare soil (hydrologic soil group B).

According to the Köppen climate classification, the climate in area 1 is Cwa subtropical and area 2 is Aw humid tropical, where both are subject to a dry winter (April to September) and hot and rainy summer (October to March). The average annual precipitation is approximately 1500 mm and 1200 mm for the areas 1 and 2 respectively. Convection is the main rainfall generating mechanism, promoting rainfall with high intensity in these regions. The soil in area 1 was classified according to the Brazilian Soil Classification System (SiBCS) as Ortic Quartzarenic Neosol (RQo) with sandy texture, well drained, acidic, and poor nutrients. Area 2 has a Dystrophic Red Argisol (PVd), with the main difference to the RQo being less sand and the presence of the greater clay content in the B horizon (between 0.50 to 1.09 m in depth) (Schiavo et al., 2010); which places it in the lower infiltration rate category of hydrologic soil (Table 1).

Table 1. Soil characteristics of the study areas.

Soil profile	Sand ($g\ kg^{-1}$)	Silt ($g\ kg^{-1}$)	Clay ($g\ kg^{-1}$)	Soil bulk density ($g\ cm^{-3}$)
Area 1* (Cerrado, 0 - 30 cm)	839	34	127	1.69
Area 1* (Bare soil, 0 - 30 cm)	865	34	101	1.64
Area 2** (0 - 24 cm)	770	110	120	1.46
Area 2** (50 - 65 cm)	610	140	250	1.46

*Ortic Quartzarenic Neosol, **Dystrophic Red Argisol.

The physiognomies of the Cerrado vary from grassland to savanna to forest. In study area 1 the physiognomy was classified as "cerrado sensu stricto denso", which is also known as cerrado woodland, and has a characteristic arborous cover of 50% to 70% and trees with heights of 5 to 8 m (Furley, 1999). This area has been preserved and there are no records of fires. The absolute density (number of individuals per unit area) is of 15,278 individual trees ha^{-1}, with a basal area (area occupied by the cross-section of tree's trunk at breast height) of 27.55 $m^2\ ha^{-1}$ and Shannon diversity index of 4.03 (Reys, 2008). Farming of area 2 included pasture before 2009, March common bean and September soybeans in 2009, corn in 2010, and millet and common bean in 2011, after which the area was fallow the remainder of 2011 and 2012.

We monitored plots with bare soil and under undisturbed cerrado (area1) from November 2011 to July 2014 (85 rainfall-runoff events), and January 2012 to July 2014 (65 rainfall-runoff events), respectively. In area 2, we monitored plots under pasture, soybeans, millet, sugarcane and bare soil from November 2012 to August 2014 (78 and 91 rainfall-runoff events for pasture/crops and bare soil, respectively). The rainfall events assessed in area 1 ranged from 7.2 to 101.4 mm, with an average of 25.1 mm. In area 2, rainfall ranged from 7.1 to 129.1 mm, with an average of 30.5 mm.

2.2 Estimation of curve number from rainfall-runoff data

The Curve Number method is based on a water budget equation to estimate the storm runoff:

$$Q = P - Ia - F \quad (1)$$

where Q is total runoff (mm); P is total rainfall (mm) ($P > Q$ and $P > Ia$); Ia is initial abstraction (mm); and F is the amount of surface retention (mm). The SCS premise is that the ratio of water retention to potential water retention is equal to the ratio of surface runoff to potential runoff (USDA, 1986; Yu, 1998):

$$\frac{Q}{P - Ia} = \frac{F}{S} \quad (2)$$

$$Ia = \lambda S \quad (3)$$

where S is potential maximum retention ($S > F$) (mm); and λ (dimensionless) is the initial abstraction ratio, equal to 0.2 according to NRCS (2004). The runoff (Q) is estimated from the combination the Eqs. (1), (2), and (3).

$$Q = \frac{(P - Ia)^2}{(P - Ia + S)}, \text{ for } P > Ia, \text{ otherwise, } Q = 0. \quad (4)$$

We computed curve numbers from the rainfall-runoff data from the five more frequently used statistical methods: the median (NRCS, 2004), geometric mean (NRCS, 2004), arithmetic mean (Bonta, 1997; Tedela et al., 2012), nonlinear, least squares fit (Hawkins, 1993), and standard asymptotic fit (Hawkins, 1993). For the median and arithmetic mean we computed the potential maximum retention and the curve numbers using the rainfall-runoff measured from the plots according to Eqs. (5) and (6), for S, Q and P in mm (Hawkins, 1993).

$$S = 5\left(P + 2Q - \sqrt{4Q^2 + 5PQ}\right) \quad (5)$$

and

$$CN = \frac{25400}{(S + 254)} \quad (6)$$

These numbers were used to obtain the median and mean for each individual plot.

For the geometric mean, we first calculated the logarithm of the event maximum potential retention S derived using Eq. (5), log S; determined the arithmetic mean of the series for each experimental plot, $\overline{\log S}$, and then calculated the geometric mean maximum potential retention, $10^{\overline{\log S}}$ (Tedela et al., 2012). Thus, the curve number was computed as:

$$CN = \frac{100}{\left(1 + \frac{10^{\overline{\log S}}}{254}\right)} \tag{7}$$

We used the nonlinear, least squares fit method by minimizing the sum of squared differences between observed and CN-calculated runoff using the Eq. (4) for each rainfall-runoff event for a given experimental plot. For this method, we used only large storms (P > 25.4 mm) to avoid bias towards larger curve numbers found with small rainfall events (Hawkins et al., 2009).

For the standard asymptotic fit method, we first rank-ordered both the rainfall and runoff time series separately, matching them in pairs from a decreasing order, and then computing the CN values from Eqs. (5) and (6) using the rank-matched pairs (Hawkins, 1993). We evaluated the CN values according to three types of behavior indentified by Hawkins (1993): standard, complacent and violent. The standard behavior occurs when the CN values decrease with the total rainfall and tend to approach a near-constant CN (called CN_∞) with rainfall increase. This behavior is the most common observed in the literature (Hawkins et al., 2009). We used the Eq. (8) to evaluate the data for standard behavior where the estimated CN_∞ is taken to be the reference CN and the k is the fitting coefficient that describes the CN(P) (curve number as a function of precipitation, P) approaches the asymptotic constant CN_∞ (Hawkins, 1993).

$$CN(P) = CN_\infty + (100 - CN_\infty)\exp^{-kP} \tag{8}$$

For the complacent behavior the calculated event curve number decreases with event rainfall increase without approaching an apparent constant value and the runoff is better

described as linearly dependent on rainfall $Q = CP$, where C is the runoff coefficient. Thus, the curve number cannot be determined from data that have this behavior, because no constant value is clearly approached (Hawkins, 1993).

Tabulated curve numbers were obtained for each land cover studied according to cover type and cover description, hydrologic conditions (based on combination factors that affect infiltration and runoff) and hydrologic soil group (NRCS, 2004). For the undisturbed cerrado, we used the woodland cover type with good hydrologic condition. For the plots under pasture we used the cover type pasture with good hydrologic condition, and for the plots under soybeans we chose the small grain cover with straight rows good hydrologic condition. For the plots under sugarcane (limited cover, straight row) and millet (partial cover, straight row) we used curve numbers obtained from Cooley and Lane (1982) for Hawaii that was recommended for use by the USDA (NRCS, 2004; Sartori et al., 2011).

2.3 Uncertainties and statistical analyses

We assessed uncertainties in curve numbers estimates for each method. For the median, we used the range of curve numbers determinate from each rainfall-runoff event. For geometric and arithmetic means methods we used the standard deviation computed from all curve numbers values estimated. For nonlinear least squares fit and asymptotic curve number, we computed the standard error (G) using values of runoff observed (Q_i), and runoff computed (Q_{ci}) from the curve number obtained by each method and the number of observations of rainfall-runoff (n) as:

$$G = \sqrt{\frac{\sum_{i=1}^{n}(Q_i - Q_{ci})^2}{n}} \tag{9}$$

We evaluated the computed runoff obtained from each method with observed runoff values using the mean bias (difference between observed and estimated runoff), coefficient of determination (CoD) and the Nash-Sutcliffe Efficiency (NSE) (Nash & Sutcliffe, 1970), Eq. (10).

$$NSE = 1 - \frac{\sum_{i=1}^{n}(Q_i - Q_{ci})^2}{\sum_{i=1}^{n}(Q_i - \overline{Q_i})^2} \quad (10)$$

We used the Student's t-test with a 95% confidence level in order to evaluate the significance of the linear correlation between the runoff observed and estimated. Furthermore, we used one-way ANOVA with a Tukey *post hoc* test at the 95% confidence level to assess if there are significant differences between the mean observed and estimated runoff from all methods studied.

3 Results and Discussion

Curve number values for plots under undisturbed cerrado ranged from 49.3 (nonlinear, least squares fit) to 73.9 (median) (Table 2). For the crop-covered plots we found the smallest curve numbers for pasture (45.2 by the nonlinear least squares) and the greatest for soybeans (85.5 by the geometric mean) and for sugarcane (79.6 by the geometric mean) (Table 2). Plots with bare soil (Ortic Quartzarenic Neosol, hydrologic soil group A) had smaller curve numbers than plots with bare soil (Dystrophic Red Argisol, hydrologic soil group B). This was expected because, despite the large sand concentration in the upper profile of the Dystrophic Red Argisol, the clay in the B horizon promotes faster soil saturation and more surface runoff than the Ortic Quartzarenic Neosol.

Table 2. Tabulated and estimated curve numbers (uncertainty ranges) for the Brazilian Cerrado.

Land cover	NRCS Table	Median	Geometric mean	Arithmetic mean	Nonlinear least squares	Asymptotic
Cerrado 1*	30	73.9 (37.6-89.1)	73.1 (59.9-83.1)	71.7 (59.7-83.8)	49.3 (47.1-51.5)	-
Cerrado 2*	30	73.3 (37.4-89.3)	72.7 (59.5-82.9)	71.4 (59.3-83.4)	49.4 (47.1-51.6)	-
Cerrado 3*	30	73.7 (38.4-89.3)	73.3 (60.4-83.2)	72.0 (60.2-83.7)	49.3 (47.2-51.5)	-
Bare soil 1*	77	85.7 (52.6-99.6)	86.9 (72.9-94.2)	84.2 (74.5-93.9)	63.4 (55.1-71.7)	73.3 (70.1-76.6)
Bare soil 2*	77	86.9 (52.6-95.8)	86.8 (76.0-93.1)	84.7 (75.2-94.1)	65.5 (56.4-74.7)	73.8 (70.4-77.3)
Bare soil 3*	77	85.0 (52.7-95.8)	85.0 (74.2-91.7)	83.1 (73.5-92.6)	65.9 (58.7-73.1)	64.7 (62.0-67.5)
Bare soil 1**	86	89.3 (61.8-98.2)	89.1 (79.1-94.6)	86.9 (78.5-95.3)	79.3 (61.2-97.4)	81.2 (78.5-83.9)
Bare soil 2**	86	88.2 (62.3-98.2)	88.9 (78.5-94.6)	86.7 (78.1-95.3)	79.1 (61.5-96.6)	81.3 (78.8-83.8)
Soybeans1**	75	83.4 (43.8-98.7)	85.5 (70.7-93.5)	82.4 (71.2-93.7)	70.7 (43.5-97.9)	78.7 (75.9-81.5)
Soybeans 2**	75	83.8 (38.5-98.2)	85.1 (70.0-93.4)	82.1 (70.4-93.7)	69.2 (54.6-83.8)	79.0 (76.7-81.3)
Millet 1**	69	76.8 (33.5-89.7)	75.9 (61.9-85.8)	74.1 (61.6-86.6)	51.2 (43.9-58.4)	56.3 (54.8-57.8)
Millet 2**	69	76.8 (34.7-89.7)	75.9 (62.2-85.8)	74.2 (61.8-86.6)	53.6 (45.2-62.1)	56.9 (55.1-58.7)
Pasture 1**	61	75.7 (32.8-90.5)	73.7 (58.4-84.8)	71.8 (58.2-85.4)	45.2 (42.1-48.4)	45.4 (44.5-46.2)
Pasture 2**	61	75.6 (32.8-89.7)	73.9 (59.3-84.6)	72.1 (59.1-85.2)	46.7 (42.8-50.5)	47.1 (46.0-48.2)
Sugarcane 1**	78	79.1 (33.0-96.2)	78.8 (63.1-89.0)	76.3 (63.2-89.4)	63.2 (49.8-76.6)	67.7 (65.6-69.8)
Sugarcane 2**	78	79.3 (33.7-98.2)	79.6 (63.3-89.8)	76.9 (63.9-89.9)	65.9 (53.2-78.7)	70.2 (67.8-72.6)

*Ortic Quartzarenic Neosol, ** Dystrophic Red Argisol. - Means complacent behavior. Uncertainties were defined for each method in the "uncertainties and statistical analyses" section.

We noted greater ranges of CN values in the plots under Cerrado, pasture and crops than the plots with bare soil (Table 2). This occurs mainly due to changes in vegetation cover and the soil surface cover during the year that tend to promote differing responses on the interception and soil surface roughness. In undisturbed Cerrado the leaf-drop late in the fall season promotes a good soil cover for the following seasons of winter and spring, thus facilitating increased water retention. Furthermore, in forest areas the leaf litter and the more porous soil tend to promote the increase of infiltration and water storage, rather than rapid overland flow (McCulloch and Robinson, 1993). On pastures the soil cover tends to change with the season wet and dry and amount of livestock per area. For the plots under crops the changes in vegetation cover and the soil surface cover occur during the agricultural cycle (tillage to harvest). Sartori et al. (2011)

found CN values for sugarcane ranging from to 44.2 (full cover, near the harvest period) to 87.1 (bare soil), which are consistent with our findings (Table 2).

We found the complacent behavior in the plots under undisturbed cerrado, i.e., no constant value was clearly approached (Fig. 2), and thus no satisfactory curve numbers were determined (Hawkins,1993). Runoff coefficients (total runoff divided by total rainfall) for the Cerraro were small ranging from 0.001 to 0.030, with an average of 0.005. In complacent behavior the runoff coefficients usually ranges from 0.005 to 0.05 (Hawkins et al., 2009). Therefore, in these cases the curve number is inappropriate and the runoff is more aptly modeled by the equation $Q = CP$, where C is the runoff coefficient.

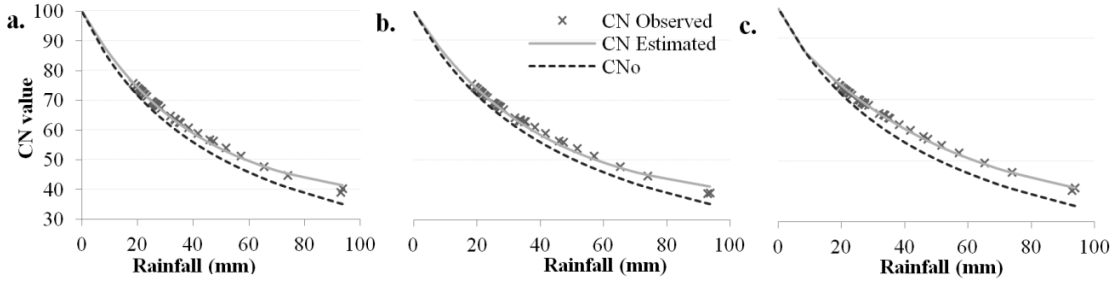

Figure 2. Complacent behavior for plots under undisturbed cerrado using rank-ordered rainfall and runoff. a. b and c means plots 1, 2 and 3, respectively. The CNo (dashed line) is the threshold under which no runoff is projected to occur ($P = 0.2S$), and was computed by equation CNo = 2540 / (25.4 + (P/2)), for P in mm.

The average runoff coefficients for the plots with bare soil (hydrologic soil group A and B), and under soybeans, sugarcane, millet and pasture and were 0.173, 0.281, 0.185, 0.087, 0.040, and 0.020, respectively. It is possible to note the influence of the soil on these values where the runoff coefficient was greater for the soybeans (hydrologic soil group B) than to the bare soil (hydrologic soil group A). For the plots with bare soil and under crops we noted that the CN values decreased with the total rainfall, tending to approach a near-constant CN with rainfall increase, featuring the standard behavior (Fig. 3). We found that CN values computed from the standard asymptotic fit were smaller than the central tendency methods (median, and geometric and arithmetic means) (Table 2). Previous studies also have reported that the central tendency methods tend to produce greater curve numbers than the standard asymptotic fit and the NRCS-tabulated (Stewart et al., 2012; Hoomehr et al., 2012; D'Asaro et al., 2014).

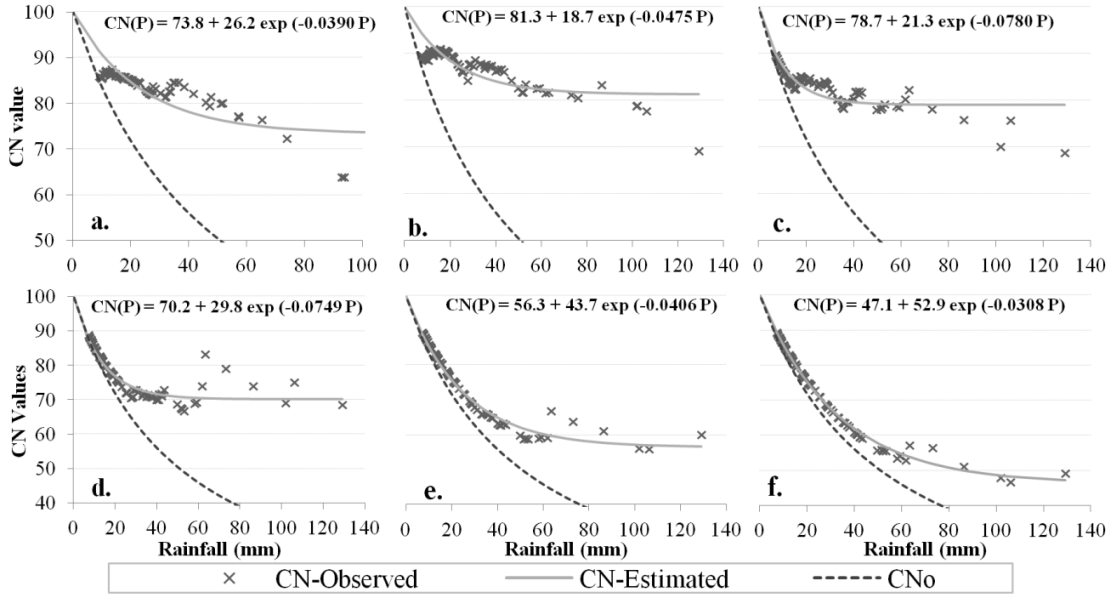

Figure 3. Standard behavior in plots under bare soil and croplands using rank-ordered rainfall and runoff: a. bare soil - hydrologic soil group A; b. bare soil - hydrologic soil group B; c. soybeans; d. sugarcane; e. millet; f. pasture. The CNo (dashed line) is the threshold under which no runoff is projected to occur (P = 0.2S) and was computed by the equation CNo = 2540 / (25.4 + (P/2)), for P in mm.

We compared the surface runoff estimated using the CN values presented in Table 2 with observed runoff and we found negative values of Nash-Sutcliffe Efficiency (NSE) for the plots under undisturbed cerrado, bare soil (hydrologic soil group A), pasture, and millet. Negative NSE values indicate that the average of the measured values is a better predictor of runoff than the model predicted values. Therefore, our results suggested that the Curve Number method was not suitable to estimate runoff under these land covers. In general, for these land cover types the modeled runoff overestimated the small observed runoff, mainly for the cerrado, pasture, and millet. For the bare soil (hydrologic soil group A), our results indicated that the amount of rainfall was not the main factor controlling surface runoff generation. The intense rainfall events and periods with several consecutive rainfall events, which promote high soil moisture contents, may have more influence on the runoff process. For example, a large rain (73.8 mm) that occured in the dry season promoted less runoff (13.7 mm) than a smaller rain event in the wet season (27.4 mm, 19.7 mm, rain and runoff, respectively).

Table 3 shows the mean bias, coefficient of determination (*CoD*), and *NSE* only for the plots with positive *NSE* and significant correlation ($p < 0.05$) between observed and estimated runoff. The central tendency methods (median, and geometric and arithmetic means) overestimated (negative bias) the surface runoff for all plots, whereas asymptotic and nonlinear

least squares underestimated runoff (positive bias). We found that the values of *CoD* and NSE were similar between the methods studied; however the standard asymptotic fit showed better values for all cover types (Table 3).

We computed the mean of observed and estimated runoff for the plots presented in Table 3. The Tukey multiple comparison tests indicated that the means of estimated runoff for all methods were not significant different ($p > 0.05$) from the observed runoff except for the nonlinear, least squares fit in the plot with bare soil (hydrologic soil group B) (Fig. 4). This method underestimated the mean observed runoff by 35%. Our results also showed that there was not significant difference between the mean runoff estimated by the central tendency methods (median, and geometric and arithmetic means) (Fig. 4). In a choice between these central tendency methods, Tedela et al. (2012) reported that the geometric mean was the better choice. This was due to the calculation of the 95 or 90% confidence intervals that allow for a probabilistic definition of the uncertainty observed in event curve numbers.

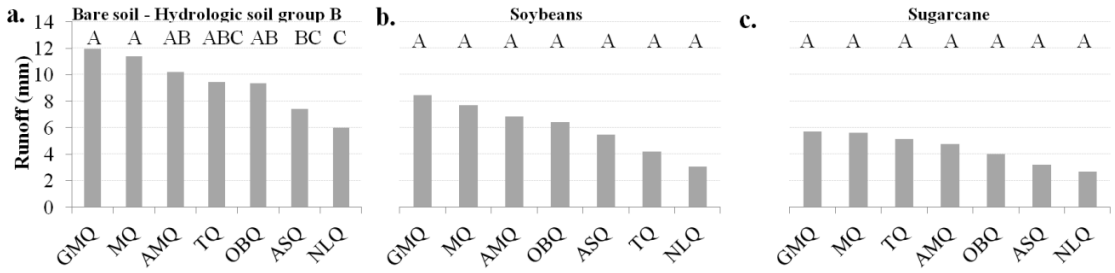

Figure 4. The ranked means of observed and computed runoff from the Tukey means test to α = 95%. Where: geometric mean curve number (GMQ), median curve number (MQ), arithmetic mean curve number (AMQ), tabulated curve number (TQ), observed runoff (OBQ), asymptotic curve number (ASQ), and nonlinear-least-squares-fit curve number (NLQ). Mean runoff with the same letter are not significantly different from each other (p > 0.05) as tested with ANOVA followed by Tukey post hoc test at the 95% confidence level.

There was a significant correlation ($r = 0.43$, $p < 0.001$) between rainfall depth and observed runoff in the cerrado. However, the largest runoff values were found for more intense rainfall events, or in periods with several consecutive rainfall events. This may indicate that other Cerrado hydrological factors, such as interception of rain by trees or by the forest floor litter may have a major influence on runoff. Rainfall of high intensity and short duration results in less interception than do low intensity, long duration events; and if rainfall is not continuous, even for short periods during an event, greater values of interception result (Crockford and Richardson,

2000). In addition, some authors have shown that the soil macroporosity has a strong influence on runoff generation processes and is greater in undisturbed forest than for crops, pasture and bare soil (Shougrakpam et al., 2010; Beven and Germann, 2013).

On undisturbed Cerrado, interception ranges from 11 to 27% of gross rainfall, with less than 1% of gross rainfall due to stemflow (Lima and Nicolielo, 1983; Lilienfein and Wilcke, 2004). Retention by forest floor litter has not been calculated for the Cerrado yet. Several authors have concluded that the forest floor properties are key factors in controlling soil hydrological processes (Molina et al., 2007; Keith et al., 2010; Neris et al., 2013). To have satisfactory results in predicting runoff using the SCS-CN method under native cerrado vegetation, it is necessary take into account interception processes, mainly by the forest floor litter. This implies that the initial abstraction ratio (λ) is different than 0.2 as suggested by the NRCS-2004, because the initial abstraction consists mainly of interception, infiltration during early stages of the storm, and surface depression storage (NRCS, 2004). Therefore, future studies should pursue for investigate the runoff generation in the Cerrado using the complete hydrograph or using rainfall simulators to estimate adequate values for the initial abstraction ratio.

We found that CN obtained from the standard table values was not adequate to estimate runoff for the undisturbed Cerrado. Tedela et al. (2012) also concluded that tabulated CN do not accurately estimate runoff in U.S. forest. However, the standard table and others CN methods presented reasonable results for bare soil and croplands (Table 2 and 3). The best CN values for the bare soil (hydrologic soil group B), soybeans, and sugarcane taking into account the greatest CoD and *NSE* were 81.2 (78.5-83.9), 78.7 (75.9-81.5), and 70.2 (67.8-72.6), respectively. These results could be useful to evaluate the hydrological process changes caused from the intense land use and land cover changes in the Cerrado (Oliveira et al., 2014).

4 Summary and Conclusions

In this study we undertook a first approach to quantify surface runoff and estimate curve numbers for the undisturbed Cerrado and for the main crops found in this biome. We measured natural rainfall-driven rates of runoff under undisturbed cerrado and bare soil (hydrologic soil group A) using three replications plots of 5 x 20 m for each treatment, and from 10 plots of 3.5 x 22.15 m, with two replications for pasture, soybeans, millet, sugarcane and bare soil (hydrologic soil group B). We monitored these plots between November 2011 and August 2014.

Our results indicated that the Curve Number method was not suitable to estimate runoff under undisturbed cerrado, bare soil (hydrologic soil group A), pasture, and millet. Therefore, in these cases the curve number is inappropriate and the runoff is more aptly modeled by the equation $Q = CP$, where C is the runoff coefficient.

The central tendency methods (median, and geometric and arithmetic means) gave higher curve numbers than the standard asymptotic fit, nonlinear, least squares fit, and the standard table. These higher curve numbers resulted in an overestimation of the estimated runoff for all plots, whereas asymptotic and nonlinear least squares underestimated runoff. However, the standard asymptotic fit showed better results for runoff estimation for bare soil, soybeans, and sugarcane than the other studied methods.

Curve number obtained from the standard table was suitable to estimate runoff for bare soil, soybeans, and sugarcane. However, CN values obtained from rainfall-runoff data (CN calibrated) provide better runoff estimate than the CN values from the standard table. In addition, we found that there was not significant difference between the mean runoff estimated by the central tendency methods (median, and geometric and arithmetic means).

We suggested curve numbers for land cover where the significant correlation with observed runoff was found, and considering the better *CoD* and *NSE* values. These CN values and ranges provide guidance for application of the curve number technique in ungauged watersheds, and to evaluate the CN calibration in other similar regions. Furthermore, these results of this study provide benchmark values that could be useful to evaluate past and future land use changes using hydrologic models and measurements in the Cerrado biome.

5 Acknowledgments

This study was supported by grants from the Fundação de Amparo à Pesquisa do Estado de São Paulo - FAPESP (10/18788-5, 11/14273-3 and 12/03764-9) and the Conselho Nacional de Desenvolvimento Científico e Tecnológico - CNPq (470846/2011-9). USDA is an equal opportunity provider and employer. The authors are grateful to the Arruda Botelho Institute (IAB) and São José farm that have allowed us to develop this study in the undisturbed cerrado. Finally, we appreciate valuable comments and careful reviews from editors, and the anonymous reviewers who helped significantly to improve this manuscript.

6 References

Ajmal, M., & Kim, T.W. (2014). Quantifying Excess Stormwater Using SCS-CN–Based Rainfall Runoff Models and Different Curve Number Determination Methods. *Journal of Irrigation and Drainage Engineering*, 04014058. doi:10.1061/(ASCE)IR.1943-4774.0000805

Arnold, J. G., Srinivasan, R., Muttiah, R. S., & Williams, J. R. (1998). Large Area Hydrologic Modeling and Assessment Part I: Model Development1. *Journal of the American Water Resources Association*, *34*(1), 73–89. doi:10.1111/j.1752-1688.1998.tb05961.x

Beven, K., & Germann, P. (2013). Macropores and water flow in soils revisited. *Water Resources Research*, *49*(6), 3071–3092.

Bonta, J. V. (1997). Determination of Watershed Curve Number Using Derived Distributions. *Journal of Irrigation and Drainage Engineering*, *123*(1), 28–36. doi:10.1061/(ASCE)0733-9437(1997)123:1(28)

Coe, M. T., Latrubesse, E. M., Ferreira, M. E., & Amsler, M. L. (2011). The effects of deforestation and climate variability on the streamflow of the Araguaia River, Brazil. *Biogeochemistry*, *105*(1-3), 119–131.

Cooley, K. R., & Lane, L. J. (1982). Modified runoff curve numbers for sugarcane and pineapple fields in Hawaii. *Journal of Soil and Water Conservation*, *37*(5), 295–298.

Costa, M. H., Botta, A., & Cardille, J. A. (2003). Effects of large-scale changes in land cover on the discharge of the Tocantins River, Southeastern Amazonia. *Journal of Hydrology*, *283*(1), 206–217.

Crockford, R. H., & Richardson, D. P. (2000). Partitioning of rainfall into throughfall, stemflow and interception: effect of forest type, ground cover and climate. *Hydrological processes*, *14*(16-17), 2903–2920.

D'Asaro, F., Grillone, G., & Hawkins, R. H. (2014). Curve Number: empirical evaluation and comparison with Curve Number handbook tables in Sicily. *Journal of Hydrologic Engineering*. 04014035. doi:10.1061/(ASCE)HE.1943-5584.0000997.

Elhakeem, M., & Papanicolaou, A. (2009). Estimation of the Runoff Curve Number via Direct Rainfall Simulator Measurements in the State of Iowa, USA. *Water Resources Management*, *23*(12), 2455–2473. doi:10.1007/s11269-008-9390-1

Furley, P. A. (1999). The nature and diversity of neotropical savanna vegetation with particular reference to the Brazilian cerrados. *Global Ecology and Biogeography*, *8*(3-4), 223–241.

Gao, G. Y., Fu, B. J., Lü, Y. H., Liu, Y., Wang, S., & Zhou, J. (2012). Coupling the modified SCS-CN and RUSLE models to simulate hydrological effects of restoring vegetation in the Loess Plateau of China. *Hydrology and Earth System Sciences*, *16*(7), 2347–2364.

Hawkins, R. (1993). Asymptotic Determination of Runoff Curve Numbers from Data. *Journal of Irrigation and Drainage Engineering*, *119*(2), 334–345. doi:10.1061/(ASCE)0733-9437(1993)119:2(334)

Hawkins, R. H., Ward, T. J., Woodward, D. E., and Van Mullen, J. A., eds. (2009). "*Curve number hydrology: State of the practice*", ASCE, Reston, VA.

Hoomehr, S., Schwartz, J. S., Yoder, D. C., Drumm, E. C., & Wright, W. (2012). Curve numbers for low-compaction steep-sloped reclaimed mine lands in the southern Appalachians. *Journal of Hydrologic Engineering*, *18*(12), 1627–1638.

Keith, D. M., Johnson, E. A., & Valeo, C. (2010). A hillslope forest floor (duff) water budget and the transition to local control. *Hydrological processes*, *24*(19), 2738–2751.

King, K. W., & Balogh, J. C. (2008). Curve numbers for golf course watersheds. *Trans. ASABE*, *51*(3), 987–996.

Knisel, W. G. (1980). CREAMS: A field-scale model for chemicals, runoff and erosion from agricultural management systems. *USDA Conservation Research Report*, (26).

Lapola, D. M., Martinelli, L. A., Peres, C. A., Ometto, J. P., Ferreira, M. E., Nobre, C. A., … Costa, M. H. (2014). Pervasive transition of the Brazilian land-use system. *Nature Climate Change*, *4*(1), 27–35.

Lilienfein, J., & Wilcke, W. (2004). Water and element input into native, agri-and silvicultural ecosystems of the Brazilian savanna. *Biogeochemistry*, *67*(2), 183–212.

Lima, W. P., & Nicolielo, N. (1983). Precipitação efetiva e interceptação em florestas de pinheiros tropicais e em reserva de cerradão. *Revista Scientia Forestalis*, 43–46.

Loarie, S. R., Lobell, D. B., Asner, G. P., Mu, Q., & Field, C. B. (2011). Direct impacts on local climate of sugar-cane expansion in Brazil. *Nature Climate Change*, *1*(2), 105–109.

McCulloch, J. S., & Robinson, M. (1993). History of forest hydrology. *Journal of Hydrology*, *150*(2), 189–216.

Mishra, S. K., Tyagi, J. V., Singh, V. P., & Singh, R. (2006). SCS-CN-based modeling of sediment yield. *Journal of Hydrology*, *324*(1), 301–322.

Molina, A., Govers, G., Vanacker, V., Poesen, J., Zeelmaekers, E., & Cisneros, F. (2007). Runoff generation in a degraded Andean ecosystem: Interaction of vegetation cover and land use. *Catena*, *71*(2), 357–370.

Nash, J. E., & Sutcliffe, J. V. (1970). River flow forecasting through conceptual models part I — A discussion of principles. *Journal of Hydrology*, *10*(3), 282–290. doi:10.1016/0022-1694(70)90255-6

Neris, J., Tejedor, M., Rodríguez, M., Fuentes, J., & Jiménez, C. (2013). Effect of forest floor characteristics on water repellency, infiltration, runoff and soil loss in Andisols of Tenerife (Canary Islands, Spain). *Catena*, *108*, 50–57.

NRCS - Natural Resources Conservation Service. (2004). "Estimation of direct runoff from storm rainfall." Chapter 10, Part 630, hydrology. *National Engineering Handbook*, Title 210. US Department of Agriculture, Washington DC.

Oliveira, P. T. S., Nearing, M. A., Moran, M. S., Goodrich, D. C., Wendland, E., & Gupta, H. V. (2014). Trends in water balance components across the Brazilian Cerrado. *Water Resources Research*, *50*, doi:10.1002/2013WR015202

Ponce, V., & Hawkins, R. (1996). Runoff Curve Number: Has It Reached Maturity? *Journal of Hydrologic Engineering*, *1*(1), 11–19. doi:10.1061/(ASCE)1084-0699(1996)1:1(11)

Reys, P. A. N. (2008). "Estrutura e fenologia da vegetação de borda e interior em um fragmento de cerrado sensu stricto no sudeste do Brasil (Itirapina, São Paulo)." Ph.D. Thesis, Universidade Estadual Paulista, Rio Claro, SP. 124pp.

Sartori, A., Hawkins, R. H., & Genovez, A. M. (2011). Reference Curve Numbers and Behavior for Sugarcane on Highly Weathered Tropical Soils. *Journal of Irrigation and Drainage Engineering*, *137*(11), 705–711. doi:10.1061/(ASCE)IR.1943-4774.0000354

Schiavo, J. A., Pereira, M. G., Miranda, L. P. M. de, Dias Neto, A. H., & Fontana, A. (2010). Caracterização e classificação de solos desenvolvidos de arenitos da formação Aquidauana-MS. *Revista Brasileira de Ciência do Solo*, *34*(3), 881–889.

Schneider, L. E., & McCuen, R. H. (2005). Statistical guidelines for curve number generation. *Journal of irrigation and drainage engineering*, *131*(3), 282–290.

Sharpley, A. N., and Williams, J. R. (1990). “EPIC - Erosion/Productivity Impact Calculator: 1.Model Documentation.” *US Department of Agriculture Technical Bulletin*, v.1768. US Government Printing Office,Washington, DC.

Shi, Z.-H., Chen, L.-D., Fang, N.-F., Qin, D.-F., & Cai, C.-F. (2009). Research on the SCS-CN initial abstraction ratio using rainfall-runoff event analysis in the Three Gorges Area, China. *Catena*, *77*(1), 1–7. doi:10.1016/j.catena.2008.11.006

Shougrakpam, S., Sarkar, R., & Dutta, S. (2010). An experimental investigation to characterise soil macroporosity under different land use and land covers of northeast India. *Journal of Earth System Science*, *119*(5), 655–674.

Soulis, K. X., Valiantzas, J. D., Dercas, N., & Londra, P. a. (2009). Investigation of the direct runoff generation mechanism for the analysis of the SCS-CN method applicability to a partial area experimental watershed. *Hydrology and Earth System Sciences*, *13*(5), 605–615. doi:10.5194/hess-13-605-2009

Stewart, D., Canfield, E., & Hawkins, R. (2011). Curve Number determination methods and uncertainty in hydrologic soil groups from semiarid watershed data. *Journal of Hydrologic Engineering*, *17*(11), 1180–1187.

Tedela, N., McCutcheon, S., Rasmussen, T., Hawkins, R., Swank, W., Campbell, J., … Tollner, E. (2012). Runoff Curve Numbers for 10 Small Forested Watersheds in the Mountains of the Eastern United States. *Journal of Hydrologic Engineering*, *17*(11), 1188–1198. doi:10.1061/(ASCE)HE.1943-5584.0000436

Tyagi, J. V., Mishra, S. K., Singh, R., & Singh, V. P. (2008). SCS-CN based time-distributed sediment yield model. *Journal of hydrology*, *352*(3), 388–403.

USDA - US Department of Agriculture. (1986). “Urban hydrology for small watersheds.” *Technical release, n. 55 (TR-55)*, Soil Conservation Service, Washington, DC.

Williams, J. R., Nicks, A. D., & Arnold, J. G. (1985). Simulator for water resources in rural basins. *Journal of Hydraulic Engineering*, *111*(6), 970–986.

Young, R. A., Onstad, C. A., Bosch, D. D., & Anderson, W. P. (1989). AGNPS: A nonpoint-source pollution model for evaluating agricultural watersheds. *Journal of soil and water conservation*, *44*(2), 168–173.

Yu, B. (1998). Theoretical Justification of SCS Method for Runoff Estimation. *Journal of Irrigation and Drainage Engineering*, *124*(6), 306–310. doi:10.1061/(ASCE)0733-9437(1998)124:6(306)

CHAPTER 4
TRENDS IN WATER BALANCE COMPONENTS ACROSS THE BRAZILIAN CERRADO

Oliveira, Paulo Tarso S., Nearing, Mark A., Moran, M. Susan, Goodrich, David C., Wendland, E. and Gupta, Hoshin V. (2014). Trends in water balance components across the Brazilian Cerrado, *Water Resources Research*, 50, 7100-7114. doi: 10.1002/2013WR015202. (Impact factor, 2013: 3.709; Qualis CAPES: A1)

Abstract

We assess the water balance of the Brazilian Cerrado based on remotely sensed estimates of precipitation (TRMM), evapotranspiration (MOD16), and terrestrial water storage (GRACE) for the period from 2003 to 2010. Uncertainties for each remotely sensed data set were computed, the budget closure was evaluated using measured discharge data for the three largest river basins in the Cerrado, and the Mann-Kendall test was used to evaluate temporal trends in the water balance components and measured river discharge. The results indicate an overestimation of discharge data, due mainly to the overestimation of rainfall by TRMM version 6. However, better results were obtained when the new release of TRMM 3B42 v7 was used instead. Our results suggest that there have been a) significant increases in average annual evapotranspiration over the entire Cerrado of 51 ± 15 mm yr^{-1}, b) terrestrial water storage increases of 11 ± 6 mm yr^{-1} in the northeast region of the Brazilian Cerrado, and c) runoff decreases of 72 ± 11 mm yr^{-1} in isolated spots and in the western part of the State of Mato Grosso. Although complete water budget closure from remote sensing remains a significant challenge due to uncertainties in the data, it provides a useful way to evaluate trends in major water balance components over large regions, identify dry periods, and assess changes in water balance due to land cover and land use change.

Keywords: hydrology, evapotranspiration, runoff, savanna, deforestation.

1 Introduction

The Brazilian Cerrado is one of the most important Brazilian biomes (being the second largest in South America) and covers an area of 2 million km^2 (~22% of the total area of Brazil). The physiognomies of the Cerrado vary from grassland to savanna to forest. Because of its endemic plant and vertebrate species, this biome has been classified as one of 25 global biodiversity hotspots (Myers et al., 2000). Most of the Cerrado is located in Brazil's central highlands. The region plays a fundamental role in water resources dynamics because it distributes fresh water to the largest basins in Brazil and South America, including the São Francisco, Tocantins, Paraná, and Paraguai. These watersheds are crucial to the provision of water supply for people and animals, to maintaining ecohydrologic functioning, to providing water for industry, agriculture, navigation and tourism, and to hydroelectric energy production.

In the last few decades, the Brazilian savanna (Cerrado) has increasingly been replaced by agricultural crops (Brannstrom et al., 2008; Sano et al., 2010; Jepson et al., 2010). Average annual deforestation were 0.69%, 0.37% and 0.32% in 2002–2008 (85,047 km^2), 2008–2009 (7637 km^2) and 2009–2010 (6469 km^2), which are greater than the average annual deforestation rates of 0.44%, 0.40% and 0.29% for the Amazon during the same periods [IBAMA/MMA/UNDP, 2011]. Marris (2005) warned that the Brazilian Cerrado is arguably under greater threat than the Amazon rain forest. By 2010, 48.5% of the area of the Cerrado had become devoted to anthropic land use, with only 50.9% remaining as native vegetation and 0.6% as water (IBAMA/MMA/UNDP, 2011). It is, therefore necessary to understand the magnitudes and consequences of these changes on hydrological processes (Costa et al., 2003; Coe et al., 2011; Loarie et al., 2011), at local, regional and continental scales.

Because 29% of the world's evaporation occurs in tropical forests and 21% occurs in savannas (Miralles et al., 2011), changes in land cover type from tropical forest and savanna to pasture and cropland have the potential to directly affect the global water balance. Savannas and forests have been classified as hotspots of reduced evapotranspiration (ET) because of deforestation (Sterling et al., 2013) and have been associated with shifts in the location, intensity and timing of rainfall events, lengthening of the dry season and changed streamflow (Wohl et al.,

2012). However, no consensus has yet emerged regarding the consequences of the Cerrado land cover change on water balance.

The use of ground-based measurements to assess water balance components remains a challenge around the globe, mainly because of inconsistent monitoring combined with high costs and a lack of data transparency and accessibility (Sheffield et al., 2009; Voss et al., 2013). Remote sensing presents a valuable tool to help fill these data gaps and has the potential to yield better regional estimates of water balance dynamics and their relationship to climate change (Sheffield et al., 2012). The recent release of the Moderate Resolution Imaging Spectroradiometer (MODIS) ET product MOD16 (Mu et al., 2011) permits a more direct accounting of the effects of land use change on ET than was possible in previous research on land use change (Lathuillière et al., 2012). In addition, the high-quality time-series precipitation data generated by the Tropical Rainfall Measuring Mission (TRMM) and the direct measurement of the terrestrial water storage change by the Gravity Recovery and Climate Experiment (GRACE) have been used successfully in several studies (Spracklen et al., 2012; Staver et al., 2011; Sheffield et al., 2009; Tapley et al., 2004).

GRACE data provide vertically integrated estimates of changes in total terrestrial water storage (TWS) which include soil moisture, surface water, groundwater and snow. These data have been combined with models from the global land data assimilation system (GLDS) (Rodell et al., 2004a), *in-situ* measurements, and other remote sensing data, to evaluate groundwater storage changes (Scanlon et al., 2012), surface water consumption (Anderson et al., 2012), regional flood potential (Reager and Famiglietti, 2009), drought (Teuling et al., 2013), reservoir storage changes (Wang et al., 2011), and water budget closure (Sheffield et al., 2009). Thus, the use of high-quality precipitation, evapotranspiration, and TWS combined with observed data for precipitation and river flow makes it possible to evaluate trends in the water balance components over time.

Sheffield et al. (2009) developed one of the first studies to estimate the large scale terrestrial water budget purely from remote sensing sources. Since then, several studies have been used remote sensing data to evaluate water balance components or water budget closure. However, the majority of these studies have been conducted in the northern hemisphere (Wang et al., 2014). In addition, evaluations of new released remote sensing data such as TRMM version 7 have been concentrated in the northern hemisphere (Amitai et al., 2012; Chen et al., 2013).

Therefore, new studies in different conditions of climate, relief, and land cover should be conducted to assess the quality of remote sensing data from the measured data.

The objective of this study is to assess the water balance dynamics for the entire Brazilian Cerrado area, identify recent temporal trends in the major components, and assess the potential consequences of land cover and land use change for the water balance. We use satellite-based TRMM, MOD16 and GRACE data for the period from 2003 to 2010 to quantify the primary water balance components of the region and to evaluate trends. Furthermore, the uncertainties are computed for each remotely sensed data set and the budget closure is evaluated from measured discharge data for the three largest river basins in the Cerrado.

2 Materials and Methods

2.1 Cerrado area

The Cerrado biome is home to the most important water sources in Brazil. It includes portions of 10 of Brazil's 12 hydrographic regions: the Tocantins (65% of the area of this hydrographic region is in the Cerrado), São Francisco (57%), Paraguai (50%), Paraná (49%), Parnaiba (46%), Occidental Atlantic Northeast (46%), Atlantic East (8%), Amazon (4%), Southeast Atlantic (1%) and Oriental Atlantic Northeast (<1%) regions (Figure 1a.). These watersheds are crucial to the water supply for people and animals, to maintaining function of ecohydrologic systems in the Cerrado and others biomes such as Pantanal (wetland) and Caatinga (semi-arid region), and to providing water for industry, agriculture, navigation and tourism. Furthermore, the Brazilian energy matrix depends on hydroelectricity for more than 80% of its total energy supply, and the largest hydroelectric facilities are on rivers in the Cerrado, such as the Itaipu, Tucuruí, Iha Solteira, Xingó and Paulo Afonso. With regards to groundwater, approximately one half of the outcrop areas of the Guarani aquifer system, one of the world's largest aquifer systems (Wendland et al., 2007), is located in the Cerrado biome. Therefore, in

terms of water resources, this biome is one of the largest and most important in Brazil and South America, and plays a strategic role in Brazilian development in several sectors.

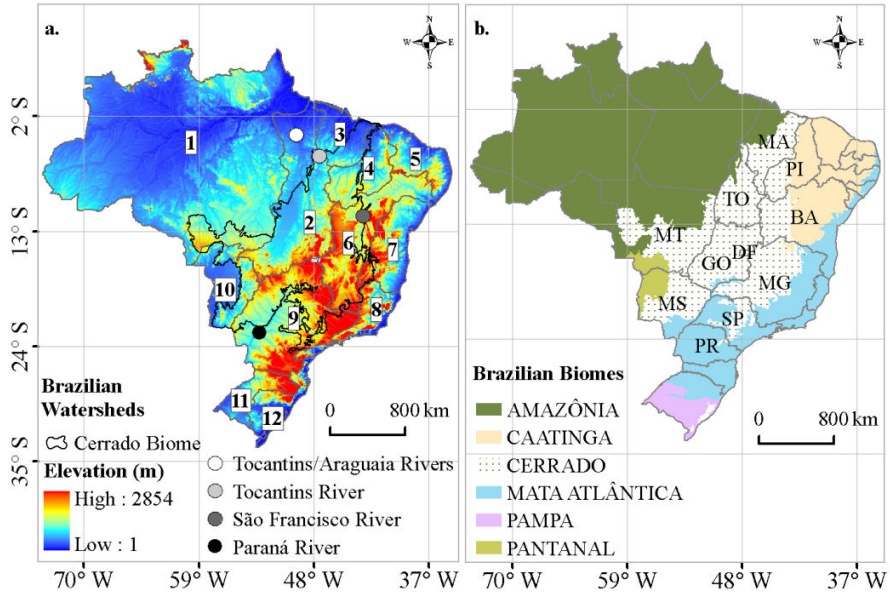

Figure 1. a. Map of Brazilian watersheds and gages for the observed discharge represented by circles. Watersheds: 1. Amazonica; 2. Tocantins; 3. Oc. A. Northeast; 4. Parnaiba; 5. Ori. A. Northeast; 6. São Francisco; 7. East Atlantic; 8. Southeast Atlantic; 9. Paraná; 10. Paraguai; 11. Uruguai; 12. South Atlantic. b. The Cerrado biome and its borders with other Brazilian biomes. States: Bahia - BA; Maranhão - MA; Tocantins - TO; Piaui - PI; Mato Grosso do Sul - MS; Mato Grosso - MT; Goiás - GO; Distrito Federal - DF; Minas Gerais - MG; São Paulo - SP and Paraná - PR.

According to the Köppen climate classification system (Peel et al., 2007), the predominant climates of the Cerrado (by percentage of the area) are the following: Aw, equatorial, winter dry (83%); Cwb, winter dry, warm temperate, warm summer (8%); Cfa, humid, warm temperate, hot summer (5%); and Cwa, dry winters, warm temperate, hot summer (4%). The average annual precipitation in the Cerrado as a whole is approximately 1500 mm, with lower values (near 700 mm) in the northeast region, in the area of transition from the Cerrado to the Caatinga biome. The highest average annual precipitation (greater than 2000 mm) is in the northwest, in the area of transition from the Cerrado to the Amazon Forest biome. The wet season is from October to March, and the dry season is April to September.

The Cerrado is bordered by 4 of the 5 Brazilian biomes (Figure 1b) and therefore has high biodiversity and a large variety of vegetation physiognomies and compositions (Ratter et al., 1997). The vegetation in the Cerrado is usually classified according to the 6 classes listed in Table 1.

Table 1. Cerrado vegetation gradient classification.

Brazilian Names	International Names	Arboreous cover (%)	Height of trees (m)
"Campo limpo"	Cerrado grassland	< 1	< 1
"Campo sujo"	Shrub Cerrado	< 5%	< 2
"Cerrado ralo"	Shrub Cerrado	5–20	2–3
"Cerrado sensu stricto"	Wooded Cerrado	20–50	3–6
"Cerrado sensu stricto denso"	Cerrado woodland	50–70	5–8
"Cerradão"	Dense Cerrado woodland	50–90	8–15

Source: Furley, 1999; Ferreira and Huete, 2004.

2.2 Data source

To evaluate the water balance in space and time, we use time-series precipitation data obtained from the Tropical Rainfall Measuring Mission (TRMM 3B42 version 6 and the new release version 7), evapotranspiration from the Moderate Resolution Imaging Spectroradiameter (MODIS) ET product MOD16, and terrestrial water storage from the Gravity Recovery and Climate Experiment (GRACE) for the years from 2003 to 2010.

The TRMM Multi-satellite Precipitation Analysis (TMPA) combines precipitation estimates from various satellite systems, as well as land surface precipitation gauge analysis where feasible. The intent of TMPA is to produce a calibration traceable back to the single “best” satellite estimate of global precipitation at fine spatial and temporal scale (0.25° × 0.25° and 3 hourly) over 50ºN-50ºS (Huffman et al., 2007). The new release of the TRMM (version 7) has been assessed in some regions showing a significant improvement in precipitation accuracy over the last version 6 (Xue et al., 2013; Chen et al., 2013; Yong et al., 2014; Ochoa et al., 2014). In this study, we use the TRMM Multi-satellite Precipitation Analysis data (TRMM 3B42 v6 and v7) provided by National Aeronautics and Space Administration (NASA) Goddard Space Flight Center (GSFC) available at http://mirador.gsfc.nasa.gov/.

To validate the TRMM 3B42 v6 and v7 data we use pluviometric measurements from 402 rain gauges (see Figure 2a) obtained in the Cerrado area between 2000 and 2005 by the Agência Nacional de Águas (ANA) and downloaded from the ANA website (http://hidroweb.ana.gov.br/). We find the correlation between TRMM and rain gauge data to be significant at the $p = 0.05$ level, with a correlation coefficient greater than 0.8. The monthly and annual values of

correlation coefficient, bias, root mean squared error, and standard deviation of differences are presented in Table 2. We also find that while TRMM v6 and v7 data both overestimate the measured data, the v7 provide better results than v6. Therefore, in this study we use TRMM 3B42 v7 to estimate the water balance over the Brazilian Cerrado.

Table 2. Relation between TRMM data and rain gauges on monthly and annual scales.

	Monthly		**Annual**	
	TRMM v6	**TRMM v7**	**TRMM v6**	**TRMM v7**
Correlation coefficient, R	0.86	0.90	0.82	0.90
Bias (mm)	6.42	5.98	95.73	61.56
Root mean squared error, RMSE (mm)	62.28	53.58	207.05	160.94
Standard deviation of differences, SD (mm)	61.17	52.45	183.63	148.74

We use evapotranspiration data provided by the Moderate Resolution Imaging Spectroradiometer (MODIS) ET product MOD16 (ftp://ftp.ntsg.umt.edu/pub/MODIS/Mirror/MOD16/), which are available at 1 km^2 spatial resolution and temporal resolution of 8-day, monthly and annual intervals. ET is estimated using a recently improved algorithm (Mu et al., 2011) that uses remote sensing inputs (MODIS satellite observations of land cover, leaf area index, albedo and fraction of absorbed photosynthetically active radiation) and daily meteorological inputs (air pressure, air temperature, humidity and radiation) to estimate ET using the Penman–Monteith equation. Ruhoff et al. (2013) inter-compare 8-day average MOD16 ET estimates and flux tower measurements between 2000 and 2002 for the sugar-cane plantation and the natural Cerrado vegetation in Brazil, and find correlation coefficients and root mean squared errors of R = 0.82, RMSE = 0.46 mm d^{-1} for sugar-cane, and R = 0.78, RMSE = 0.78 mm d^{-1} for Cerrado. They conclude that the MOD16 data provides accurate ET estimates, mainly over the long term (monthly and annual scales), and thus shows potential for spatial and temporal monitoring of ET in Brazil. Loarie et al. (2011) use data from 10 eddy covariance flux towers to validate ET estimates from MOD16 for the Brazilian Cerrado between 2000 and 2006. Their results indicate that, compared with observed data, annual ET averages vary less than ±4% for the savanna areas, ±5% in the tropical forest areas and ±13% in pasture/agriculture areas of the Cerrado.

The Gravity Recovery and Climate Experiment (GRACE) satellites have provided, since mid-2002, measurements of month-to-month variations of Earth's gravity field by measuring the distance between two orbiting satellites. Variations in Earth's gravity field are attributed to

changes in terrestrial water storage (TWS) after removal of atmospheric and ocean bottom pressure changes (Tapley et al., 2004). These data have been successfully used for hydrological studies in regions larger than 200,000 km^2 (Famiglietti and Rodell, 2013). The GRACE project provides time variable GRACE global gravity solutions from three processing centers: Geoforschungs Zentrum Potsdam (GFZ), the Jet Propulsion Laboratory (JPL), and the Center for Space Research (CSR) at the University of Texas. We use the direct measurement of TWS provided by GRACE release 05, available with spatial resolution of 1° × 1° (Landerer and Swenson, 2012). GRACE land data were processed by Sean Swenson (NASA MEaSUREs Program), and are available via the Jet Propulsion Laboratory's TELLUS website at http://grace.jpl.nasa.gov with monthly temporal resolution.

To evaluate the water budget closure, we use observed discharge data from the three largest river basins in the Cerrado, Paraná, São Francisco and Tocantins (Figure 1a). The data are available at http://hidroweb.ana.gov.br/, and the main features of time series of discharge studied are presented in the Table 3.

Table 3. Main features of the discharge time series.

Location	**River basin**	**Area (km^2)**	**Average annual precipitation (mm)**	**Time series (years)**
22° 42'S and 53° 10'W	Paraná	670,000	1450	1985 - 2010
11° 33'S and 43° 16'W	São Francisco	345,000	950	1955 - 2012
5° 47'S and 47° 28'W	Tocantins	298,559	1600	1974 - 2012
3° 45'S and 49° 38'W	Tocantins/Araguaia	742,300	1700	1978 - 2012*

* This time series was not used to evaluate water budget because in the measured data was not continuous through the study period (2003-2010). This time series was used to evaluate long time trends in the Tocantins/Araguaia River Basin.

2.3 Water balance dynamics

The water balance equation (Eq. 1) is based on the principle of mass conservation, also known as the continuity equation. To analyze the water balance of the Cerrado biome, we use a simplified equation, considering only the largest inputs and outputs at the monthly and annual time scales.

$$\frac{dS}{dt} = P - ET - Q \quad (1)$$

where S is the water storage change with time, P is precipitation, ET is evapotranspiration and Q is runoff.

Each monthly GRACE grid represents the mass anomaly defined as the difference in the masses for that month (m) and the baseline average over Jan 2004 to Dec 2009. As the GRACE data are given as mass anomalies for approximately 30-day observation periods at irregularly spaced intervals, the computation of monthly TWS change to approximate dS/dt is not straightforward. In this study the simple derivative method is used to estimate TWS change at a monthly scale. This method corresponds to the difference between two GRACE data points, which represents the average change in storage between the observation periods (Long et al., 2014; Wang et al., 2014):

$$\frac{dS}{dt} \approx \frac{TWS}{dt} \approx \frac{TWS(t+1) - TWS(t)}{\Delta t} \quad (2)$$

To make the other water balance components comparable with the TWS change at monthly steps, we use the monthly average of precipitation (TRMM), evapotranspiration (MOD16), and observed discharge to account for their contribution to the mass change (Rodell et al., 2004b; Sheffield et al., 2009; Wang et al., 2014):

$$\frac{dS}{dt} = \left(\frac{P_{(t+1)} + P_t}{2}\right) - \left(\frac{ET_{(t+1)} + ET_t}{2}\right) - \left(\frac{Q_{(t+1)} + Q_t}{2}\right) \quad (3)$$

We use equation 3 to estimate dS/dt and to assess the TWS change from GRACE at monthly scale. Furthermore, these results are used to discuss the seasonality of water balance in the Brazilian Cerrado. The annual water budget is computed to estimate the runoff as the residual of equation 1 and the results are assessed from the observed discharge (Table 3). In addition, the

results of annual water balance components are used to estimate trends in each water balance component across the Brazilian Cerrado (see section 2.4).

2.4 Uncertainty and trend analysis

The computed annual runoff is obtained as a residual of precipitation (TRMM), evapotranspiration (MOD 16) and terrestrial water storage (GRACE) (equation 1). Uncertainties in the runoff estimates are determined for each pixel from the method of moments (MOM) derived from a first order approximation of the Taylor series expansion (Refsgaard et al., 2007). If the components are independent of each other (no covariance between any two components), this MOM expansion reduces to Gaussian error propagation (Armanios and Fisher, 2014). Such an approach has been used reliably in numerous hydrological studies where the water budget was computed from GRACE and other remote sensing data (Rodell et al., 2004b; Sheffield et al., 2009; Voss et al., 2013; Armanios and Fisher, 2014; Long et al., 2014). The 95% confidence limits on the residual (runoff) are calculated as $\pm 2\sigma_{runoff}$.

$$\sigma_{runoff} = \sqrt{\sigma^2{}_{TRMM} + \sigma^2{}_{MOD16} + \sigma^2{}_{GRACE}} \quad (4)$$

where σ is the error estimated to each component.

The error estimated in TRMM v7 data is computed as the standard deviation of differences between TRMM and the value at each of the 402 corresponding rain gauges (see section 2.2), and then an error map is developed by kriging. To estimate the error in MOD16 data we use the Cerrado land cover map of 2010 [IBAMA/MMA/UNDP, 2011] to find the regions corresponding to native Cerrado and anthropic (pasture/agriculture) vegetation. Then we use the error values estimated by Loarie et al. (2011) for these two land cover types (±4% for the Cerrado and ±13% in pasture/agriculture areas) to estimate the uncertainties associated with the average ET values (2003-2010) for the entire Cerrado.

GRACE data have two distinct causes of error. The first is the loss of signal due to measurement error (based on the GRACE footprint) and the second is the "leakage" error (the contamination of a signal with a stronger adjacent signal) (Reager and Famiglietti, 2013). Thus, data preprocessing is necessary, which includes application of a destriping filter and a spherical harmonic filter cutoff at degree 60, with subsequent rescaling to restore much of the energy removed by these filtering processes (Swenson and Wahr, 2006; Proulx et al., 2013). The gridded fields of leakage, GRACE measurement errors, and scale factor have been processed by Sean Swenson (NASA MEaSUREs Program), and are available at http://grace.jpl.nasa.gov. The total error at each GRACE grid point is obtained by summing leakage and measurement errors in quadrature according to Landerer and Swenson (2012). More details about GRACE error estimation is provided by Landerer and Swenson (2012) and Swenson and Wahr (2006). Errors in TWS change used in equation 4 were computed from uncertainties in TWS anomaly for back and forward months added in quadrature (Long et al., 2014).

We analyze the annual values of precipitation, evapotranspiration, terrestrial water storage and runoff obtained from remote sensing data, and observed long-term discharge data to determine if there are statistically significant trends in the study period. The trend analysis is performed at each pixel using the Mann-Kendall test with Sen's slope estimates, with a 0.05 significance level (95% confidence level) using Matlab 7.12.0 (the p-value is the probability of getting a value of the test statistic at least as extreme as the one that was actually observed, assuming that the null hypothesis is true - i.e. time series values are independent, identically distributed). We use the statistically significant values of Sen's slope at each pixel to create trends maps using ArcGis 9.3 software.

3 Results and Discussion

3.1 Evaluation of estimated errors

Figure 2a shows that the main source of uncertainty in the computed runoff of the water budget is uncertainty in the TRMM data. In general, TRMM data from version 6 tend to overestimate rainfall in the Brazilian Cerrado, mainly in the southern portion, although there is underestimation in northeastern areas as well. Previous studies have reported overestimation in southern Brazil, and underestimation in the northeastern Cerrado and Amazon regions (Franchito et al., 2009; Rozante et al., 2010). However, we find that the new version 7 of TRMM notably reduces the bias from the measured precipitation data from 9.5% to 6%. Other similar research has shown significant improvement for TRMM 3B42 v7, thus indicating its potential for application in hydrological studies (Amitai et al., 2012; Xue et al., 2013; Chen et al., 2013). Furthermore, to evaluate overall annual water balance these errors are reasonable, representing less than 10% of the annual rainfall average over the entire Cerrado.

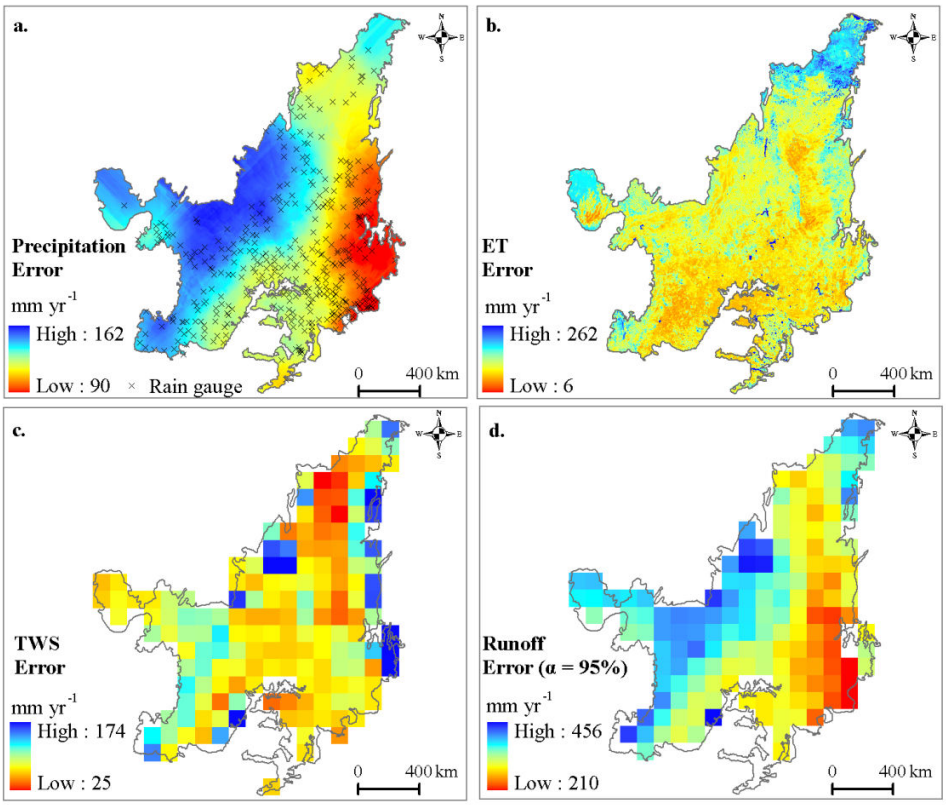

Figure 2. Errors computed for each water balance component.

Figure 2b shows that the errors estimated for ET are largest in the northern and smallest in the central and southern regions. We use the PROBIO land cover (PROBIO, 2004) and MOD16 ET data to evaluate the ET range in 2002 for the main cover classes of the Cerrado biome (Table 4), and find that the ranges of ET values obtained by MOD16 are similar to values obtained in previous studies that used eddy covariance flux towers or measurements of soil water balance (Table 4 and 5). For example, for the "Cerrado sensu stricto" we find mean and standard deviation values of 938.6 ± 323.2 mm yr^{-1} for the ET obtained from MOD16 data, whereas the values reported in the literature for this cover type range from 830.5 to 994.0 mm yr^{-1} (Table 4). ET values of reforestation presented in Table 4 are similar to the values obtained in studies of eucalyptus, i.e., 1179.5 ± 78.5 mm yr^{-1} (Cabral et al., 2010), which is the main type of reforested former cropland in the Cerrado area. The average of 2.6 ± 0.9 mm day^{-1} reported by Meirelles et al. (2011) for the *Brachiaria brizantha* pasture in the Brazilian savanna region is comparable to the annual values presented in Table 4. Croplands are not classified in the used PROBIO map, so no comparison between ET results for cropland cover is done.

Table 4. Studies of evapotranspiration in the Brazilian Cerrado.

Latitude	Longitude	State	Years	Precipitation	Land cover	Evapotranspiration	Method	Authors
21° 37'S	47° 38'W	SP	2005–2009	1478	Cerrado sensu stricto	830.5 mm yr^{-1}	Eddy covariance	Bruno, 2009
21° 35'S	47° 36'W	SP	2004–2005	1217	Cerrado sensu stricto	981.0 mm yr^{-1}	Eddy covariance	Bruno, 2009
21° 35'S	47° 36'W	SP	2005–2006	725	Cerrado sensu stricto	820.0 mm yr^{-1}	Eddy covariance	Bruno, 2009
21° 35'S	47° 36'W	SP	2006–2007	1721	Cerrado sensu stricto	994.0 mm yr^{-1}	Eddy covariance	Bruno, 2009
21° 35'S	47° 36'W	SP	2007–2008	1618	Cerrado sensu stricto	942.0 mm yr^{-1}	Eddy covariance	Bruno, 2009
15°56'S	47° 53'W	DF	2001–2003	1440	Cerrado Denso	823.0 mm yr^{-1}	Eddy covariance	Giambelluca et al., 2009
15°56'S	47°53'W	DF	2001–2003	1440	Campo Cerrado	689.0 mm yr^{-1}	Eddy covariance	Giambelluca et al., 2009
15°56'S	47°51'W	DF	1998–1999	1017	Campo Sujo	861.9 mm yr^{-1}	Eddy covariance	Santos et al., 2003
15°56'S	47°53'W	DF	1996–1998	1500	Cerrado denso	dry season = 1–4 mm day^{-1} and wet season = 5–8 mm day^{-1}	Water balance in soil (depth of 7.5 m)	Oliveira et al., 2005
15°56'S	47°53'W	DF	1996–1998	1500	Campo Sujo	dry season = 0–9 mm day^{-1} and wet season = 4–5 mm day^{-1}	Water balance in soil (depth of 4 m)	Oliveira et al., 2005
15°33'S	47°36'W	DF	2002–2006	1453	Cerrado sensu stricto	dry season = 20–25 mm $month^{-1}$ and wet season = 75–85 mm $month^{-1}$	Water balance in soil (depth of 7 m)	Garcia-Montiel et al., 2008
11°24'S	55°19'W	MT	1999–2000	2095	Transitional Amazonia–Cerrado forest	2.82 (± 0.33) mm day^{-1}	Eddy covariance	Vourlitis et al., 2002
9° 49'S	50° 08'W	AM	2003/2004 2004/2005 2005/2006	1692 1471 1914	Transitional Amazonia–Cerrado forest	1361 mm yr^{-1} 1318 mm yr^{-1} 1317 mm yr^{-1}	Eddy covariance	Borma et al., 2009

Years = length of record, Elevation (m), Precipitation = average annual precipitation (mm), Methods = evapotranspiration calculation methods. States: AM, Amazonas; MT, Mato Grosso; DF, Distrito Federal and SP, São Paulo.

Table 5. Average and standard deviation of annual evapotranspiration in the Cerrado biome in 2002.

Main land cover*	**Evapotranspiration (mm yr^{-1})**	**Area** (%)**
"Cerradão"	1272.0 ± 363.7	1.19
"Cerrado sensu stricto denso"	1268.5 ± 313.0	5.82
Savanna ("cerrado sensu stricto")	938.6 ± 323.2	46.88
Reforestation	1040.8 ± 258.1	1.01
Cropland	731.0 ± 239.4	10.32
Pasture	720.7 ± 202.6	29.29

*The main land cover classes, PROBIO map, year 2002, 1:250,000. **Percentage of area occupied by the land cover types.

The total errors from GRACE (the sum of leakage and measurement errors in quadrature) (Figure 2c) are in agreement with those reported in the literature (Landerer and Swenson, 2012; Proulx et al., 2013). Runoff uncertainties, at 95% significance (Figure 2d), are larger, and for some regions and years are larger than estimated runoff (Figure 3). However, the estimated values are similar to those from previous studies such as Sheffield et al. (2009) and Armanios and Fisher (2014), in which runoff was obtained as a residual of remote sensing data. We note that the greatest uncertainty values are concentrated in the western region, but in general the values are less than 300 mm yr^{-1} (Figure 2d).

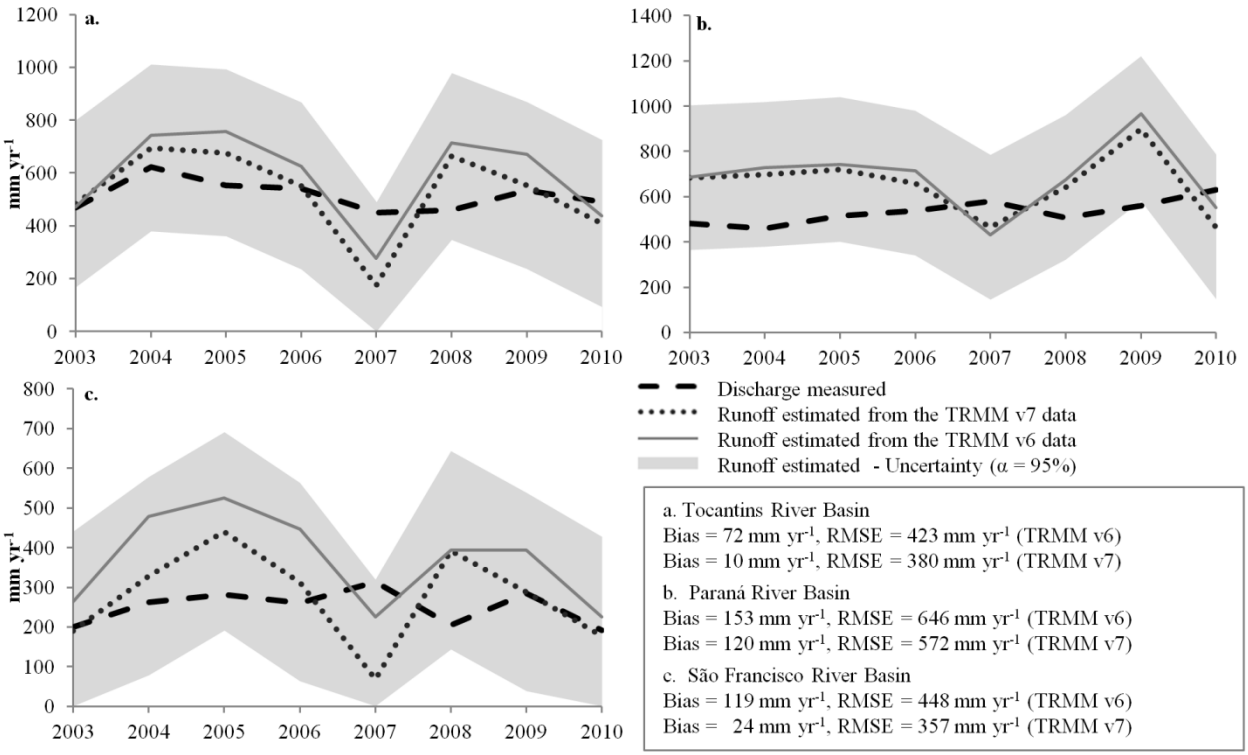

Figure 3. Comparison between runoff estimated and observed discharge. The area in grey color represents the uncertainty estimated with 95% significance in accordance with equation 2.

The runoff computed as a residual of the water budget equation using the TRMM v6 data overestimates the *in-situ* discharge, due mainly to TRMM v6 overestimation of the rainfall. Similar results are reported by (Sheffield et al., 2009) and (Gao et al., 2010). However, we note an improvement in results when the runoff is computed using the TRMM v7 data (Figure 3). The biases for Tocantins and São Francisco river basin when using TRMM v7 are around 7 times less than the biases computed using TRMM v6. The uncertainties estimated for runoff (presented at 95% significance) are high, and for some regions and years are larger than the runoff estimate itself (as obtained from the water budget equation). However, its important to note that the measured discharge values are themselves not precise, with uncertainties ranging between 2% (under ideal conditions) to over 20% (Sauer and Meyer, 1992). Further, we find the behavior of increases and decreases in the estimated runoff and measured discharge to be similar, except for 2007 in the Paraná and São Francisco River basins, which indicate a slight increase in discharge whereas the estimated runoff decreases in that year.

3.2 Water budget and trends in the Cerrado

The water storage change (dS/dt) computed from equation 1 shows a significant correlation with TWS change obtained from GRACE data for all watersheds studied (Figure 4 d. e. and f.). Our results indicate that GRACE data may represent the TWS change in the Brazilian Cerrado satisfactorily; allowing assessment of the seasonality of the water balance in this region. These results are consistent with those reported by Almeida et al. (2012) and Frappart et al. (2013) for the Amazon region. The El Niño events of 2007 and 2010 are probably responsible for the major droughts in the watersheds studied. In these years the drought season was longer than in the other years; i.e. the amount of rainfall between April to September (dry season in the Cerrado) was low, causing less water storage and more dryness in the period (Figure 4 a. b and c.). In 2007 the total rainfall in those months was on average 40% lower than the average rainfall (260 mm, 310 mm and 152 mm) in the same period in Tocantins, Parana and São Francisco river basins, respectively.

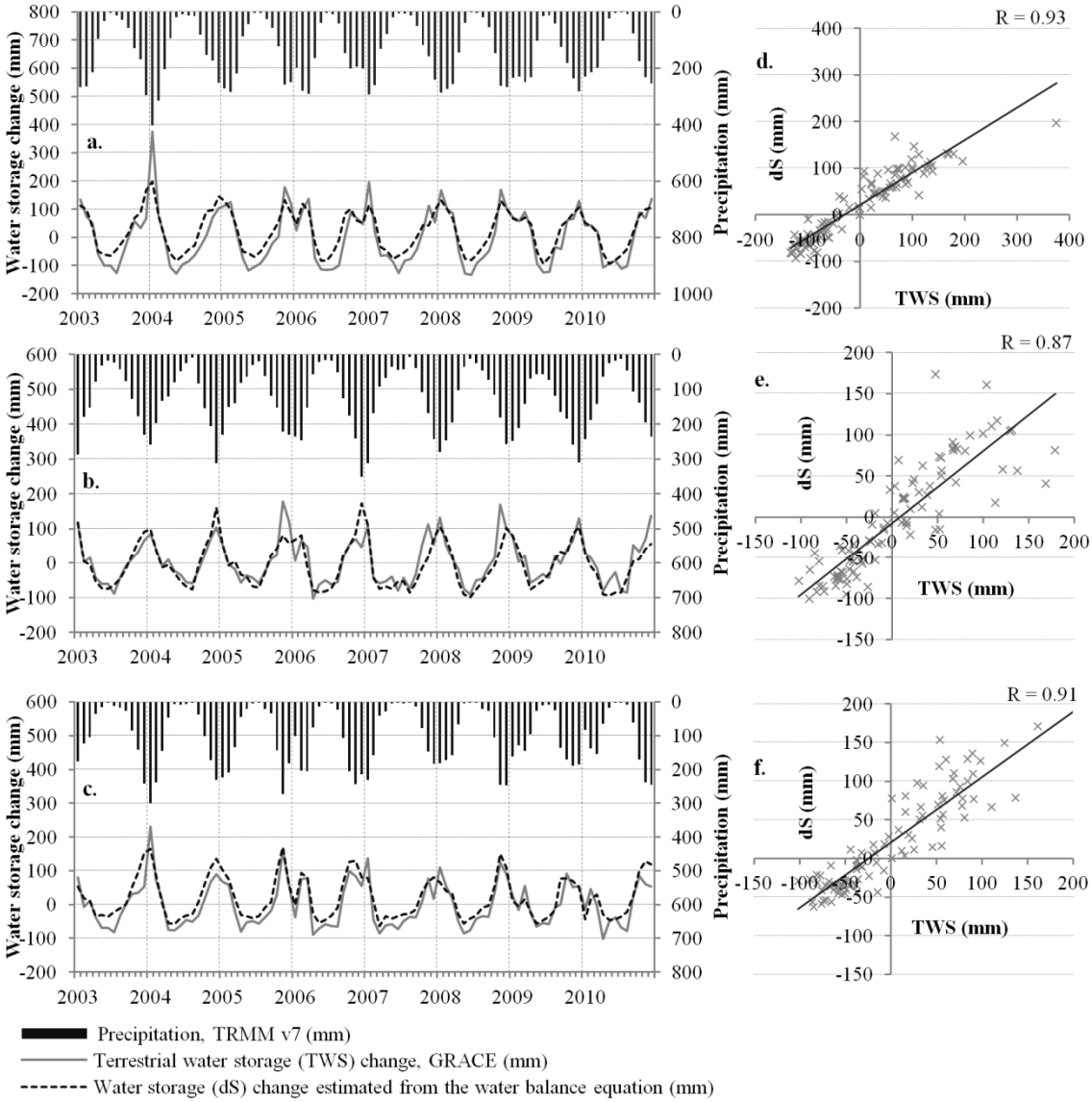

Figure 4. Monthly water storage change (d*S*) estimated from the water balance equation (equation 1) and the TWS obtained from GRACE data, and coefficients of correlation between them, (a and d) the Tocantins River basin, (b and e) the Parana River basin, and (c and f) the São Francisco River basin.

There is a correspondence in time of the severe 2010 drought in the Amazonia (Lewis et al., 2011), with the one experienced in the Brazilian Cerrado, though the 2005 Amazonian drought was not recorded in the Cerrado with the same severity (Marengo et al., 2008). Although the drought years observed for the Tocantins, São Francisco, and Paraná River basins occurred in similar periods (Figure 4a, b and c.), it is possible to identify different features in each river basin, mainly between São Francisco and Tocantins, the driest and the wettest basins, respectively. The São Francisco river basin had lower precipitation and water storage than the Tocantins River basin (on average less than 28% and 70%, respectively).

The major drought occurred in 2007, when annual precipitation (1201 mm) was ~20% less than the mean for the entire period. The States of Bahia-BA, the north of Minas Gerais-MG, Piaui-PI and Maranhão-MA had several regions with water deficits (ET > P). This can be noted in the São Francisco River basin where some of these states are located (Figure 5d). These regions have borders with the Caatinga biome and receive less rainfall and more radiation than other regions of the Cerrado (Hastenrath, 2012), consequently less water storage and runoff (Figures 4c and 5d). The 2007 drought was considered severe especially in the north of Minas Gerais-MG and in the Brazilian northwest, with a shortage on water availability, accompanied by crop loss and hydroelectric production loss. On November 2007, the Sobradinho reservoir (which has water springs in the Cerrado area) stored only 15% of its total volume capacity, and an emergency was decreed in 158 cities in the State of Paraiba (Marengo, 2008).

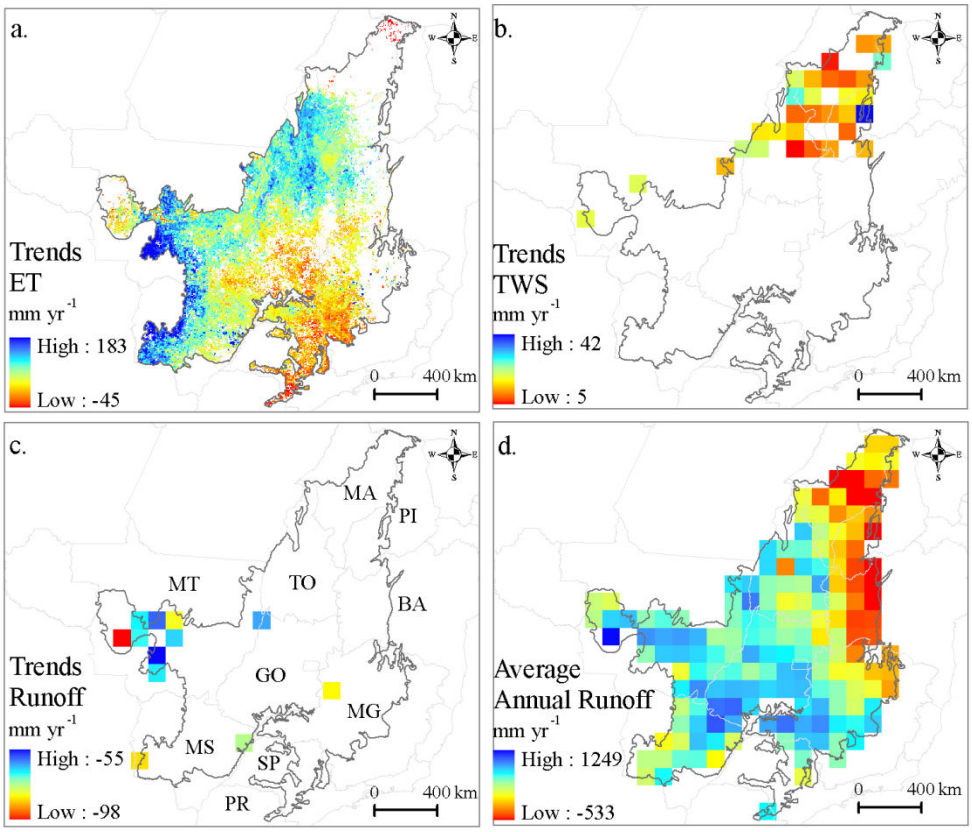

Figure 5. Significant trends in annual water balance components between 2003 and 2010 for: a. evapotranspiration, b. terrestrial water storage and c. runoff. White means no trend. We did not find any significant trends in annual precipitation. d. Average annual runoff (2003 - 2010). Each trend analysis was evaluated using Mann-Kendall test and with Sen's slope estimates (95% confidence level).

The annual ET tended to decrease in the western part of Mato Grosso-MT, North of Maranhão-MA and part of São Paulo-SP and Minas Gerais-MG up to 45 mm yr^{-1} on average during the study period (Figure 5a). The states of MT and MA had the greatest deforestation index, representing about 40% of the total deforestation between 2002-2010 (IBAMA/MMA/UNDP, 2011). However, we find a significant trend of increasing annual ET on average over the entire Cerrado of 51 ± 15 mm yr^{-1}, and changes as large as 183 mm yr^{-1} averaged over the western parts of Mato Grosso and Mato Grosso do Sul (near the Pantanal - wetland Biome) and northern parts of Tocantins-TO (near the Amazon rainforest Biome) (Figure 5a). Our results are consistent with those presented by Zeng et al. (2012), who found the global land ET increased from 1982 to 2009 with the Amazon and part of Cerrado biome having the highest rates of ET increase.

We can suggest at least three hypotheses to explain the increase in annual ET. The first is that anthropic activities that reduce ET, such as deforestation, can be offset by other anthropic activities that act in an opposite manner, such as irrigation and reservoir creation (Gordon et al., 2005; Sterling et al., 2013). The second is that the land use change in the Cerrado biome of the pasture to crops (Phalan et al., 2013) could have increased the ET in the study period. To evaluate this hypothesis, we examine annual ET data in an area of the 45 km^2 that was deforested in 2009, located in the State of Maranhão-MA (42.87ºW 3.32ºS). These data indicate that the initial consequence of deforestation was an ET decrease of 36% (429 mm) between 2008 and 2009, followed in the second year by an ET increase to a level near the pre-deforestation level (Figure 6). In other words, new crop cultivation in the area of deforestation decreased the ET for only a year, after which it returned to a level not statistically different from the original native vegetation. Loarie et al. (2011) reported similar results in two other Cerrado areas (located in States of Mato Grosso-MT and São Paulo-SP). They found that conversion of Cerrado to pasture led to a decrease of ET, whereas conversion of pasture to sugarcane led to an increase of ET. Therefore, land use and land cover change promote changes in ET, and for large regions with multiple types of land use change and weather variation it becomes difficult to evaluate changes in this component, due to compensation between activities that increase and decrease ET (Gordon et al., 2005). The third hypothesis is that the ET increases have been accelerating due to increased evaporative demand associated with rising radiative forcing, atmospheric CO_2 concentrations, and temperatures (Jung et al., 2010). All these hypotheses must be carefully studied in the future

with a long enough data period to evaluate the factors that are influencing the ET changes in this region.

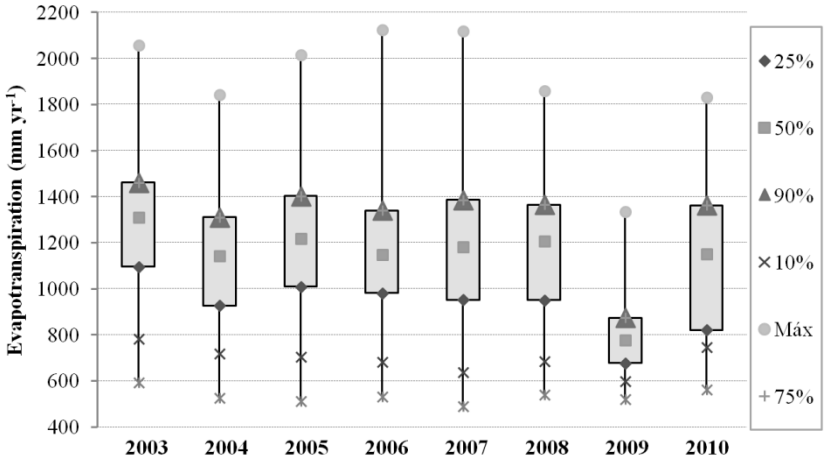

Figure 6. Evapotranspiration in an area of 45 km^2 that was deforested in 2009, located in the State of Maranhão-MA (42.87ºW 3.32ºS). We used the values of all the pixels (Number of pixels, N=54) in this polygon to develop this figure.

Figure 5b indicates that a significant increasing trend in annual terrestrial water storage (TWS) with average changes of 11 ± 6 mm yr^{-1}, in the States of Maranhão-MA, Piaui-PI and Tocantins-TO, northeast region of the Brazilian Cerrado. The TWS values tend to increase with changes in land uses that promote more infiltration, percolation, and groundwater recharge. Note that the native Cerrado tends to promote more infiltration than areas used for pasture and cropland. Meanwhile, the canopy interception values in the native Cerrado vegetation are approximately 20% of gross rainfall (Oliveira et al., 2014) and the greater use of water by native Cerrado vegetation for transpiration (Giambelluca et al., 2009) tends to result in smaller groundwater recharge than for pasture and cropland (Lucas et al., 2012). In a Cerrado region, Wendland et al. (2007) found values of groundwater recharge ranging from 145 to 703 mm yr^{-1} in pasture, 324 - 694 mm yr^{-1} in orange citrus, and 37 to 48 mm yr^{-1} in Eucalyptus. Therefore, increasing trends in TWS found in the northeast region of the Brazilian Cerrado may indicate a deforestation process or other changes in the land use and cover that promot more infiltration and groundwater recharge, such as crops or pasture.

Despite the fact that precipitation does not show a significant trend during the study period, probably because of the relatively short time series available, we find that estimated annual runoff tends to decrease by an average of 72 ± 11 mm yr^{-1} in a few isolated spots and in the western of the State of Mato Grosso-MT (Figure 5c). From the analysis using the long-term data (1952-2012), we note a significant trend in decreasing discharge for the Tocantins

(18.3 km^3 yr^{-1}) and Tocantins/Araguaia (40.3 km^3 yr^{-1}) River basins (Figure 7a and b); whereas we do not find any trend in the São Francisco and Paraná River basins (Figure 7c and d). In two watersheds located in the headwater of Tocantins and Araguaia Rivers (areas = 175,360 km^2 and 82,632 km^2), previous studies have reported that annual mean discharge increased 24% from the 1979 to 1998, and 25% between 1970 to 1990 in these two rivers, respectively (Costa et al., 2003; Coe et al., 2011). However, the difference between the watersheds sizes studied in the present paper and in these two previous studies may have caused different results. Some previous large-scale studies have presented results that do not agree with the results from a more detailed scale (Wilk et al., 2001; Costa et al., 2003). In other words, the response times for watersheds are dependent on the scale studied. Thus, in small watersheds it is usually easier to find a response to land use and land cover changes on the water balance components than in large watersheds.

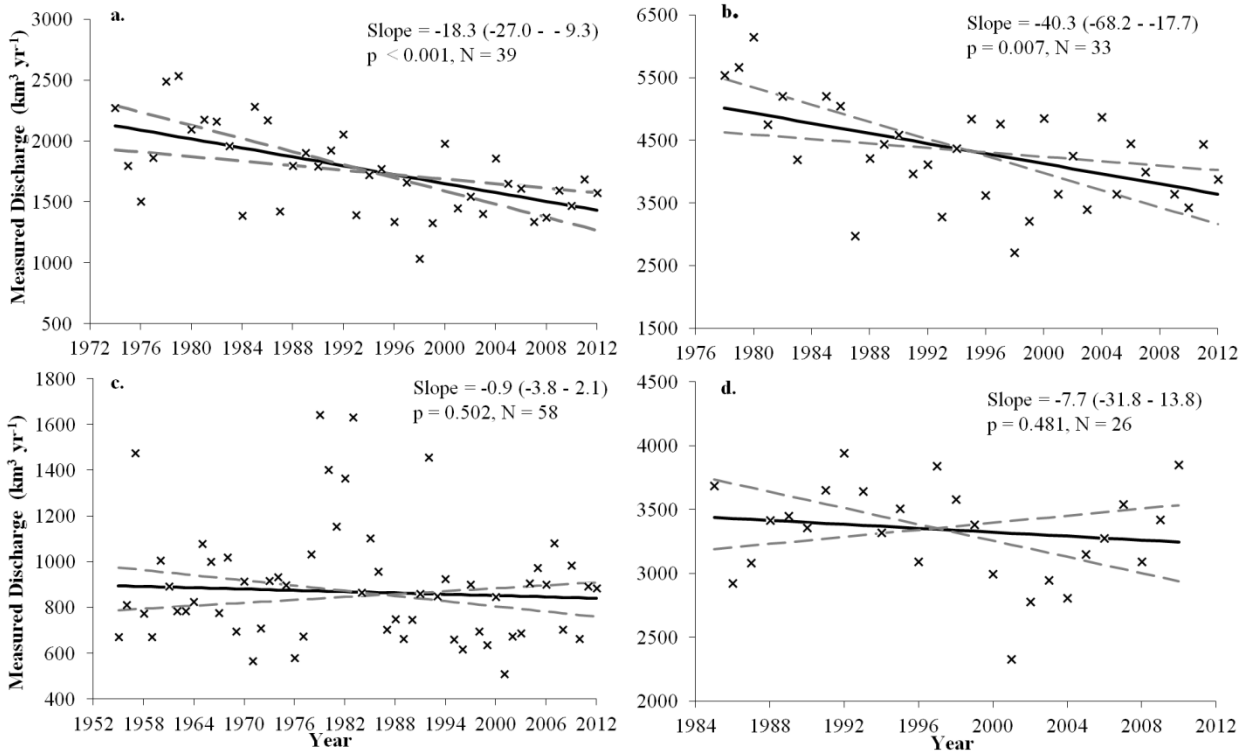

Figure 7. Long-term of observed annual discharge for: a. Tocantins River; b. Tocantins/Araguaia River basin; c. São Francisco River basin, and d. Paraná River basin. Where the p values less than 0.05 show significant trend to measured discharge.

4 Conclusions

We evaluate the water budget for the Brazilian Cerrado from remote sensing data of precipitation (TRMM), evapotranspiration (MOD16), and terrestrial water storage (GRACE) for the period from 2003 to 2010. We assess trends in each water balance component obtained from remote sensing data, and in observed discharge using the Mann-Kendall test and with Sen's slope estimates with a 0.05 significance level. The uncertainties are computed for each remotely sensed data set and the budget closure is evaluated from *in-situ* discharge data for the three biggest river basins in the Cerrado, Paraná, São Francisco and Tocantins.

The main source of water budget uncertainty in the estimated runoff arises from errors in the TRMM precipitation data. In general, TRMM v6 data tend to overestimate the ground-measured rainfall in the Brazilian Cerrado, mainly in the southern part, although there is an underestimation in the northeast. However, our results show that the new version of TRMM 3B42 v7 notably reduces the bias between TRMM and the measured precipitation data from 9.5% to 6%, thus improving its potential application in hydrological studies.

We note that the water storage change (dS/dt) computed as a residual of the water budget equation using remote sensing data (TRMM and MOD16) and measured discharge data shows a significant correlation with TWS change obtained from the GRACE data for all watersheds studied. The results indicate that the GRACE data may provide a satisfactory representation of water storage change for large areas in the Brazilian Cerrado.

We conclude that water budget closure from remote sensing remains a challenge due to uncertainties in the data. However, this approach demonstrates the potential to evaluate trends in water balance components over large regions, identify drier periods, and assess changes in water balance due to land cover and land use changes.

Our results also indicate that deforestation promotes a significant decrease in evapotranspiration at the local level. However, deforestation alone cannot account for all of the recent changes in water balance in the Cerrado, because other anthropic activities such as irrigation and reservoir creation also act to modify the water balance. In other words, the response time to watershed change is dependent on the scale studied. Therefore, water balance results obtained for small areas can be different that those over larger areas, illustrating the need to study the responses at different scales.

5 Acknowledgments

This study was supported by grants from the Fundação de Amparo à Pesquisa do Estado de São Paulo - FAPESP (10/18788-5, 11/14273-3 and 12/03764-9) and the Conselho Nacional de Desenvolvimento Científico e Tecnológico - CNPq (470846/2011-9). USDA is an equal opportunity provider and employer. The authors are grateful to Sean Swenson of the National Center for Atmospheric research for GRACE data processing, and to Qiaozhen Mu, National Aeronautics and Space Administration, and Agência Nacional de Águas (ANA) for providing ET data (from MOD16), TRMM data and observed rainfall and measured discharge data, respectively. We also thank Dr. Matthew Rodell (Chief, Hydrological Sciences Laboratory, NASA/GSFC) for helping in the data analysis. Finally, we appreciate valuable comments and careful reviews from editors, the reviewer Dr. Augusto Getirana (Hydrological Sciences Laboratory, NASA/GSFC), and other four anonymous reviewers who helped significantly to improve this manuscript.

6 References

Almeida, F. G. V. de, Calmant, S., Seyler, F., Ramillien, G., Blitzkow, D., Matos, A. C. C., & Silva, J. S. (2012). Time-variations of equivalent water heights'from Grace Mission and in-situ river stages in the Amazon basin. *Acta Amazonica*, *42*(1), 125–134. doi:10.1590/S0044-59672012000100015

Amitai, E., Unkrich, C. L., Goodrich, D. C., Habib, E., & Thill, B. (2012). Assessing Satellite-Based Rainfall Estimates in Semiarid Watersheds Using the USDA-ARS Walnut Gulch Gauge Network and TRMM PR. *Journal of Hydrometeorology*, *13*(5), 1579–1588. doi:10.1175/JHM-D-12-016.1

Anderson, R. G., Lo, M.-H., & Famiglietti, J. S. (2012). Assessing surface water consumption using remotely-sensed groundwater, evapotranspiration, and precipitation: Surface water consumption. *Geophysical Research Letters*, *39*(16), n/a–n/a. doi:10.1029/2012GL052400

Armanios, D. E., & Fisher, J. B. (2014). Measuring water availability with limited ground data: assessing the feasibility of an entirely remote-sensing-based hydrologic budget of the Rufiji Basin, Tanzania, using TRMM, GRACE, MODIS, SRB, and AIRS: Measuring water availability with limited ground data. *Hydrological Processes*, *28*(3), 853–867. doi:10.1002/hyp.9611

Borma, L. S., da Rocha, H. R., Cabral, O. M., von Randow, C., Collicchio, E., Kurzatkowski, D., … Artaxo, P. (2009). Atmosphere and hydrological controls of the evapotranspiration over a floodplain forest in the Bananal Island region, Amazonia. *Journal of Geophysical Research*, *114*(G1). doi:10.1029/2007JG000641

Brannstrom, C., Jepson, W., Filippi, A. M., Redo, D., Xu, Z., & Ganesh, S. (2008). Land change in the Brazilian Savanna (Cerrado), 1986–2002: Comparative analysis and implications for land-use policy. *Land Use Policy*, *25*(4), 579–595. doi:10.1016/j.landusepol.2007.11.008

Bruno, R.D. (2009), Balanço de água em microbacias de cerrado restrito e eucalipto: um estudo de caso com medidas observacionais, Ph.D. thesis, IAG, University of São Paulo, São Paulo, Brazil. (90pp)

Cabral, O. M. R., Rocha, H. R., Gash, J. H. C., Ligo, M. A. V., Freitas, H. C., & Tatsch, J. D. (2010). The energy and water balance of a Eucalyptus plantation in southeast Brazil. *Journal of Hydrology*, *388*(3-4), 208–216. doi:10.1016/j.jhydrol.2010.04.041

Chen, S., Hong, Y., Gourley, J. J., Huffman, G. J., Tian, Y., Cao, Q., … Xue, X. (2013). Evaluation of the successive V6 and V7 TRMM multisatellite precipitation analysis over the Continental United States: Evaluation of successive tmpa over conus. *Water Resources Research*, *49*(12), 8174–8186. doi:10.1002/2012WR012795

Coe, M. T., Latrubesse, E. M., Ferreira, M. E., & Amsler, M. L. (2011). The effects of deforestation and climate variability on the streamflow of the Araguaia River, Brazil. *Biogeochemistry*, *105*(1-3), 119–131. doi:10.1007/s10533-011-9582-2

Costa, M. H., Botta, A., & Cardille, J. A. (2003). Effects of large-scale changes in land cover on the discharge of the Tocantins River, Southeastern Amazonia. *Journal of Hydrology*, *283*(1-4), 206–217. doi:10.1016/S0022-1694(03)00267-1

Famiglietti, J. S., & Rodell, M. (2013). Water in the Balance. *Science*, *340*(6138), 1300–1301. doi:10.1126/science.1236460

Ferreira, L. G., & Huete, A. R. (2004). Assessing the seasonal dynamics of the Brazilian Cerrado vegetation through the use of spectral vegetation indices. *International Journal of Remote Sensing*, *25*(10), 1837–1860. doi:10.1080/0143116031000101530

Franchito, S. H., Rao, V. B., Vasques, A. C., Santo, C. M. E., & Conforte, J. C. (2009). Validation of TRMM precipitation radar monthly rainfall estimates over Brazil. *Journal of Geophysical Research*, *114*(D2). doi:10.1029/2007JD009580

Frappart, F., Seoane, L., & Ramillien, G. (2013). Validation of GRACE-derived terrestrial water storage from a regional approach over South America. *Remote Sensing of Environment*, *137*, 69–83. doi:10.1016/j.rse.2013.06.008

Furley, P. A. (1999). The nature and diversity of neotropical savanna vegetation with particular reference to the Brazilian cerrados. *Global Ecology and Biogeography*, *8*(3-4), 223–241. doi:10.1046/j.1466-822X.1999.00142.x

Gao, H., Tang, Q., Ferguson, C. R., Wood, E. F., & Lettenmaier, D. P. (2010). Estimating the water budget of major US river basins via remote sensing. *International Journal of Remote Sensing*, *31*(14), 3955–3978. doi:10.1080/01431161.2010.483488

Garcia-Montiel, D. C., Coe, M. T., Cruz, M. P., Ferreira, J. N., da Silva, E. M., & Davidson, E. A. (2008). Estimating Seasonal Changes in Volumetric Soil Water Content at Landscape Scales in a Savanna Ecosystem Using Two-Dimensional Resistivity Profiling. *Earth Interactions*, *12*(2), 1–25. doi:10.1175/2007EI238.1

Giambelluca, T. W., Scholz, F. G., Bucci, S. J., Meinzer, F. C., Goldstein, G., Hoffmann, W. A., … Buchert, M. P. (2009). Evapotranspiration and energy balance of Brazilian savannas with contrasting tree density. *Agricultural and Forest Meteorology*, *149*(8), 1365–1376. doi:10.1016/j.agrformet.2009.03.006

Gordon, L. J., Steffen, W., Jonsson, B. F., Folke, C., Falkenmark, M., & Johannessen, A. (2005). Human modification of global water vapor flows from the land surface. *Proceedings of the National Academy of Sciences*, *102*(21), 7612–7617. doi:10.1073/pnas.0500208102

Hastenrath, S. (2012). Exploring the climate problems of Brazil's Nordeste: a review. *Climatic Change*, *112*(2), 243–251. doi:10.1007/s10584-011-0227-1

Huffman, G. J., Bolvin, D. T., Nelkin, E. J., Wolff, D. B., Adler, R. F., Gu, G., … Stocker, E. F. (2007). The TRMM Multisatellite Precipitation Analysis (TMPA): Quasi-Global, Multiyear, Combined-Sensor Precipitation Estimates at Fine Scales. *Journal of Hydrometeorology*, *8*(1), 38–55. doi:10.1175/JHM560.1

IBAMA/MMA/UNDP. Monitoramento do desmatamento nos biomas Brasileiros por satélite. available at: http://siscom.ibama.gov.br/monitorabiomas/cerrado/index.htm.

Jepson, W., Brannstrom, C., & Filippi, A. (2010). Access Regimes and Regional Land Change in the Brazilian Cerrado, 1972–2002. *Annals of the Association of American Geographers*, *100*(1), 87–111. doi:10.1080/00045600903378960

Jung, M., Reichstein, M., Ciais, P., Seneviratne, S. I., Sheffield, J., Goulden, M. L., … Zhang, K. (2010). Recent decline in the global land evapotranspiration trend due to limited moisture supply. *Nature*, *467*(7318), 951–954. doi:10.1038/nature09396

Landerer, F. W., & Swenson, S. C. (2012). Accuracy of scaled GRACE terrestrial water storage estimates: ACCURACY OF GRACE-TWS. *Water Resources Research*, *48*(4), n/a–n/a. doi:10.1029/2011WR011453

Lathuillière, M. J., Johnson, M. S., & Donner, S. D. (2012). Water use by terrestrial ecosystems: temporal variability in rainforest and agricultural contributions to evapotranspiration in Mato Grosso, Brazil. *Environmental Research Letters*, *7*(2), 024024. doi:10.1088/1748-9326/7/2/024024

Lewis, S. L., Brando, P. M., Phillips, O. L., van der Heijden, G. M. F., & Nepstad, D. (2011). The 2010 Amazon Drought. *Science*, *331*(6017), 554–554. doi:10.1126/science.1200807

Loarie, S. R., Lobell, D. B., Asner, G. P., Mu, Q., & Field, C. B. (2011). Direct impacts on local climate of sugar-cane expansion in Brazil. *Nature Climate Change*, *1*(2), 105–109. doi:10.1038/nclimate1067

Long, D., Longuevergne, L., & Scanlon, B. R. (2014). Uncertainty in evapotranspiration from land surface modeling, remote sensing, and GRACE satellites. *Water Resources Research*, *50*(2), 1131–1151. doi:10.1002/2013WR014581

Lucas, M.C., R.C. Guanabara, and E. Wendland (2012), Estimativa de recarga subterrânea em área de afloramento do Sistema Aquífero Guarani, *Boletín Geológico y Minero* 123(3), 311-323.

Marengo, J. A., Nobre, C. A., Tomasella, J., Oyama, M. D., Sampaio de Oliveira, G., de Oliveira, R., … Brown, I. F. (2008). The Drought of Amazonia in 2005. *Journal of Climate*, *21*(3), 495–516. doi:10.1175/2007JCLI1600.1

Marengo, J.A. (2008), Vulnerabilidade, impactos e adaptação à mudança do clima no semi-árido do Brasil, *Parcerias Estratégicas* 13, 149-176.

Marris, E. (2005). Conservation in Brazil: The forgotten ecosystem. *Nature*, *437*(7061), 944–945. doi:10.1038/437944a

Meirelles, M. L., Franco, A. C., Farias, S. E. M., & Bracho, R. (2011). Evapotranspiration and plant-atmospheric coupling in a Brachiaria brizantha pasture in the Brazilian savannah region: Evapotranspiration and plant-atmospheric coupling. *Grass and Forage Science*, *66*(2), 206–213. doi:10.1111/j.1365-2494.2010.00777.x

Miralles, D. G., De Jeu, R. A. M., Gash, J. H., Holmes, T. R. H., & Dolman, A. J. (2011). Magnitude and variability of land evaporation and its components at the global scale. *Hydrology and Earth System Sciences*, *15*(3), 967–981. doi:10.5194/hess-15-967-2011

Mu, Q., Zhao, M., & Running, S. W. (2011). Improvements to a MODIS global terrestrial evapotranspiration algorithm. *Remote Sensing of Environment*, *115*(8), 1781–1800. doi:10.1016/j.rse.2011.02.019

Myers, N., Mittermeier, R. A., Mittermeier, C. G., Da Fonseca, G. A., & Kent, J. (2000). Biodiversity hotspots for conservation priorities. *Nature*, *403*(6772), 853–858.

Ochoa, A., Pineda, L., Willems, P., & Crespo, P. (2014). Evaluation of TRMM 3B42 (TMPA) precipitation estimates and WRF retrospective precipitation simulation over the Pacific-Andean basin into Ecuador and Peru. *Hydrology and Earth System Sciences Discussions*, *11*(1), 411–449. doi:10.5194/hessd-11-411-2014

Oliveira, P.T.S., Wendland, E., Nearing, M.A. & Martins, J.P. (2014). Interception of rainfall and surface runoff in the Brazilian Cerrado. Geophysical Research Abstracts 16, EGU2014-4780.

Oliveira, R. S., Bezerra, L., Davidson, E. A., Pinto, F., Klink, C. A., Nepstad, D. C., & Moreira, A. (2005). Deep root function in soil water dynamics in cerrado savannas of central Brazil. *Functional Ecology*, *19*(4), 574–581. doi:10.1111/j.1365-2435.2005.01003.x

Peel, M. C., Finlayson, B. L., & McMahon, T. A. (2007). Updated world map of the Köppen-Geiger climate classification. *Hydrology and Earth System Sciences*, *11*(5), 1633–1644. doi:10.5194/hess-11-1633-2007

Phalan, B., Bertzky, M., Butchart, S. H. M., Donald, P. F., Scharlemann, J. P. W., Stattersfield, A. J., & Balmford, A. (2013). Crop Expansion and Conservation Priorities in Tropical Countries. *PLoS ONE*, *8*(1), e51759. doi:10.1371/journal.pone.0051759

PROBIO (2004), Projeto de Conservação e Utilização Sustentável da Diversidade Biológica Brasileira. Mapeamento dos biomas brasileiros, escala 1:250,000. Brasilia, DF, Brazil.

Proulx, R. A., Knudson, M. D., Kirilenko, A., VanLooy, J. A., & Zhang, X. (2013). Significance of surface water in the terrestrial water budget: A case study in the Prairie Coteau using GRACE, GLDAS, Landsat, and groundwater well data: Prairie Coteau Terrestrial Water Budget. *Water Resources Research*, *49*(9), 5756–5764. doi:10.1002/wrcr.20455

Ratter, J. (1997). The Brazilian Cerrado Vegetation and Threats to its Biodiversity. *Annals of Botany*, *80*(3), 223–230. doi:10.1006/anbo.1997.0469

Reager, J. T., & Famiglietti, J. S. (2009). Global terrestrial water storage capacity and flood potential using GRACE. *Geophysical Research Letters*, *36*(23). doi:10.1029/2009GL040826

Reager, J. T., & Famiglietti, J. S. (2013). Characteristic mega-basin water storage behavior using GRACE: CHARACTERISTIC Water Storage Behavior Using Grace. *Water Resources Research*, *49*(6), 3314–3329. doi:10.1002/wrcr.20264

Refsgaard, J. C., van der Sluijs, J. P., Højberg, A. L., & Vanrolleghem, P. A. (2007). Uncertainty in the environmental modelling process – A framework and guidance. *Environmental Modelling & Software*, *22*(11), 1543–1556. doi:10.1016/j.envsoft.2007.02.004

Rodell, M. (2004). Basin scale estimates of evapotranspiration using GRACE and other observations. *Geophysical Research Letters*, *31*(20). doi:10.1029/2004GL020873

Rodell, M., Houser, P. R., Jambor, U., Gottschalck, J., Mitchell, K., Meng, C.-J., … Toll, D. (2004). The Global Land Data Assimilation System. *Bulletin of the American Meteorological Society*, *85*(3), 381–394. doi:10.1175/BAMS-85-3-381

Rozante, J. R., Moreira, D. S., de Goncalves, L. G. G., & Vila, D. A. (2010). Combining TRMM and Surface Observations of Precipitation: Technique and Validation over South America. *Weather and Forecasting*, *25*(3), 885–894. doi:10.1175/2010WAF2222325.1

Ruhoff, A. L., Paz, A. R., Aragao, L. E. O. C., Mu, Q., Malhi, Y., Collischonn, W., … Running, S. W. (2013). Assessment of the MODIS global evapotranspiration algorithm using eddy covariance measurements and hydrological modelling in the Rio Grande basin. *Hydrological Sciences Journal*, *58*(8), 1658–1676. doi:10.1080/02626667.2013.837578

Sano, E. E., Rosa, R., Brito, J. L. S., & Ferreira, L. G. (2010). Land cover mapping of the tropical savanna region in Brazil. *Environmental Monitoring and Assessment*, *166*(1-4), 113–124. doi:10.1007/s10661-009-0988-4

Santos, A. J. B., Silva, G. T. D. A., Miranda, H. S., Miranda, A. C., & Lloyd, J. (2003). Effects of fire on surface carbon, energy and water vapour fluxes over campo sujo savanna in central Brazil. *Functional Ecology*, *17*(6), 711–719. doi:10.1111/j.1365-2435.2003.00790.x

Sauer VB, and RW. Meyer (1992), Determination of error in individual discharge measurements. *U.S. Geological Survey Open-file Report 92–144*: 21pp.

Scanlon, B. R., Longuevergne, L., & Long, D. (2012). Ground referencing GRACE satellite estimates of groundwater storage changes in the California Central Valley, USA: GRACE groundwater depletion Central Valley CA. *Water Resources Research*, *48*(4), W04520. doi:10.1029/2011WR011312

Sheffield, J., Ferguson, C. R., Troy, T. J., Wood, E. F., & McCabe, M. F. (2009). Closing the terrestrial water budget from satellite remote sensing: WATER BUDGET FROM REMOTE SENSING. *Geophysical Research Letters*, *36*(7), n/a–n/a. doi:10.1029/2009GL037338

Sheffield, J., Wood, E. F., & Roderick, M. L. (2012). Little change in global drought over the past 60 years. *Nature*, *491*(7424), 435–438. doi:10.1038/nature11575

Spracklen, D. V., Arnold, S. R., & Taylor, C. M. (2012). Observations of increased tropical rainfall preceded by air passage over forests. *Nature*, *489*(7415), 282–285. doi:10.1038/nature11390

Staver, A. C., Archibald, S., & Levin, S. A. (2011). The Global Extent and Determinants of Savanna and Forest as Alternative Biome States. *Science*, *334*(6053), 230–232. doi:10.1126/science.1210465

Sterling, S. M., Ducharne, A., & Polcher, J. (2012). The impact of global land-cover change on the terrestrial water cycle. *Nature Climate Change*, *3*(4), 385–390. doi:10.1038/nclimate1690

Swenson, S., & Wahr, J. (2006). Post-processing removal of correlated errors in GRACE data. *Geophysical Research Letters*, *33*(8). doi:10.1029/2005GL025285

Tapley, B. D. (2004). GRACE Measurements of Mass Variability in the Earth System. *Science*, *305*(5683), 503–505. doi:10.1126/science.1099192

Teuling, A. J., Van Loon, A. F., Seneviratne, S. I., Lehner, I., Aubinet, M., Heinesch, B., … Spank, U. (2013). Evapotranspiration amplifies European summer drought: EVAPOTRANSPIRATION AND SUMMER DROUGHTS DROUGHTS. *Geophysical Research Letters*, *40*(10), 2071–2075. doi:10.1002/grl.50495

Voss, K. A., Famiglietti, J. S., Lo, M., de Linage, C., Rodell, M., & Swenson, S. C. (2013). Groundwater depletion in the Middle East from GRACE with implications for transboundary water management in the Tigris-Euphrates-Western Iran region:

GROUNDWATER DEPLETION IN THE MIDDLE EAST FROM GRACE. *Water Resources Research*, *49*(2), 904–914. doi:10.1002/wrcr.20078

Vourlitis, G. L., Filho, N. P., Hayashi, M. M. S., de S. Nogueira, J., Caseiro, F. T., & Campelo, J. H. (2002). Seasonal variations in the evapotranspiration of a transitional tropical forest of Mato Grosso, Brazil: TROPICAL FOREST EVAPOTRANSPIRATION. *Water Resources Research*, *38*(6), 30–1–30–11. doi:10.1029/2000WR000122

Wang, H., Guan, H., Gutiérrez-Jurado, H. A., & Simmons, C. T. (2014). Examination of water budget using satellite products over Australia. *Journal of Hydrology*, *511*, 546–554. doi:10.1016/j.jhydrol.2014.01.076

Wang, X., de Linage, C., Famiglietti, J., & Zender, C. S. (2011). Gravity Recovery and Climate Experiment (GRACE) detection of water storage changes in the Three Gorges Reservoir of China and comparison with in situ measurements: GRACE DETECTION OF WATER STORAGE CHANGES IN TGR. *Water Resources Research*, *47*(12), W12502. doi:10.1029/2011WR010534

Wendland, E., Barreto, C., & Gomes, L. H. (2007). Water balance in the Guarani Aquifer outcrop zone based on hydrogeologic monitoring. *Journal of Hydrology*, *342*(3-4), 261–269. doi:10.1016/j.jhydrol.2007.05.033

Wilk, J., Andersson, L., & Plermkamon, V. (2001). Hydrological impacts of forest conversion to agriculture in a large river basin in northeast Thailand. *Hydrological Processes*, *15*(14), 2729–2748. doi:10.1002/hyp.229

Wohl, E., Barros, A., Brunsell, N., Chappell, N. A., Coe, M., Giambelluca, T., … Ogden, F. (2012). The hydrology of the humid tropics. *Nature Climate Change*. doi:10.1038/nclimate1556

Xue, X., Hong, Y., Limaye, A. S., Gourley, J. J., Huffman, G. J., Khan, S. I., … Chen, S. (2013). Statistical and hydrological evaluation of TRMM-based Multi-satellite Precipitation Analysis over the Wangchu Basin of Bhutan: Are the latest satellite precipitation products 3B42V7 ready for use in ungauged basins? *Journal of Hydrology*, *499*, 91–99. doi:10.1016/j.jhydrol.2013.06.042

Yong, B., Chen, B., Gourley, J. J., Ren, L., Hong, Y., Chen, X., … Gong, L. (2014). Intercomparison of the Version-6 and Version-7 TMPA precipitation products over high and low latitudes basins with independent gauge networks: Is the newer version better in both real-time and post-real-time analysis for water resources and hydrologic extremes? *Journal of Hydrology*, *508*, 77–87. doi:10.1016/j.jhydrol.2013.10.050

Zeng, Z., Piao, S., Lin, X., Yin, G., Peng, S., Ciais, P., & Myneni, R. B. (2012). Global evapotranspiration over the past three decades: estimation based on the water balance equation combined with empirical models. *Environmental Research Letters*, *7*(1), 014026. doi:10.1088/1748-9326/7/1/014026

CHAPTER 5

EXPLORING THE IMPORTANCE OF THE UNDISTURBED BRAZILIAN SAVANNAH ON RUNOFF AND SOIL EROSION PROCESSES

Oliveira, Paulo Tarso S., Nearing, Mark .A., and Wendland, E. Exploring the importance of the undisturbed brazilian savannah on runoff and soil erosion processes. *Earth Surface Processes and Landforms*. Under Review. (Impact factor, 2013: 2.695; Qualis CAPES: A1)

Abstract

The Brazilian Cerrado is a large and important economic and environmental region that is experiencing major loss of its natural landscapes due to pressures of food and energy production, which has caused large increases in soil erosion. However the magnitude of the soil erosion increases in this region is not well understood, in part because scientific studies of surface runoff and soil erosion are scarce or nonexistent in native Cerrado vegetation. In this study we measured natural rainfall-driven rates of runoff and soil erosion under native cerrado vegetation and bare soil to compute the Universal Soil Loss Equation (USLE) cover and management factor (C-factor) to help evaluate the likely effects of land use change on soil erosion rates. Replicated data on precipitation, runoff, and soil loss on plots (5 x 20 m) under bare soil and native cerrado were collected for 55 erosive storms occurring in 2012 and 2013. We found average runoff coefficient of ~20% for the plots under bare soil and less than 1% under native cerrado vegetation. The mean annual soil losses in the plots under bare soil and cerrado were 15.25 t $ha^{-1}yr^{-1}$ and 0.17 t ha^{-1} yr^{-1}, respectively. The erosivity–weighted C-factor for the native cerrado vegetation was 0.013. Surface runoff, soil loss and C-factor were greatest in the summer and fall. Our results suggest that though soil erosion under undisturbed Cerrado is important, shifts in land use from the native to cultivated vegetation may result in orders of magnitude increases in soil loss rates. These results provide benchmark values that will be useful to evaluate past and future land use changes using soil erosion models and measurements.

Keywords: deforestation; infiltration; runoff; soil and water conservation; USLE.

1 Introduction

Land use changes have led to several environmental impacts at local, regional and global scales. The conversion of natural landscapes to the production of food and energy is one of the most common land use changes that lead to major impacts on ecosystem function (Foley et al., 2005). In Brazil, deforestation is threatening the Cerrado (Marris 2005), one of the richest biomes in the world in terms of the biodiversity (Myers et al., 2000). This biome covers an area of 2 million km^2 (~22% of the total area of Brazil), however, more than half of the area of the Cerrado has been transformed into pasture and cropland (Klink and Machado 2005). Between the years of 2002–2008, 2008–2009 and 2009–2010 the average annual deforestation rates were 0.69%, 0.37% and 0.32%, which are on the order of or greater than that for the Amazon rain forest during the same periods, which were 0.44%, 0.40% and 0.29% (IBAMA/MMA/UNDP 2011).

Brazil is currently one of the world's largest producers and exporters of grain and beef (FAO 2012), and the majority of those are produced in the Cerrado. For the years of 2009–2010, 54% of the nation's soybeans, 95% of its cotton, 23% of its coffee, 55% of its beef and 41% of its milk were produced in the Cerrado (EMBRAPA 2012). This region also plays a fundamental role in water resource dynamics because it distributes fresh water to the largest basins in Brazil and South America. Furthermore, the largest hydroelectric plants (comprising 80% of the Brazilian energy matrix), such as the Itaipu, Tucuruí, Ilha Solteira, Xingó and Paulo Afonso, are on rivers in the Cerrado. Deforestation is driven by food production and national economic development, however, the associated changes impact water balance dynamics and have the potential to degrade soil and water resources. These changes also have the potential to directly and adversely affect hydroelectricity plants. Balancing economic development with the conservation of the Cerrado is a major challenge for Brazil.

Change from native vegetation to pasture and crops potentially increases runoff rates, soil erosion rates and sediment yields (Wohl et al., 2012; Davidson et al., 2012). Therefore, it is fundamentally important to quantify soil erosion on native vegetation (undisturbed lands) to have benchmarks for assessing erosion under other land uses (Zimmermann et al., 2012). The gold standard for quantifying soil erosion rates in any environment, including native vegetation, is using soil erosion plots under natural rainfall, however, these studies are expensive and time consuming (Nearing et al., 2000). Thus, there is a dearth of such

measurements in native vegetation worldwide (Robichaud et al., 2010), and we did not find any studies on native Cerrado vegetation. This lack of knowledge results in a lack of specificity in erosion and runoff predictions for forest management activities (Robichaud et al., 2010) and to development and use of soil erosion models (Özhan et al., 2005).

Despite limitations in the Universal Soil Loss Equation (USLE) (Wischmeier and Smith 1978) and its revised version (RUSLE) (Renard et al., 1997), these are the most widely employed erosion models in the world (Kinnell, 2010). USLE is composed of six factors (rainfall erosivity – R; soil erodibility – K; slope length – L; slope steepness – S; cover and management – C; and conservation practices – P), which multiplied together result in the estimated average annual soil loss (A). Although by definition USLE-estimated soil loss is equally sensitive to each of the factors, given the usual ranges of the factors the topographic factor (LS) and the cover and management (C-factor) have been shown to be the two factors that most greatly influence the USLE model's overall efficiency (Risse et al., 1993). The C-factor is defined as a non-dimensional number between zero and one that represents a rainfall erosivity-weighted ratio of soil loss from land under specified, vegetated conditions to the corresponding loss from continuous bare fallow (Wischmeier and Smith 1978). In Brazil, there have been few studies on C-factors, and no studies under native Cerrado vegetation.

Studies of the C-factor are needed to use the USLE and other models widely employed in Brazil, such as RUSLE and Soil Water Assessment Tool (SWAT) (Arnold et al., 1998). In addition, this factor is used in the Brazilian program of payment for environmental service, called "water producer". However, C-factor values used in this program, in general, are based in standard values developed for conditions in the United States (ANA, 2008). The use of the USLE factors developed in such a different geographic environment can lead to uncertainties in soil erosion estimates. Thus, studies *in situ* are crucial to accurately use soil erosion models for the application of programs for payment for environmental services and to promote soil and water conservation.

The objectives of this study were to measure natural rainfall-driven rates of runoff and soil erosion under native Cerrado and bare soil conditions and to derive associated USLE C-factor values. The information is crucial for applying models in the area to assess impacts of land use changes, and has significance for native vegetation regions worldwide.

2 Materials and Methods

2.1 Study area

This study was conducted in a native cerrado area located in the municipality of Itirapina, São Paulo State, Brazil (latitude 22°10' S, longitude 47°52' W and average elevation of 780 m) (Figure 1).

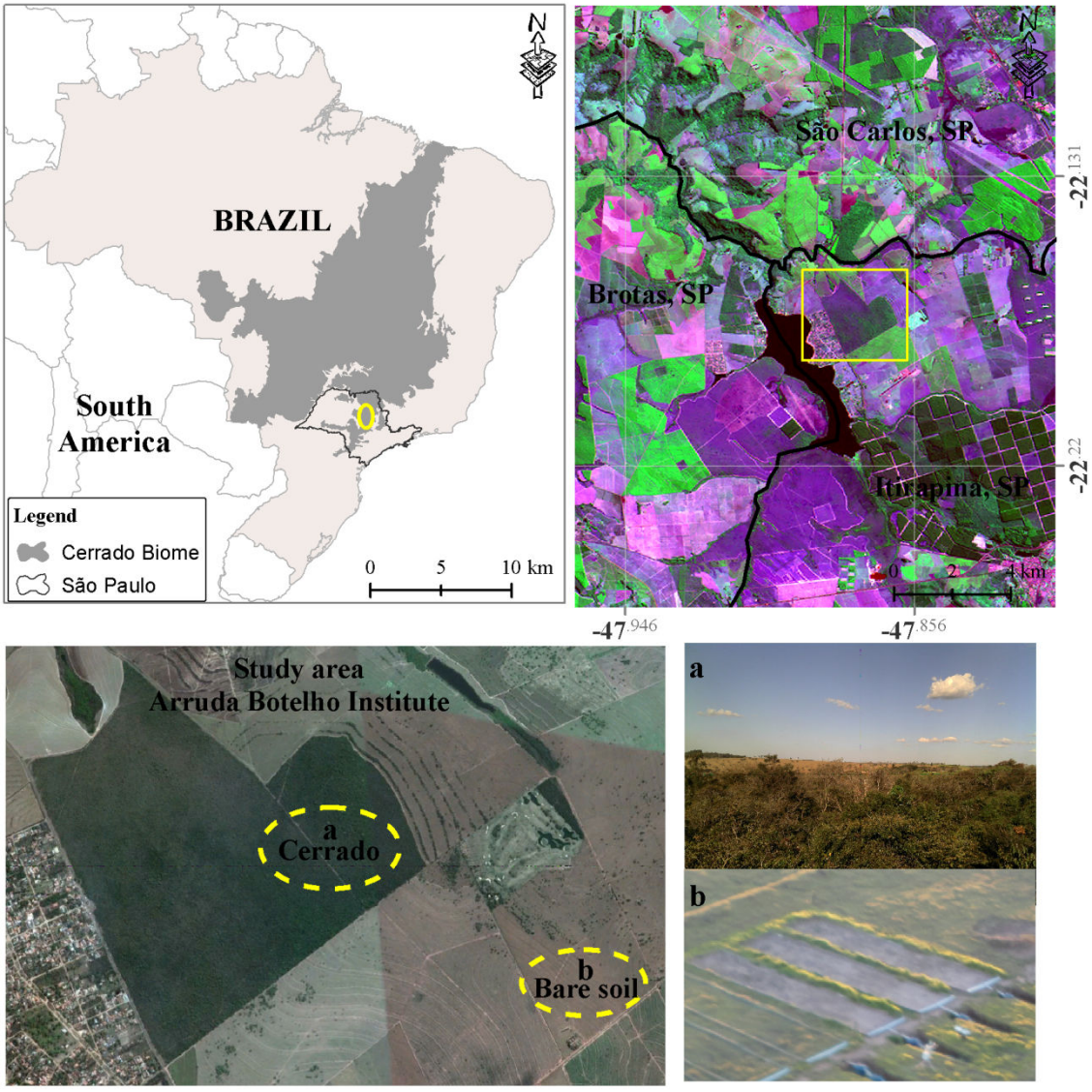

Figure 1. Study area and research plots.

The physiognomies of the Cerrado as a whole vary from grassland to savanna to forest. In the study area the physiognomy was classified as "cerrado sensu stricto denso", which is also known as cerrado woodland and has a characteristic arborous cover of 50% to 70% and tree heights of 5 to 8 m (Furley 1999). This area has been preserved and there are no records of fires. The absolute density was of 15,278 individuals trees per hectare, with a basal area of 11.44 m^2 ha^{-1} and Shannon diversity index of 4.03 in our study area, which are similar to values found in other Cerrado areas (Reys 2008). According to the Köppen climate classification system, the climate in this area is Cwa subtropical, with a dry winter (April to September) and hot and rainy summer (October to March). The average annual precipitation is approximately 1500 mm. The soil is classified in the Brazilian Soil Classification System (SiBCS) as Ortic Quartzarenic Neosol (RQo) with sand texture (85.7% sand, 1.7% silt, and 12.6% clay), and bulk density of 1.7 g cm^{-3}.

We used 100 m^2 experimental plots of 5 m width and 20 m length, with slope steepness of approximately 0.09 m m^{-1}, which is approximately standard for USLE unit plots (The USLE unit plot is 72 feet, or 22 m, in length, at 9% slope). Runoff and soil loss were measured for each erosive rain (see definition below) under the native cerrado vegetation and bare soil. Each treatment had three replications and plots on bare soil were located about 1 km from the plots under native cerrado vegetation. Plots under bare soil were built with three storage tanks with 310 liters capacity each and two splitters of one seventh, i.e. one seventh were collected in the second tank and one forty ninth in the third tank. In the plots under native cerrado vegetation only one storage tank with a capacity 310 liters for each plot was used to collect runoff and soil loss (Figure 2).

Figure 2. Experimental plots under native cerrado vegetation (above) and bare soil (below) showing the runoff collection system.

We monitored the plots for 55 erosive storms occurring during 2012 and 2013. The runoff data for each event were obtained by measuring the height of the water in the collecting tanks at the ends of the plots. For sediment measurements we collected a sample of 1000 ml taken from the tank while stirring manually, which was the standard method used in the original development of the USLE, along with the deposition of sediment in the approach to the tank. The samples were oven-dried at 105 ºC for 24 h and then weighed to compute the total sediment amount. Soil loss for each event was calculated as the total sediment divided by the plot area.

2.2 Rainfall erosivity (R-Factor)

We used an automated tipping bucket rain gauge (model TB4) to measure rainfall depth on a 10 min interval. This rain gauge was located in an open area in front of the plots under bare soil. The erosivity index (EI_{30}) was computed for each rainfall event. Periods of rainfall were considered to be isolated events when they were separated by periods of precipitation between 0 (no rain) and 1.0 mm for at least 6 h, and were classified as erosive events when

6.0 mm of rain fell within 15 min or 10.0 mm of rain fell over a longer time period (Oliveira et al., 2013). Only erosive events were used in calculating rainfall erosivity.

Erosive rainfall data were processed using the Chuveros software to calculate the USLE erosivity (Cassol et al., 2008), following the methods used for the USLE. Rainfall hyetographs were analyzed by identifying time segments with similar intensities, and for each segment the kinetic energy was estimated by:

$$e = 0.119 + 0.0873 \log_{10} i \quad (1)$$

where e is the kinetic energy (MJ ha^{-1} mm^{-1}) and i represents time segments of rainfall intensity (mm h^{-1}) (Wischmeier and Smith, 1978).

The values obtained using Eq. 1 were multiplied by the amount of rain in the respective uniform segment to express the kinetic energy of the segment in MJ ha^{-1}. The total kinetic energy of rain (E_{ct}) was obtained by summing the kinetic energy of all the time segments of rain (Oliveira et al., 2013). The event erosivity, EI_{30}, was computed as the product of the maximum rain intensity during a 30-minute period (I_{30}) and the E_{ct}.

$$EI_{30} = E_{ct} I_{30} \quad (2)$$

where EI_{30} is the rainfall erosivity index (MJ mm ha^{-1} h^{-1}), E_{ct} is the total calculated kinetic energy of the rain (MJ ha^{-1}), and I_{30} is the maximum rain intensity during a 30-minute period (mm h^{-1}) (Wischmeier and Smith, 1978). Rainfall erosivity (R-Factor) for any period of time is computed as the sum of EI_{30} values occurring during the period.

2.3 Cover and management (C-factor)

The cover and management (C-factor) was computed considering the 55 erosive storms occurring in 2012 and 2013. We used the erosivity-weighted average values of soil loss for each treatment to compute the C-factor. This factor was estimated for the soil loss from the native cerrado vegetation divided by the soil loss from bare soil (Soil Loss Ratio - SLR), and

the fraction of the erosive rainfall index (FEI_{30}) for each time interval. The values were then summed and divided by the total FEI_{30} for the entire period of study (Eq. 3):

$$C = (SLR_1 * FEI30_1 + SLR_2 * FEI30_2 + ... + SLR_n * FEI30_n) / \sum^{n} FEI30 \quad (3)$$

where SL*R* is the average soil loss by replicated plots under the native cerrado vegetation divided by the average soil loss from replicated plots under bare soil (dimensionless), FEI_{30} = $EI_{30}\ storm / \sum EI_{30}$ (dimensionless).

2.4 Statistical analyses

We used the Student's t-test with a 95% confidence level in order to evaluate the significance of the linear correlation between the surface runoff and soil loss in the plots under bare soil and undisturbed cerrado, and between FEI_{30} and SLR.

3 Results and Discussion

3.1 Runoff and soil loss under native cerrado vegetation

The measured annual precipitation was 1247.4 mm and 1113.0 mm for 2012 and 2013, with 31 and 24 erosive rainfall events each year, resulting in a rainfall erosivity index of 3644.0 MJ mm ha^{-1} h^{-1} and 3089.5 MJ mm ha^{-1} h^{-1}, respectively. The erosive rainfall represented 80% of the total precipitation and was concentrated in the wet season, which generally runs from October through March (Figure 3). The high rainfall in the month of May, 2013 was atypical in that May is not generally considered to be part of the rainy season in the area. The six months of October through March together represented 73% of the total

erosivity for the study period. In 2012 the monthly rainfall was greatest in January and December; however the highest value of erosivity occurred in February. Similarly in 2013 the months of January and November had the greatest rainfall while May and October had the greatest erosivity (Figure 3). This difference between months of maximum rainfall and maximum erosivity occurred because greater values of precipitation do not necessarily produce greater values of erosivity due to variation in rainfall intensity, and hence energy, patterns (Oliveira et al., 2013).

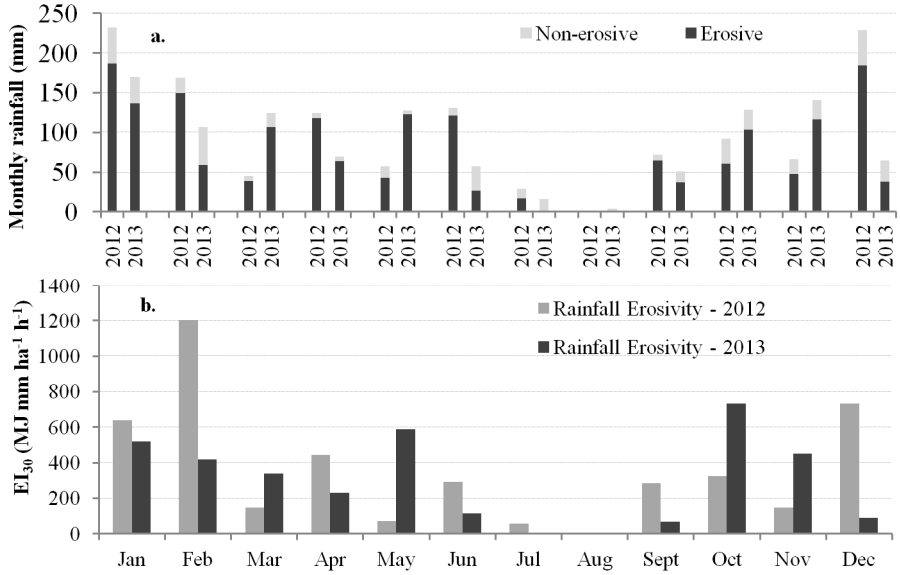

Figure 3. Monthly rainfall (a) and storm erosivity indices (b), EI_{30}, in 2012 and 2013.

In the plots on bare soil, the runoff coefficient for individual rainfall events (total runoff divided by total rainfall) ranged from 0.003 to 0.860 with an average value and standard deviation of 0.212 ± 0.187. The highest values were found for larger, more intense rainfall events, or in periods with several consecutive rainfall events, which induced high soil moisture contents and consequently greater runoff generation. Moreover, the runoff coefficient found for the bare soil plots (~20%) indicates that the soil in the study area (sandy soil) has a high infiltration capacity. In forest areas the leaf litter and the more porous soil tend to promote the increase of infiltration and water storage, rather than rapid overland flow (McCulloch and Robinson 1993). Runoff coefficients ranged from 0.001 to 0.030 with an average of less than 1% (0.005 ± 0.005) in the plots under undisturbed cerrado.

We found a significant correlation coefficient between surface runoff and soil loss for the plots under bare soil and undisturbed cerrado, $R = 0.73$ ($p < 0.0001$) and $R = 0.72$ ($p < 0.0001$), respectively. However, the relative seasonal trends were not identical for the native cerrado and the bare plots. Precipitation and rainfall erosivity index (EI_{30}) were greatest in

summer, followed by spring, fall, and then winter. Runoff and soil loss from the bare plots followed the same relative trend. However, for the native cerrado plots there was more runoff, and a greater runoff coefficient, in the winter than in the spring. This occurred because in 2012 the rainfall events in the winter had longer duration than they did in the spring, promoting more surface runoff and soil loss. For example, the amount rain on 06/20/2013 was 74 mm and had a duration of 45 minutes, which is not expected during this season that is generally dry. In 2013 the surface runoff and soil loss were larger in the spring than in the winter (the expected scenario) for the plots under native cerrado and bare soil because the rainfall events were not as long-lasting as in the winter of 2012. In the plots under native cerrado vegetation the greatest surface runoff and soil erosion values were concentrated in the summer and fall seasons (Figure 4a and c). The values found in these periods (summer and fall) represent, respectively, 77% and 78% of the total surface runoff and soil erosion measured on the native cerrado plots during the study period. This happened because the leaf-drop late in the fall season promotes a good soil cover for the following seasons of winter and spring, thus facilitating increased water retention and protection against soil erosion. However, by the summer the accelerated litter decomposition left the soil more exposed. Decomposition is faster in this season because of the summer heat and moisture.

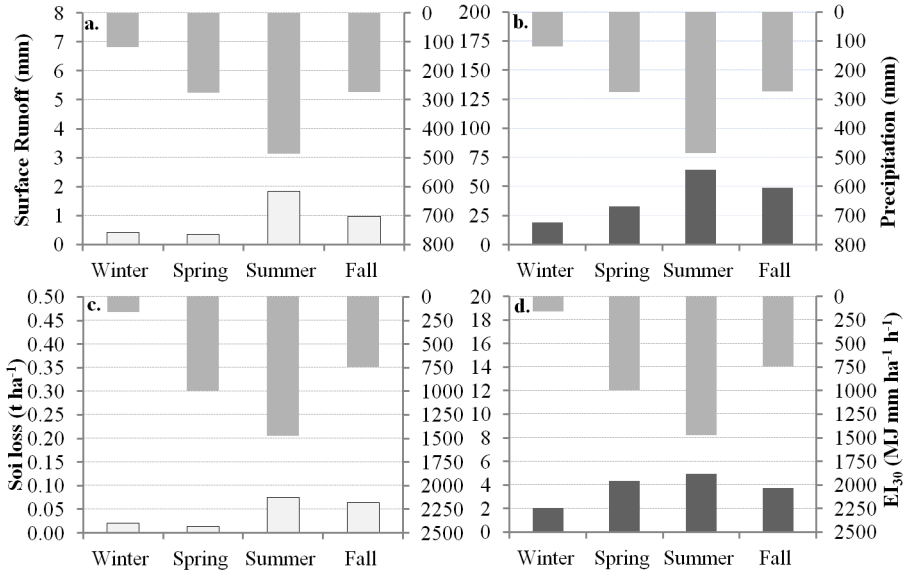

Figure 4. Average values for two years of surface runoff and soil loss in plots under native cerrado vegetation (a and c) and bare soil (b and d) for each season. Seasons: winter (June 1 to August 31); Spring (September 1 to November 30); Summer (December 1 to February 28) and Fall (March 1 to May 31).

Canopy interception in this native cerrado vegetation site was evaluated in a previous study with measured value of 17.4% of rainfall, where throughfall and stemflow were 81.0% and 1.6% of rainfall, resptvilly (Oliveira et al., 2014). However, knowledge about interception in the native cerrado vegetation is incomplete, particularly regarding the interception by ground cover at the soil surface. Despite that we did not quantify the forest floor cover in the cerrado, we can infer that the forest floor had a strong influence on runoff and soil erosion in the native cerrado vegetation. We noted that in the summer, when the soil was more exposed (Figure 5b) than the winter and spring (Figure 5a), the runoff and soil erosion tended to be greater. In addition, we found on the metal plot borders (Figure 5c and d) evidence of greater splash in the summer. Under forest vegetation raindrop diameters typically increase due to the interception process, thereby potentially increasing the splash effect and consequently the soil loss (Nanko et al., 2004; Geißler et al., 2012). Future studies should be undertaken to evaluate the effects of the cerrado vegetation on interception, runoff and soil erosion.

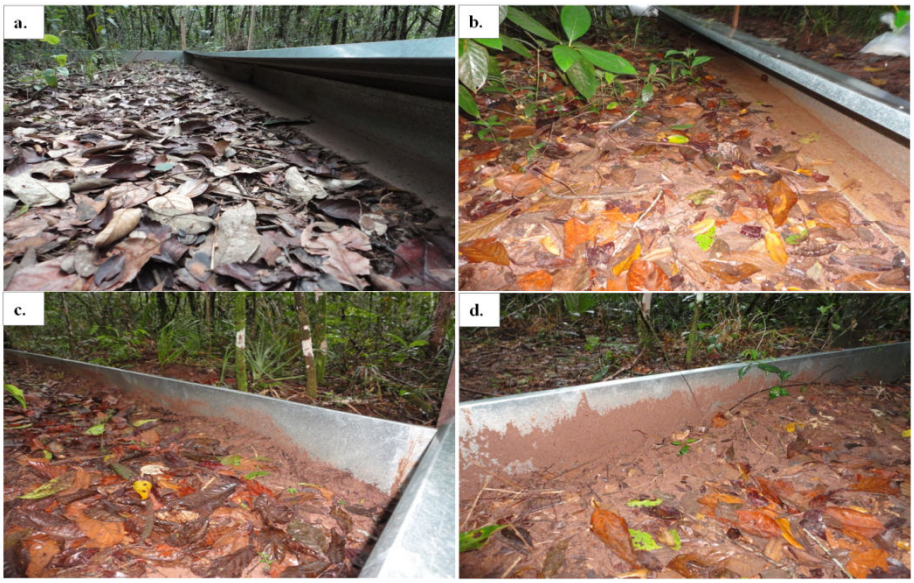

Figure 5. Forest floor of the plots under cerrado: a. in the winter and b. in the summer; c. and d. splash effects in the summer season.

The soil losses measured under bare soil and cerrado were 15.68 t $ha^{-1}yr^{-1}$ and 0.24 t ha^{-1} yr^{-1} in 2012, and 14.82 t ha^{-1} yr^{-1}, 0.11 t ha^{-1} yr^{-1} in 2013, respectively, with means of total soil loss during the study period of 15.25 t ha^{-1} yr^{-1} and 0.17 t ha^{-1} yr^{-1}. These results were consistent with those presented by Bruijnzeel (2004), who found annual soil loss for several natural tropical forests ranging 0.03 to 6.2 t ha^{-1} yr^{-1} with an average of the 0.3 t ha^{-1} yr^{-1}. Our study conditions represent the most common form of the undisturbed cerrado, however, there are others parts of the biome that vary from grassland ("campo limpo") to forest ("cerradão")

that should also be studied to provide benchmarked values to evaluate past and future land use and land cover change from soil erosion models and measurements.

In the plots under bare soil and native cerrado vegetation, the coefficients of variation among replicated plots for runoff from individual storms ranged from 2.6 to 73.1% and 2.1 to 95.0%, with average of 27.1% and 40.0%. For the soil loss we found values ranging from 6.3 to 103.3% and 1.2 to 124.2%, with average of 42.2% and 43.7%, respectively, for bare soil and cerrado. In addition, we noted that the coefficients of variation were larger on small observed values of runoff and soil erosion than on large observed values. These results are comparable with the high coefficients of variation found in studies on plots under natural rainfall discussed in Nearing et al., (1999) and Gómez et al., (2001). The coefficients of variation found here highlight the importance of studying soil erosion from replicated field plots. Further, in soil erosion models generally there are several inputs (climate, soil type, land cover, topographic, and etc.), and a deterministic output response, generating unique rather than probabilistic predictions or ranges of potential values for runoff and soil erosion, for example. However, these results presented here and by Wendt *et al*. (1986); Nearing *et al.* (1999); and Gómez *et al.* (2001) have shown that in natural conditions there may be a range of responses to surface runoff and soil erosion for similar measurable inputs (precipitation, land cover, and etc). Therefore, the coefficients of variation found here should be considered and used in future studies to evaluate expected prediction capability for erosion models in the Brazilian Cerrado.

3.2 C-factor for the native cerrado vegetation

The annual C-factor computed during 2012 and 2013 for the plots under native cerrado vegetation was 0.013. Although the cerrado studied was an undisturbed area, e.g., without any management, tillage or on the fire influences, there were changes in the canopy, forest floor, and soil moisture during the year promoted mainly by the weather and the vegetation dynamics (Giambelluca et al., 2009). These changes produced different responses to runoff, soil erosion, and consequently to the soil loss ratio (SLR) and C-factor. Furthermore, there were significant differences in the rainfall erosivity between the seasons (Oliveira et al., 2013), with the rainfall erosivity concentrated in the wet season. The greatest FEI_{30}, SLR and

C-factor values were found in the summer and fall for the two years studied (Table 1). Although the greatest values of FEI_{30} and SLR were in these two seasons, our results have shown that there was no significant correlation between FEI_{30} and SLR for all events ($p = 0.06$). This result indicates that soil loss in the plots under bare soil had greater correlation with rainfall erosivity than the plots under undisturbed cerrado. This statement can be verified by the coefficient of correlation between soil loss with rainfall erosivity of $R = 0.57$ ($p < 0.0001$) and $R = 0.31$ ($p = 0.02$) for the plots under bare soil and cerrado respectively.

Table 1. Results by year for erosivity index (EI_{30}), fraction of the erosive rainfall index (FEI_{30}), Soil Loss Ratio (SLR) and C-factor.

	EI_{30}		**FEI_{30}**		**SLR**		**C-factor**	
	2012	**2013**	**2012**	**2013**	**2012**	**2013**	**2012**	**2013**
Winter	303.7	14.7	0.0833	0.0048	0.0442	0.0033	0.0163	0.0033
Spring	757.5	1231.4	0.2079	0.3986	0.0445	0.0231	0.0026	0.0029
Summer	1921.5	1028.2	0.5273	0.3328	0.4605	0.1626	0.0209	0.0127
Fall	661.3	815.2	0.1815	0.2639	0.2741	0.0803	0.0202	0.0125
Total annual	3644.0	3089.5	-	-	-	-	0.0166	0.0087

We found the greatest annual values for EI_{30}, FEI_{30}, SLR, and C-factor in 2012. These results show an example of weather variability in Brazilian climate (Oliveira et al., 2013), and suggest that is important to continue the research in the native Cerrado vegetation in order to evaluate if the results found in the present study will vary significantly over the years and to improve our knowledge about this factor in the Cerrado. Furthermore, this kind of study is important to improve knowledge on overland flow generation and soil erosion processes occurring in forested areas, particularly considering expected climate change (Butzen et al., 2014).

The C-factor obtained in the present study was almost half of the value previously reported for the Atlantic Forest Biome and greater than that reported for the Caatinga Biome (Table 2). We found that there have been very few studies on soil erosion under undisturbed natural vegetation in the entire world (Montgomery et al., 2007; Robichaud et al., 2010) and several authors have used the C-factor developed for the United States (Wischmeier and Smith, 1978; Dissmeyer and Foster, 1981) to map soil erosion using geographic information systems (Irvem et al., 2007; Oliveira et al., 2011). Another common approach is to estimate the C-factor using remotely sensed data (Bargiel et al., 2013; Durigon et al., 2014). However, both of these methods to obtain the C-factor produce uncertainties and can compromise the quality of soil erosion predictions. Therefore, the computation of the C-factor using field data

is crucial to evaluate soil erosion predictions and to generate local information that can be used in models of soil erosion.

Table 2. Previous studies of C-factors in Brazil.

Land use	C-factor (annual)	Source
Native cover (Cerrado Biome)	0.013	Present Study
Native cover (Atlantic Forest Biome)	0.02	Martins *et al.* 2010
Native cover (Pampa Biome)	0.01	Oliveira 2011
Native cover (Caatinga Biome)	0.0015	Albuquerque et al. 2005
Caatinga 'regeneration process'	0.0017	Albuquerque et al. 2005
Eucalyptus grandis	0.30	Martins *et al.* 2010
Eucalyptus saligna	0.10	Oliveira 2011
Eucalyptus urophylla, maidenii and E. globulus	0.03	Oliveira 2011
Corn with several manegements	0.025 - 0.156	De Maria and Lombardi Neto 1997
Corn (Dk, Cp and Nt)	0.1097, 0.0809 and 0.0610	Bertol *et al.* 2002
Oat (Dk, Cp and Nt)	0.0671, 0.0409 and 0.0372	Bertol *et al.* 2002
Soybeans (Dk, Cp and Nt)	0.1437, 0.0807 and 0.0455	Bertol *et al.* 2001
Wheat (Dk, Cp and Nt)	0.2158, 0.1854 and 0.0558	Bertol *et al.* 2001
Coffee	0.0866 - 0.1412 (average, 0.1126)	Prochnow *et al.* 2005
Palma (downhill)	0.5103	Albuquerque *et al.* 2005
Palma (in level)	0.2355	Albuquerque *et al.* 2005

Dk = disk harrow, Cp = chisel plow and Nt = no-tillage.

Previous studies have shown that, in general, the C-factors for Brazilian crops cover an approximate 10-fold range, from 2 to 39-times greater than the C-factor for undisturbed cerrado (Table 2). Montgomery *et al.* (2007) reported results from other parts the world, concluding that rates of soil erosion under conventional agriculture are in mean 124-fold greater than under undisturbed native vegetation. We also found reported C-factor values for Eucalyptus, the main planted forest in Brazil, ranging from 3 to 23-times greater than the C-factor for undisturbed cerrado (Table 2). Borrelli and Schütt (2014) concluded that soil loss in a planted forest was 21 times greater than that for an undisturbed forest in Central Italy. Therefore, we might expect that the current conversion of unidsturbed cerrado to crops (Jepson et al., 2010; Phalan et al., 2013) or planted forest will likely increase significantly the soil erosion rates in the region. For Brazil to develop economically and maintain the quality of its natural resources, such as soil and water, we must understand the soil erosion processes under undisturbed areas and pasture/crops. From this knowledge a soil erosion model adjusted to Brazilian conditions may be useful to delineate areas best suited for crop, pasture and native vegetation.

4 Conclusions

In this paper we undertook a first approach to quantify runoff and soil erosion on land in native cerrado vegetation from experimental plots under natural rainfall. We measured soil erosion rates under native cerrado vegetation and bare soil to compute the USLE cropping factor (C-factor) to help evaluate the likely effects of land use change on the soil erosion rates. Replicated data on precipitation, runoff, and sediment amounts under native cerrado and bare soil were collected for 55 erosive storms occurring in 2012 and 2013. This study represents a first step toward filling the information gap on soil erosion in native cerrado vegetation, and provides a better understanding of the magnitude of the soil erosion impacts promoted by the recent deforestation in the Brazilian Cerrado.

We found an average runoff coefficient of ~20% for the plots under bare soil and less than 1% under native cerrado vegetation. The means of annual soil losses in the plots under bare soil and cerrado were 15.25 t $ha^{-1}yr^{-1}$ and 0.17 t ha^{-1} yr^{-1}, respectively. These results provide benchmark values that will be useful to evaluate past and future land use changes using soil erosion models and measurements.

Studies on soil erosion and the C-factor for many common crops in Brazil (such as: sugar cane, rice, beans, potato, cotton, millet, among others), fruit trees, pasture, and for the undisturbed Amazon rainforest and Pampa Biome are generally lacking. Furthermore, it is important to continue the research in the native Cerrado vegetation to evaluate if the results found in the present study will vary significantly over the years and to improve our knowledge about this factor in other parts of the Cerrado. Therefore, new experimental field studies of runoff and soil erosion processes need to be undertaken at different scales, including plots, hillslopes, and watersheds, to improve soil and water conservation technologies in Brazil.

The annual C-factor for the plots under native cerrado vegetation was 0.013. Our results showed that the surface runoff, soil erosion and C-factor for the undisturbed cerrado changes between seasons. The greatest C-factor values were found in the summer and fall. We found that there have been relatively few scientific studies on runoff, soil erosion and C-factors under undisturbed, natural vegetation in the past, and several researchers have used the C-factor developed in the United States to map soil erosion using geographic information

systems. The use of this factor, without on-site knowledge, produces uncertainties that can compromise the quality of soil erosion predictions and assessments. By first understanding and quantifying soil erosion processes and rates under both undisturbed areas and pasture or crops, we can then more confidently apply a soil erosion model to represent specific local conditions. This study represents a step toward that goal.

5 Acknowledgments

The authors thank the Fundação de Amparo à Pesquisa do Estado de São Paulo - FAPESP (10/18788-5, 11/14273-3 and 12/03764-9) and the Conselho Nacional de Desenvolvimento Científico e Tecnológico - CNPq (470846/2011-9) for making this study possible. We would like to thank the Arruda Botelho Institute (IAB) and São José farm that have allowed us to develop this study in the native Cerrado vegetation. USDA is an equal opportunity provider and employer.

6 References

Albuquerque, A. W. de, M. Filho, G., Santos, J. R., Costa, J. P. V., & Souza, J. L. (2005). Determinação de fatores da equação universal de perda de solo em Sumé, PB. *Revista Brasileira de Engenharia Agrícola E Ambiental*, *9*(2), 153–160. doi:10.1590/S1415-43662005000200001

ANA, Agência Nacional de Àguas. Manual Operativo do Programa Produtor de Água. Superintendência de Usos Múltiplos, Brasília: ANA, 2008.

Arnold, J. G., Srinivasan, R., Muttiah, R. S., & Williams, J. R. (1998). LARGE AREA HYDROLOGIC MODELING AND ASSESSMENT PART I: MODEL DEVELOPMENT. *Journal of the American Water Resources Association*, *34*(1), 73–89. doi:10.1111/j.1752-1688.1998.tb05961.x

Bargiel, D., Herrmann, S., & Jadczyszyn, J. (2013). Using high-resolution radar images to determine vegetation cover for soil erosion assessments. *Journal of Environmental Management*, *124*, 82–90. doi:10.1016/j.jenvman.2013.03.049

Bertol, I., Schick, J., & Batistela, O. (2001). Razão de perdas de solo e fator c para as culturas de soja e trigo em três sistemas de preparo em um cambissolo húmico alumínico. *Revista Brasileira de Ciência Do Solo*, *25*(2), 451–461. doi:10.1590/S0100-06832001000200021

Bertol, I., Schick, J., & Batistela, O. (2002). Razão de perdas de solo e fator C para milho e aveia em rotação com outras culturas em três tipos de preparo de solo. *Revista Brasileira de Ciência Do Solo*, *26*(2), 545–552. doi:10.1590/S0100-06832002000200029

Borrelli, P., & Schütt, B. (2014). Assessment of soil erosion sensitivity and post-timber-harvesting erosion response in a mountain environment of Central Italy. *Geomorphology*, *204*, 412–424. doi:10.1016/j.geomorph.2013.08.022

Bruijnzeel, L. A. (2004). Hydrological functions of tropical forests: not seeing the soil for the trees? *Agriculture, Ecosystems & Environment*, *104*(1), 185–228. doi:10.1016/j.agee.2004.01.015

Butzen, V., Seeger, M., Wirtz, S., Huemann, M., Mueller, C., Casper, M., & Ries, J. B. (2014). Quantification of Hortonian overland flow generation and soil erosion in a Central European low mountain range using rainfall experiments. *CATENA*, *113*, 202–212. doi:10.1016/j.catena.2013.07.008

Cassol, E. A., Eltz, F. L. F., Martins, D., Lemos, A. M. de, Lima, V. S. de, & Bueno, A. C. (2008). Erosividade, padrões hidrológicos, período de retorno e probabilidade de ocorrência das chuvas em São Borja, RS. *Revista Brasileira de Ciência Do Solo*, *32*(3), 1239–1251. doi:10.1590/S0100-06832008000300032

Davidson, E. A., de Araújo, A. C., Artaxo, P., Balch, J. K., Brown, I. F., C. Bustamante, M. M., … Wofsy, S. C. (2012). The Amazon basin in transition. *Nature*, *481*(7381), 321–328. doi:10.1038/nature10717

De Maria I.C., & Lombardi Neto F. (1997). Razão de perdas de solo e fator C para sistemas de manejo da cultura do milho. *Revista Brasileira de Ciência do Solo*, 21, 263-270.

Dissmeyer, G. E., & Foster, G. R. (1981). Estimating the cover-management factor (C) in the universal soil loss equation for forest conditions. *Journal of Soil and Water Conservation*, *36*(4), 235–240.

Durigon, V. L., Carvalho, D. F., Antunes, M. A. H., Oliveira, P. T. S., & Fernandes, M. M. (2014). NDVI time series for monitoring RUSLE cover management factor in a tropical watershed. *International Journal of Remote Sensing*, *35*(2), 441–453. doi:10.1080/01431161.2013.871081

EMBRAPA, Empresa Brasileira de Pesquisa Agropecuária. Apresentação. available at: http://www.cpac.embrapa.br/unidade/apresentacao/

FAO, Food and Agricultural commodities production. Country rank in the world, by commodity. available at: http://faostat.fao.org/site/339/default.aspx

Foley, J. A. (2005). Global Consequences of Land Use. *Science*, *309*(5734), 570–574. doi:10.1126/science.1111772

Furley, P. A. (1999). The nature and diversity of neotropical savanna vegetation with particular reference to the Brazilian cerrados. *Global Ecology and Biogeography*, *8*(3-4), 223–241. doi:10.1046/j.1466-822X.1999.00142.x

Geißler, C., Kühn, P., Böhnke, M., Bruelheide, H., Shi, X., & Scholten, T. (2012). Splash erosion potential under tree canopies in subtropical SE China. *CATENA*, *91*, 85–93. doi:10.1016/j.catena.2010.10.009

Giambelluca, T. W., Scholz, F. G., Bucci, S. J., Meinzer, F. C., Goldstein, G., Hoffmann, W. A., … Buchert, M. P. (2009). Evapotranspiration and energy balance of Brazilian savannas with contrasting tree density. *Agricultural and Forest Meteorology*, *149*(8), 1365–1376. doi:10.1016/j.agrformet.2009.03.006

Gómez, J. ., Nearing, M. ., Giráldez, J. ., & Alberts, E. . (2001). Analysis of sources of variability of runoff volume in a 40 plot experiment using a numerical model. *Journal of Hydrology*, *248*(1-4), 183–197. doi:10.1016/S0022-1694(01)00402-4

IBAMA/MMA/UNDP. Monitoramento do desmatamento nos biomas Brasileiros por satélite. available at: http://siscom.ibama.gov.br/monitorabiomas/cerrado/index.htm.

İrvem, A., Topaloğlu, F., & Uygur, V. (2007). Estimating spatial distribution of soil loss over Seyhan River Basin in Turkey. *Journal of Hydrology*, *336*(1-2), 30–37. doi:10.1016/j.jhydrol.2006.12.009

Jepson, W., Brannstrom, C., & Filippi, A. (2010). Access Regimes and Regional Land Change in the Brazilian Cerrado, 1972–2002. *Annals of the Association of American Geographers*, *100*(1), 87–111. doi:10.1080/00045600903378960

Kinnell, P. I. A. (2010). Event soil loss, runoff and the Universal Soil Loss Equation family of models: A review. *Journal of Hydrology*, *385*(1-4), 384–397. doi:10.1016/j.jhydrol.2010.01.024

Klink, C. A., & Machado, R. B. (2005). Conservation of the Brazilian Cerrado. *Conservation Biology*, *19*(3), 707–713. doi:10.1111/j.1523-1739.2005.00702.x

Marris, E. (2005). Conservation in Brazil: The forgotten ecosystem. *Nature*, *437*(7061), 944–945. doi:10.1038/437944a

Martins, S. G., Silva, M. L. N., Avanzi, J. C., Curi, N., & Fonseca, S. (2010). Cover-management factor and soil and water losses from eucalyptus cultivation and Atlantic Forest at the Coastal Plain in the Espírito Santo State, Brazil. *Scientia Forestalis*, **38**, 517-526.

McCulloch, J. S. G., & Robinson, M. (1993). History of forest hydrology. *Journal of Hydrology*, *150*(2-4), 189–216. doi:10.1016/0022-1694(93)90111-L

Montgomery, D. R. (2007). Soil erosion and agricultural sustainability. *Proceedings of the National Academy of Sciences*, *104*(33), 13268–13272. doi:10.1073/pnas.0611508104

Myers, N., Mittermeier, R. A., Mittermeier, C. G., da Fonseca, G. A. B., & Kent, J. (2000). Biodiversity hotspots for conservation priorities. *Nature*, *403*(6772), 853–858. doi:10.1038/35002501

Nanko, K., Hotta, N., & Suzuki, M. (2004). Assessing raindrop impact energy at the forest floor in a mature Japanese cypress plantation using continuous raindrop-sizing instruments. *Journal of Forest Research*, *9*(2), 157–164. doi:10.1007/s10310-003-0067-6

Nearing, M. A. (2000). Measurements and Models of Soil Loss Rates. *Science*, *290*(5495), 1300b–1301. doi:10.1126/science.290.5495.1300b

Nearing, M. A., Govers, G., & Norton, L. D. (1999). Variability in Soil Erosion Data from Replicated Plots. *Soil Science Society of America Journal*, *63*(6), 1829. doi:10.2136/sssaj1999.6361829x

Oliveira, A.H. (2010). Erosão hídrica e seus componentes na sub-bacia hidrográfica do horto florestal terra dura, Eldorado do Sul (RS). PhD dissertation, Universidade Federal de Lavras (UFLA), Lavras, Brazil. 181pp.

Oliveira, P. T. S., Sobrinho, T. A., Rodrigues, D. B. B., & Panachuki, E. (2011). Erosion Risk Mapping Applied to Environmental Zoning. *Water Resources Management*, *25*(3), 1021–1036. doi:10.1007/s11269-010-9739-0

Oliveira, P. T. S., Wendland, E., & Nearing, M. A. (2013). Rainfall erosivity in Brazil: A review. *CATENA*, *100*, 139–147. doi:10.1016/j.catena.2012.08.006

Oliveira, P.T.S., Wendland, E., Nearing, M.A. & Martins, J.P. (2014). Interception of rainfall and surface runoff in the Brazilian Cerrado. Geophysical Research Abstracts 16, EGU2014-4780.

Özhan, S., Balcı, A. N., Özyuvaci, N., Hızal, A., Gökbulak, F., & Serengil, Y. (2005). Cover and management factors for the Universal Soil-Loss Equation for forest ecosystems in the Marmara region, Turkey. *Forest Ecology and Management*, *214*(1-3), 118–123. doi:10.1016/j.foreco.2005.03.050

Phalan, B., Bertzky, M., Butchart, S. H. M., Donald, P. F., Scharlemann, J. P. W., Stattersfield, A. J., & Balmford, A. (2013). Crop Expansion and Conservation Priorities in Tropical Countries. *PLoS ONE*, *8*(1), e51759. doi:10.1371/journal.pone.0051759

Prochnow, D., Dechen, S. C. F., De Maria, I. C., Castro, O. M. de, & Vieira, S. R. (2005). Razão de perdas de terra e fator C da cultura do cafeeiro em cinco espaçamentos, em Pindorama (SP). *Revista Brasileira de Ciência Do Solo*, *29*(1), 91–98. doi:10.1590/S0100-06832005000100010

Renard, K.G., Foster, G.R., Weesies, G.A., Mccool, D.K., & Yoder, D.C. (1997). *Predicting soil erosion by water: A guide to conservation planning with the Revised Universal Soil Loss Equation (RUSLE).* Washington: USDA Agriculture Handbook, n.703.

Reys, P. A. N. (2008). *Estrutura e fenologia da vegetação de borda e interior em um fragmento de cerrado sensu stricto no sudeste do Brasil (Itirapina, São Paulo)*. PhD dissertation, Universidade Estadual Paulista, Rio Claro, Brazil. (124pp)

Risse, L. M., Nearing, M. A., Laflen, J. M., & Nicks, A. D. (1993). Error Assessment in the Universal Soil Loss Equation. *Soil Science Society of America Journal*, *57*(3), 825. doi:10.2136/sssaj1993.03615995005700030032x

Robichaud, P. R., Wagenbrenner, J. W., & Brown, R. E. (2010). Rill erosion in natural and disturbed forests: 1. Measurements: RILL EROSION IN FORESTS, 1. *Water Resources Research*, *46*(10), n/a–n/a. doi:10.1029/2009WR008314

Wendt, R. C., Alberts, E. E., & Hjelmfelt, A. T. (1986). Variability of Runoff and Soil Loss from Fallow Experimental Plots1. *Soil Science Society of America Journal*, *50*(3), 730. doi:10.2136/sssaj1986.03615995005000030035x

Wischmeier, W.H., & Smith, D.D. (1978). *Predicting rainfall erosion losses. A guide to conservation planning*. Washington: USDA Agriculture Handbook, n. 537, 58p.

Wohl, E., Barros, A., Brunsell, N., Chappell, N. A., Coe, M., Giambelluca, T., … Ogden, F. (2012). The hydrology of the humid tropics. *Nature Climate Change*. doi:10.1038/nclimate1556

Zimmermann, A., Francke, T., & Elsenbeer, H. (2012). Forests and erosion: Insights from a study of suspended-sediment dynamics in an overland flow-prone rainforest catchment. *Journal of Hydrology*, *428-429*, 170–181. doi:10.1016/j.jhydrol.2012.01.039

GENERAL CONCLUSIONS

The literature review presented in the **first chapter** reveals that the annual rainfall erosivity in Brazil ranges from 1672 to 22,452 MJ mm ha^{-1} h^{-1} yr^{-1}. The lowest values are found in the northeastern region, and the highest values are found in the north region and the southeastern region. The rainfall erosivity tends to increase from east to west, particularly in the northern part of the country. There are few studies on erosivity in Brazil and that these studies are concentrated in the south and southeast regions. In addition, the number of years of data used in most of those studies was less than the recommended standard for the application of RUSLE (20 years of data). The regression equations of rainfall erosivity cannot be extrapolated to a generalized form without underestimating or overestimating the erosivity values. Studies must be conducted on the local climate to determine which equation is best suited to the desired region. There are 73 regression equations to calculate rainfall erosivity in Brazil. These equations can be useful to map rainfall erosivity for the entire country. To this end, techniques already established in Brazil may be used for the interpolation of rainfall erosivity, such as geostatistics and artificial neural networks.

The empirical model developed in the **second chapter** showed a satisfactory agreement with observed ET and better results than from the product MOD16 ET. From this empirical model it is possible to compute ET at daily, monthly and annual scales for undisturbed cerrado areas with similar characteristics of hydroclimatology and phenology that observed in the PDG site. Furthermore, from this approach is possible to assess the ET for large areas of the Cerrado with a good spatial and temporal resolution (250 m and 16 days), therefore, it may be useful for monitoring evapotranspiration dynamics in this region. From the results of this chapter was possible to conclude that the canopy interception may range from 4 to 20% of gross precipitation in the cerrado and that stemflow values are around 1% of gross precipitation. The average runoff coefficient was less than 1% in the plots under undisturbed cerrado and that the deforestation has the potential to increase up to 20 fold the runoff coefficient value. As only little excess water runs off (either by surface water or groundwater) the water storage in the undisturbed cerrado (IAB site) may be estimated by the difference between precipitation and evapotranspiration. The results provide benchmark values of water

balance dynamics in the undisturbed Cerrado that will be useful to evaluate past and future land use in different sceneries of water scarcity and climate change for this region.

The results found in the **third chapter** show that the Curve Number method was not suitable to estimate runoff under undisturbed cerrado, bare soil (hydrologic soil group A), pasture, and millet. Therefore, in these cases the curve number is inappropriate and the runoff is more aptly modeled by the equation $Q = CP$, where C is the runoff coefficient. Curve number obtained from the standard table was suitable to estimate runoff for bare soil, soybeans, and sugarcane. However, CN values obtained from rainfall-runoff data (CN calibrated) provide better runoff estimate than the CN values from the standard table. In addition, there was not significant difference between the mean runoff estimated by the central tendency methods (median, and geometric and arithmetic means). In this chapter were suggested curve numbers for land cover where the significant correlation with observed runoff was found, and considering the better *CoD* and *NSE* values. These CN values and ranges provide guidance for application of the curve number technique in ungauged watersheds, and to evaluate the CN calibration in other similar regions. Furthermore, these results of this study provide benchmark values that could be useful to evaluate past and future land use changes using hydrologic models and measurements in the Cerrado biome.

In the **fourth chapter**, the study indicates that the main source of water budget uncertainty in the estimated runoff arises from errors in the TRMM precipitation data. In general, TRMM v6 data tend to overestimate the ground-measured rainfall in the Brazilian Cerrado, mainly in the southern part, although there is an underestimation in the northeast. However, our results show that the new version of TRMM 3B42 v7 notably reduces the bias between TRMM and the measured precipitation data from 9.5% to 6%, thus improving its potential application in hydrological studies. The water storage change (dS/dt) computed as a residual of the water budget equation using remote sensing data (TRMM and MOD16) and measured discharge data shows a significant correlation with TWS change obtained from the GRACE data for all watersheds studied. The results indicate that the GRACE data may provide a satisfactory representation of water storage change for large areas in the Brazilian Cerrado. The results show that water budget closure from remote sensing remains a challenge due to uncertainties in the data. However, this approach demonstrates the potential to evaluate trends in water balance components over large regions, identify drier periods, and assess changes in water balance due to land cover and land use changes.

The results presented in the **fifth chapter** indicate an average runoff coefficient of ~20% for the plots under bare soil and less than 1% under native Cerrado vegetation. The means of annual soil losses in the plots under bare soil and Cerrado were 15.25 t $ha^{-1}yr^{-1}$ and 0.17 t ha^{-1} yr^{-1}, respectively. These results provide benchmark values that will be useful to evaluate past and future land use changes using soil erosion models and measurements. The annual C-factor for the plots under native Cerrado vegetation was 0.013. The results showed that the surface runoff, soil erosion and C-factor for the undisturbed Cerrado changes between seasons. The greatest C-factor values were found in the summer and fall. There have been relatively few scientific studies on runoff, soil erosion and C-factors under undisturbed, natural vegetation in the past, and several researchers have used the C-factor developed in the United States to map soil erosion using geographic information systems. The use of this factor, without on-site knowledge, produces uncertainties that can compromise the quality of soil erosion predictions and assessments. By first understanding and quantifying soil erosion processes and rates under both undisturbed areas and pasture or crops, we can then more confidently apply a soil erosion model to represent specific local conditions. This study represents a step toward that goal.

The chapters presented in this doctoral thesis were already published or are under review in peer reviewed journals. The process of elaboration of these chapters provided great advances in the methodological delineation and discussion aspects, mainly with the valuable contributions and cooperation of co-authors, and constructive criticisms from the international journals reviewers and editors.

APPENDIX:

General details about the experimental area located at the 'Instituto Arruda Botelho - IAB'

The IAB site is a 300 ha, undisturbed woodland located in the municipality of Itirapina, São Paulo State (latitude 22°10' S, longitude 47°52' W, elevation: 780 m). The climate in the IAB site is similar to that for the PDG (Cwa subtropical), with an average annual precipitation of 1506 mm and temperature of 20.8 ºC.

Soil characteristics of the IAB site

The soil is classified as Ortic Quartzarenic Neosol with sandy texture in the entire profile (85.7% sand, 1.7% silt, and 12.6% clay), and soil bulk density of 1.7 g cm^{-3}. Figure 1 shows the soil collected at the IAB site and some of results are presented in the Figure 2 and 3.

Figure 1. Samples from soil profile at the IAB site.

Universidade de São Paulo
Escola Superior de Agricultura "Luiz de Queiroz"
Departamento de Ciência do Solo

Interessado: **8354 Paulo Tarso Sanches de Oliveira**
Endereço: AV Trabalhador Sancarlense 400 Cx.Postal 359
Parque Arnold Schimidt Sao Carlos SP CEP 13566590
Propriedade: FAZENDA SAO JOSE - CERRADÃO Município: ITIRAPINA - SP

Tipo de Análise: SF3
Requisição: **3267**
Data de Emissão: 20/9/2012
Concluídas em: 19/7/2012

Resultado de Análise Granulométrica

Identif. da Amostra	Areias (g/kg)						Silte (g/kg)	Argilas (g/kg)		Floculação (%)	Classe de Textura
	AMG	AG	AM	AF	AMF	AT		c/disp.	água		
0-31CM	16	105	382	339	3	844	31	125	100	20	**ar.**
31-78CM	15	98	369	328	29	839	34	127	101	20	**ar.**
78-175CM	18	99	315	287	37	756	11	234	70	70	**md-ar.**

Métodos: Bouyoucos (densímetro); S.S.S.A. Book Series: 5 Methods of Siol Analysis Part4;
Classe de diametro (mm) U.S.D.A..
5 frações de areia: muito grossa (MG) = 2 a 1; grossa (G) = 1 a 0,5; média (M) = 0,5 a 0,25;
fina (F) = 0,25 a 0,10; muito fina (MF) = 0,10 a 0,05; areia total (AT) = 2 a 0,05;
silte = 0,05 a 0,002; argila total < 0,002; argila água < 0,002.
2 frações de areia: grossa (G) = 2 a 0,25 e fina (F) = 0,25 a 0,05; areia total (AT) = 2 a 0,05;
silte = 0,05 a 0,002; argila total < 0,002.
Classe de textura: Argila (c/ dispersante) até 149 g/kg = arenosa (ar); de 150 a 249 g/kg
= média arenosa (md-ar); de 250 a 349 g/kg = média argilosa (md-arg);
de 350 a 599 g/kg = argilosa (arg); de 600 g/kg ou superior - muito argilosa (m-arg).
Observações:
Amostra coletada pelo interessado; (#) elemento não determinado.
Este documento pode ser reproduzido somente por completo.
Os resultados deste relatório se referem somente às amostras enviadas ao laboratório.

Signatário Autorizado

Av. Pádua Dias, 11 CEP 13418-260 - Piracicaba, SP - Brasil fone (19) 3417-2117 / 3417-2159 - Fax (19) 3417-2135
e-mail: LSO.LAB@USP.BR - Home-page: http:// www.solos.esalq.usp.br

Figure 2. Physical characteristics of soil at the IAB site.

UNIVERSIDADE DE SÃO PAULO
ESCOLA SUPERIOR DE AGRICULTURA "LUIZ DE QUEIROZ"
DEPARTAMENTO DE CIÊNCIA DO SOLO
Av. Pádua Dias, 11 • • CEP 13418-900 • Piracicaba, SP - Brasil
Fone (19) 3417-2117 • Fax (19) 3417 2135
http://www.solos.esalq.usp.br

Cliente: **Paulo Tarso Sanches de Oliveira**
Dep. de Eng.Hidráulica e Saneamento (EESC-USP)-SÃO CARLOS

Nº
Estado: SP

RESULTADOS DE ANÁLISES

AMOSTRA	POROSIDADE			UMIDADE VOLUMÉTRICA			DENSIDADE		CONDUTIVIDADE HIDRÁULICA*
	PT	MAC	MIC	-0,06 MPa	-0,033 MPa	-1,5 MPa	SOLO	PARTÍCULAS	
	---------- cm³/cm³ ----------						-------- g/cm³ --------		---- mm/h ----
01 (20 cm)	0.3594	0.1692	0.1902	0.2739	0.1292	0.0930	1.69	2.64	102.279
02 (50 cm)	0.3215	0.1156	0.2059	0.3485	0.1440	0.0972	1.80	2.65	11.302
03 (100 cm)	0.3338	0.1229	0.2109	0.3410	0.1404	0.0914	1.77	2.66	19.813

PT, porosidade total; MAC, macroporosidade; MIC, microporosidade. *: do solo saturado.

Piracicaba, 15 de agosto de 2012.

Prof. Dr. Alvaro Pires da Silva
Responsável

Figure 3. Physical characteristics of soil at the IAB site.

Meteorological station installed at the IAB.

We installed a 11 m instrumental platform to measure basic above-canopy meteorological and soil variables. A datalogger (Campbell CR1000, Logan UT, USA) sampled the weather station and soil data every 15 s and recorded averages on a 10 min basis. Figure 4 and 5 shows details of the instrument platform installed at the IAB.

Figure 4. Instrument platform installed at the IAB.

Figure 5. Some sensors installed on the instrument platform.

We also have monitored other meteorological station approximately 1 km of the instrument platform installed in the undisturbed Cerrado. In this other area there are plots under pasture, sugarcane and bare soil (Figure 6).

Figure 6. Location of the meteorological stations installed in the cerrado and bare soil areas.

Canopy interception

Canopy interception (CI) was computed as the difference between the gross precipitation (P_g) and the net precipitation (P_n), where P_g is the total precipitation that fell at the top of the canopy and P_n is computed as the sum of two components: throughfall (TF) and stemflow (SF). We measured the P_g from an automated tipping bucket rain gauge (model TB4) located above the canopy at 10 m height. TF was obtained from 15 automated tipping bucket rain gauges (Davis Instruments, Hayward, CA) distributed below the cerrado canopy and randomly relocated every month during the wet season (Figure 7). Each rain gauge was installed considering an influence area of 10 x 10 m.

Figure 7. Automated tipping bucket rain gauges (Davis Instruments, Hayward, CA) distributed below the cerrado canopy.

SF was measured on 12 trees using a plastic hose wrapped around the trees trunks, sealed with neutral silicone sealant, and a covered bucket to store the water (Figure 8). Selected trees to be monitored were divided into two groups considering the diameter at breast height (DBH). Therefore, we monitored 7 trees with 5 cm < DBH < 20 cm and 5 trees with DBH > 20 cm. The volume of water in each SF collector was measured after each rainfall event that generated stemflow.

Figure 8. Collectors of throughfall.

Plots under undisturbed cerrado and bare soil

We used 100 m^2 experimental plots of 5 m width and 20 m length, with slope steepness of approximately 0.09 m m^{-1}, which is approximately standard for USLE unit plots (The USLE unit plot is 72 feet, or 22 m, in length, at 9% slope). Runoff and soil loss were measured for each erosive rain under the native cerrado vegetation and bare soil. Each treatment had three replications and plots on bare soil were located about 1 km from the plots under native cerrado vegetation. The boundaries of the plots were made using galvanized sheet placed 30 cm above the soil and into the soil to a depth of 30 cm (Figure 9 and 10).

Figure 9. Details of boundaries of the experimental plots.

Surface runoff was collected in storage tanks at the end of each plot. Plots under bare soil were built with three storage tanks with 310 liters capacity each and two splitters of one seventh, i.e. one seventh were collected in the second tank and one forty ninth in the third tank. In the plots under cerrado vegetation only one storage tank with a capacity of 310 liters

for each plot was used to collect runoff and soil loss because of the expected lower runoff amounts from those plots (Figure 10).

Figure 10. Experimental plots under bare soil (above) and undisturbed cerrado vegetation (below) showing the surface runoff and soil erosion collection system.